Research & Development

2017

**Selected Collection from Synergy 2017 International Conference
organized by the Faculty of Mechanical Engineering,
Szent István University**

Contents

Contents

Total quality management in the context
of industry 4.0

S. SADER[1], I. HUSTI[2], M. DARÓCZI[3]

[1]Ph.D. Student, Doctoral School of Engineering, Szent István University
Páter K. u. 1., Gödöllő, H-2103, Hungary
[2] Institute of Engineering Management, Faculty of Mechanical Engineering,
Szent István University, Páter K. u. 1., Gödöllő, H-2103, Hungary,
[3]Institute of Engineering Management, Faculty of Mechanical Engineering,
Szent István University, Páter K. u. 1., Gödöllő, H-2103, Hungary,

Abstract

Industry 4.0 (I4.0) is the fourth industrial revolution, emerged since 2011, aims at developing the new "Smart Factory", by utilizing the technological development such as Internet of Things (IoT), Cyber Physical Systems (CPS), Cloud Computing, and Big Data. I4.0 emerged as a result of the growing demand of more individualized and complex products, considering its quality and the responsiveness to market demand. In this paper, a review for the I4.0 literature was made, aligned with TQM principles, suggested areas where I4.0 can serve to successfully implement TQM principles.

Keywords

Industry 4.0, TQM, Total Quality Management, Smart Factory, Production systems

1. Introduction

Industry 4.0 (I4.0) is known as the technological development occurred in industry from embedded systems to intelligent Cyber Physical Systems (Scheer, 2013). It was firstly suggested and adopted by the German Government in its High-Tech Strategy 2020 (Scheer, 2013), introduced in 2011 during the Hannover fair event (Qin, Liu, & Grosvenor, 2016). Industry 4.0, abbreviated by (I 4.0) aims at utilizing the new technological systems such as Internet of Things (IoT), Cloud Computing, and Big Data to revolutionize the industry to an intelligent manufacturing systems (Trappey et al., 2016), where production facilities and warehousing facilities are connected to each other in the form of Cyber Physical Systems (Henning et al., 2013).

The name (Industry 4.0) stands for the fourth industrial revolution. As illustrated in Figure 1, the first three revolutions represent the development of industry since the first revolution, emerged during the 18th century, and relied on mechanical power generated from steam and water. The second revolution, emerged during the 20s century, advanced the industry to mass production lines,

where production process was divided into stages, building on the experience of labor gained from the repeated work, responding to the increased market demand. This period was known by the use of conveyor to transfer products between machines automatically. The third revolution, came as a result of integrating the programmable logic controllers (PLC), which were invented during the 1970s and facilitated the automation of industrial production, minimizing the efforts needed by labor. Recently, the computer systems were developed and integrated in the industry and this utilization was developed until Internet of Things (IoT) brought to stage and launched the new fourth industrial revolution which was agreed to be known as Industry 4.0 (Keller et al., 2014; Qin et al., 2016; Scheer, 2013).

The need for I4.0 came from the fact that 17% of the GDP generated in European countries accumulated from industry, offering 32 million job positions. However, this large economical sector in Europe, is being challenged by the aging community of the EU countries, and concurrently, the accelerating development of other competing industrial economies such as China and Asia and other developing countries (Qin et al., 2016). Accordingly, Industry 4.0 was innovated and supported by the German Government in order to maintain the leading industrial position of Germany (Scheer, 2013), Supported by the new development of smart IT solutions including data gathering tools (sensors), and intelligent analysis systems (software) provided the ability to analyze big data collected from production processes as well as during the whole production chain, translate it to a user friendly computer interface, replacing the traditional monitoring tools, and providing a key enabler for industrial effectiveness and efficiency. Hence, a bedrock for Industry 4.0 development (Scheer, 2013).
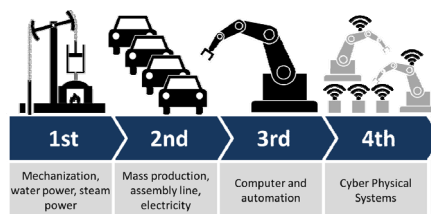
Figure 1. Illustration of Industry 4.0, showing the four "industrial revolutions"
(Source: Christoph Roser: http://www.allaboutlean.com)

Industry 4.0 changed the production from a centralized to a de-centralized process, made it possible to advance the production from a traditional machining process to a more interactive and complex process where the product communicate with the machine, telling it what to do (Scheer, 2013). Additionally, the support of intelligent CPS provided the ability of the machine to gather data, analyze, learn, and decide independently (Lee, Bagheri, & Kao, 2015). This feature paved the way to offer a new generation of industry, where factories are intelligent enough having the ability to self-plan and self-adapt to

provide more customized products and fulfilling the customer expectations autonomously (Witkowski, 2017).

The current common production strategy depends mainly on mass production in order to minimize the production cost per-unit, and to fulfill the expanding market need of this product (economies of scale). However, in the recent decade, customers are increasingly demanding more than ever before, looking for more customized and detailed products that differs from each other. Industry 4.0 opened the door for more customized products that is flexible to preserve the mass production and fulfills the customers' requirements in more details at the same time.

The impact of Industry 4.0 was not only to introduce a new known as "Smart Factory", but it also introduced the "Smart Product" term, where products are embedded with sensors and smart processors, which carry the customer experience and provide the feedback to the supplier about the performance of the products in field (Qin et al., 2016). A real case example for industry 4.0 applications is the "Technology Initiative SmartFactoryKL" which is a research and development project funded by leading industrial suppliers, in order to act as a university and research center, for building a model of factory that is totally smart and supported by high end technologies (Zuehlke, 2010). The equipment of the factory was built to produce liquid soap, where clients can specify their needs at any number, and chose from different colors. The plant was able to combine requirements and demand, and produce the customized products at any number of bottles. The plant was built in a modular construction, where each function is independent and autonomous, and the product is being customized according to customer demand.

Another example of smart product, is the "Smart Vehicle". Where the vehicle is linked with sensors to collect information about the vehicle operation, driver, routs, and conditions. This data is being transmitted to a data cloud server, where it is analyzed and transferred and friendly displayed useful and valuable information to humans. The data could be the driver skills practices, route prediction, and the health of the vehicle (Qin et al. 2016).

However, Industry 4.0 is still a new phenomenon, and till now it is not implemented widely and several industries are in the testing and development stage. Thus, Industry 4.0 needs further research on several areas to identify its impact on industry, human, product and the economy.

Additionally, industry 4.0 still have some ambiguities in terms of security and safety issues. Connectivity problems and the lack of expertise that are needed to run the utilized high technologies effectively could cause significant damages when happening. Failure during production entails expensive costs and could be harmful for human being (Mrugalska & Wyrwicka, 2017).

2. Total quality management (TQM):

Total Quality Management (TQM) is a managerial approach that leads an organization to achieve a world-class position by insuring that its products and services satisfies customers, meeting their requirements and expectations (Yusof

& Aspinwall, 2000). The Term "Total Quality Management – TQM" was first suggested and leaded by the American scientist Deming, who traveled from the United States of America to Japan in order to help the Japanese industrial firms to recover from the World War II. During his work, he implemented the statistical quality control and process control, as tools to trace production errors and to identify the source of products' defects (Kanji, 1990). Later on, he met with Juran, who was stressing to focus on customers' satisfaction through producing fit-to-use products that fulfills the customers' needs. Shortly, both Deming and Juran successfully caught the attention of market all over the world, their new ideas increased the production rates in Japan, and contributed very strongly to the Japanese well-known successful industrial miracle (Kanji, 1990).

Since then, the philosophy of TQM has been enhanced and expanded, several TQM principles were identified in order to guide the good implementation of TQM at organizations. The goal was to benefit business stakeholders, where everyone at the organization as well as the business processes are cooperating to produce value-for-money products and services, that fulfils and positively exceed the customers' expectations (Dale, 2015). Researchers found strong evidences that TQM has improved the organizational effectiveness, flexibility, competitiveness, excellence, creating positive attitude, and a source of creating continuous improvement culture at the organization (Anu P. Anil & Satish, 2016).

There are several approaches to implement TQM, in their paper (Anu P. Anil & Satish, 2016) suggested 30 general practices for successful TQM implementation. Accordingly, a literature review was conducted for the most known TQM gurus research and quality models, such as Juran, Malcom Baldrige National Quality Award, European Quality Award, Deming Prize and others, through which they obtained a final list (as in table 1 below) of critical 18 frequently suggested success factors for implementing TQM practices.

Table 1. TQM Critical success factors

1	Leadership and top management commitment	7	Education and training	13	Quality culture
2	Continuous improvement	8	Strategic management	14	Benchmarking
3	Supplier quality management	9	SPC usage	15	Process and product design
4	Customer focus	10	Quality information analysis	16	Process management
5	Employees involvement	11	Quality assurance	17	Product Innovation
6	Employees empowerment	12	Quality citizenship	18	Knowledge management

(Source: Anu P. Anil & Satish, 2016)

However, (Anu P. Anil & Satish, 2016) did not mention an important approach to implement TQM which is the International Standard Organization

Model (ISO 9001:2015 model), it is widely adopted as one of the best practices to achieve TQM excellence.

The recent version of ISO 9001:2015 was approved on the basis of ISO 9001:2008 version. The benefits of implementing this system is the ability to provide high quality products and services that fulfills customers' requirements, continuously enhance their satisfaction, addressing the risks and opportunities associated with organization's context and objectives, and conformity to specified quality management system requirements (International Organization for Standardization, 2015).

According to the recently released (ISO 9001:2015, 2015), Quality management principles consisted of seven principles which are: customer focus, leadership, engagement of people, process approach, improvement, evidence-based decision making, and relationship management. Where those principles are summarized as following:

- Customer Focus: it is the primary focus of quality management, meeting customers' requirements and strive to exceed their expectations. Such goal is achieved by understanding the organization's customers, grouping them, communicate with them, aligning the organization's objectives to customers' needs and expectations. Other supporting activities to this goal is to measure and monitor customer satisfaction, and take proper actions and modify products when needed. It is also important to maintain sustainable relationships with customers. The outcomes of this goals are measured by several indicators such as customers' loyalty, satisfaction, growth of customers' base, improved reputation of the organization and increased market share.

- Leadership: the role of leadership is important to ensure unity of purpose between all leadership levels toward achieving the organization's quality goals. This implies that the leadership is responsible to communicate the organization's vision, mission, strategies and policies to all managerial levels. It is also important to encourage an organizational wide commitment to quality principles, which means that everybody at the organization shares the same believes and habits, including leaders. Additionally, it is important to train people at the organization and delegate authorities and responsibilities to them, this need proper training and clear accountability policy.

- Engagement of people: it is important to engage people of the organization in achieving the organization's quality objectives. Empowerment, recognition, enhancement of competences, support personal development, and encouraging initiatives, all will contribute to the excellence of the organization, improve business activities, building a creative, motivating and trust environment. It will improve the satisfaction of employees, and will support and promote the organizational values among all people.

- Process approach: activities and processes of the organization should be understood, consistent, managed and coherent with the whole system of the organization. It is necessary to identify the system objectives to

understand the necessary processes to achieve them. Managing processes needs authorities, responsibilities and accountability policies to be identified. It is important to understand the interdependencies of processes and the interrelations to achieve the quality objectives of the organization effectively and efficiently. Performance monitoring, analysis, transparency is important to evaluate processes and take correction actions or optimize processes when needed. Risks affecting the system should be addressed to avoid downtime and emergency maintenance.

– Improvement: continuous improvement is essential for organization development, it will maintain its innovative position among competitors, continuously enhancing processes' performance, supporting organizational capability and customers' satisfaction. Continuous improvement will enhance the organization ability to avoid risks and react to opportunities. Improvements include development of new products and services as well as processes. Successful organizations support the culture of continuous improvement by admiring innovators and recognize improvements.

– Evidence-based decision making: measuring, analyzing, monitoring key performance indicators will support the process of decision making. Decisions taken on the basis of transparent, accurate, secure, reliable and balanced information will provide an effective, efficient, and improved decisions that prove their correctness in the future.

– Relationship management: identifying stakeholders of the organization and their relationships will enhance the organization's production supply chain. Suppliers, partners, customers, investors, employees, etc. relations should be managed in a collaborative manner in order to unify the efforts of the organization toward its goals.

According to previous listed ISO 9001:2015 TQM principles, and based on the interpretation of each item as explained in the ISO9000:2015 fundamentals and vocabulary document, this paper suggests a simple matching of the 18th principles list in table 1, and the seven principle of TQM of the ISO9001:2015 standard. Accordingly, this paper aims at suggesting an Industry 4.0 based approach toward successful implementation of the ISO 9001:2015 principles.

Table 2. TQM principles VS. 18th principles in Table 1

ISO 9001:2015 TQM principles	18th Principles identified in Table 1
Customer focus	4
leadership	1,8,12,13
engagement of people	5,6,13
process approach	9,10,11,15,16
improvement	2,7,14,15,17
evidence-based decision making	11,18
relationship management	3

3. Total quality management in the context of industry 4.0

As a result of the previous discussions, Industry 4.0 can serve the successful implementation of the seven TQM principles through the following means:

– **Customer Focus**: Industry 4.0 will enable organizations to improve their customers' satisfaction through improving their products and services, fulfilling and strive to exceed customers' requirements and expectations. Industry 4.0 will enable industries to provide customized products at a regular time, away from the complexity of changing mass production systems. Moreover, Industry 4.0 will provide businesses with early forecasting about consumption behavior and trends, thus, providing a competitive advantage for the business by providing proper products at the proper time.

– **Leadership**: Evidences showed that Industry 4.0 had a great impact on information flow over the production line, integrating the business processes and supporting the ERP systems to optimize manufacturing management (Lee, Kao, & Yang, 2014). I4.0 provided transparent production processes, thus, aligning resources such as labor and machines to demand will be efficient and optimized.

– **Engagement of people**: Industry 4.0 will support the communication and collaboration of all players inside the organization, it will stimulate innovation, encourage individual contributions. Data provided by I4.0 outcomes will help people at their respective positions to use this data to avoid risks and suggest solutions, hence, be more initiative.

– **Process approach**: Industry 4.0 will support the transparency of business and production processes in the organization, it will help to optimize processes, improve efficiency and resources allocation. I4.0 will facilitate tracing production bottleneck, defects' sources, and minimize production cost. Additionally, it will improve the supply chain responsiveness, through total integration from market demand back to suppliers (Wang, He, & Xu, 2017). I4.0 will provide accurate information about processes (time, risks, resources, critical constraints) thus, it will help the planning level of key-processes to maintain continuity and efficiency.

– **Improvement**: Industry 4.0 will provide a basis for continuous improvements at the product, process and the business level for an organization. Totally connected production and supply chain will improve performance and responsiveness of the system. Experiments showed the ability of products (automobile industry as an example) to send information to the producing companies about operating problems, thus, enhancing future products to overcome such problems.

– **Evidence-based decision making**: Industry 4.0 and the new IT solutions such as big data, afforded a great capacity to improve the decision making process. Machines are self-learned, connected to each other forming a collaborative community, collecting and analyzing data, providing ability to make independent decisions. Experiments show that Industry 4.0 techniques were able to send earlier prognostics about machine health, reducing downtime and afford maintenance on time.

Table 3. TQM VS. I4.0 Interaction

TQM principles	Qualitative & Quantitative measures	Industry 4.0 contributions
Customer Focus	– Improved customer satisfaction & loyalty, – growth in customers' base, – Improved organization's reputation.	– Improved responsiveness, – Customized product/customer, – Smart prediction of market demand.
Leadership	– Unity of purpose among the organization, – Aligned strategies, policies, processes and resources, – Effective communication between all administrative levels.	– Smart allocation of resources, – High coordination among all levels of the organization, – Effective evaluation for results.
Engagement of people	– Increase motivation of people, – Increasing innovative ideas, – Enhanced people satisfaction, – Self-evaluation and self-improvement culture.	– Improved communication and collaboration, – Facilitating innovation and sharing of ideas.
Process approach	– Identify key processes and points of improvements, – Optimized performance and effective process management, – Manage processes, and interrelations, as well as dependencies.	– Transparent, interconnected, dynamic processes, – Self-learning, early prediction of errors, – Less downtime, early maintenance prediction.
Improvement	– Responsive systems to customer requirements, – Enhanced ability to react to development of processes, products and market needs, – Support drivers for innovation.	– Active dynamic interaction with market needs, – Instant re-configuration of production processes to respond to improvement requests, – Motivating for change environment.
Evidence-based decision making	– Clear and agreed decision making process, – Data availability and clarity, – Effective past decisions, – Analyze and evaluate data using suitable methods and tools.	– Rich information and analytics dashboards about production, machines, markets, etc. – Early prediction of failures, thus, anticipating early reactions, – Early evidence to correct or support decisions.
Relationship management	– Stakeholders are identified and suitable communication tools to each are known, – Stakeholders are satisfied and their feedback is considered, – Suppliers are responding to materials requests on time and at the required quality, – Supply chain is stable and no downtime due to lack supply.	– Easy identification and communication tools, – The ability to hire segmentation of stakeholders based on priorities, – Stronger collaboration with providers and partners to encourage continuous improvements.

    – **Relationship management**: total integration and effective communication between all stakeholders of an organization became one of the benefits of I4.0. Suppliers are connected with production systems, understanding the organization needs, and responsive to markets demand more than ever before.

The above discussion is summarized in table 3 below. Qualitative and quantitative measures are identified, accordingly, the contribution of I4.0 is determined.

Conclusions

Industry 4.0 provided a "stone rock" support for a successful implementation of TQM principles. Although this paper reviewed several factors to obtain a successful TQM implementation, but the paper highlighted the seven TQM principles identified by ISO9001:2015 model. This model is very popular and widely implemented worldwide. However, this paper only conducted and matched the possibilities offered by I4.0 to support the implementation of TQM in a theoretical approach. Accordingly, it is very important to use a quantitative approach to measure the real impact to utilize I4.0 to support TQM. Finding an effective interface that connect I4.0 with TQM requires experimental research. Thus, this paper appeals an industrial partner who is interested to ensure good implementation of the TQM principles toward obtaining ISO 9001:2015 principles and jointly developing Industry 4.0 technologies at the organization.

References

[1] Anu P. Anil, & Satish, K. P. (2016). Investigating the Relationship Between TQM Practices and Firm's Performance: A Conceptual Framework for Indian Organizations. *Procedia Technology*, *24*, 554–561. https://doi.org/10.1016/j.protcy.2016.05.103

[2] Dale, B. (2015). Total Quality Management. *Wiley Encyclopedia of Management*, 1–4. https://doi.org/10.1002/9781118785317.weom100042

[3] Henning, Kagermann (National Academy of Science and Engineering). Wolfgang, Wahlster (German Research Center for Artificial Intelligence). Johannes, H. (Deutsche P. A. (2013). *Recommendations for implementing the strategic initiative INDUSTRIE 4.0. Final report of the Industrie 4.0 WG*. https://doi.org/10.13140/RG.2.1.1205.8966

[4] International Organization for Standardization. (2015). ISO 9001_2015.pdf. International Organization for Standardization. Retrieved from https://www.iso.org/news/2015/09/Ref2002.html

[5] Kanji, G. K. (1990). Total quality management: the second industrial revolution. *Total Quality Management*, *1*(1), 3–12. https://doi.org/10.1080/09544129000000001

[6] Keller, M., Rosenberg, M., Brettel, M., & Friederichsen, N. (2014). How Virtualization, Decentrazliation and Network Building Change the Manufacturing Landscape: An Industry 4.0 Perspective. *International Journal of Mechanical, Aerospace, Industrial, Mechatronic and Manufacturing Engineering*, *8*(1), 37–44. https://doi.org/scholar.waset.org/1999.8/9997144

[7] Lee, J., Bagheri, B., & Kao, H. A. (2015). A Cyber-Physical Systems architecture for Industry 4.0-based manufacturing systems. *Manufacturing Letters*, *3*, 18–23. https://doi.org/10.1016/j.mfglet.2014.12.001

[8] Lee, J., Kao, H. A., & Yang, S. (2014). Service innovation and smart analytics for Industry 4.0 and big data environment. *Procedia CIRP*, *16*, 3–8. https://doi.org/10.1016/j.procir.2014.02.001

[9] Mrugalska, B., & Wyrwicka, M. K. (2017). Towards Lean Production in Industry 4.0. *Procedia Engineering*, *182*, 466–473. https://doi.org/10.1016/j.proeng.2017.03.135

[10] Qin, J., Liu, Y., & Grosvenor, R. (2016). A Categorical Framework of Manufacturing for Industry 4.0 and beyond. *Procedia CIRP*, *52*, 173–178. https://doi.org/10.1016/j.procir.2016.08.005

[11] Scheer, A. W. (2013). *Industrie 4.0. Germany Trade and Invest*. https://doi.org/10.1007/978-3-642-36917-9

[12] Trappey, A. J. C., Trappey, C. V., Hareesh Govindarajan, U., Chuang, A. C., & Sun, J. J. (2016). A review of essential standards and patent landscapes for the Internet of Things: A key enabler for Industry 4.0. *Advanced Engineering Informatics*. https://doi.org/10.1016/j.aei.2016.11.007

[13] Wang, L., He, J., & Xu, S. (2017). The Application of Industry 4.0 in Customized Furniture Manufacturing Industry. In *MATEC Web of Conferences* (Vol. 100, p. 3022). https://doi.org/10.1051/matecconf/201710003022

[14] Witkowski, K. (2017). Internet of Things, Big Data, Industry 4.0 – Innovative Solutions in Logistics and Supply Chains Management. *Procedia Engineering*, *182*, 763–769. https://doi.org/10.1016/j.proeng.2017.03.197

[15] Yusof, S. M., & Aspinwall, E. (2000). Total quality management implementation frameworks: Comparison and review. *Total Quality Management*, *11*(3), 281–294. https://doi.org/10.1080/0954412006801

[16] Zuehlke, D. (2010). SmartFactory-Towards a factory-of-things. *Annual Reviews in Control*, *34*(1), 129–138. https://doi.org/10.1016/j.arcontrol.2010.02.008

Dimensions of green warehouses –
a literature review

W. A. H. AL-ZAIDI, Cs. B. ILLÉS

Department of Business Economics and Management,
Faculty of Economics and Social Sciences, Szent István University
Páter K. u. 1., Gödöllő, H-2100, Hungary

Abstract

Warehouses represent an integral and cost effective part of supply chain and serves as a hub for raw materials, goods-in-process, finished goods and other storage related information. As warehouses play a significant role in total cost, environmental impacts and customers' service, this formulated the main motivation to study this subject.

In the "greening" process, warehouses seek to find the way of cutting operational costs while maintaining productivity and efficiency by reducing waste and decreasing energy costs. The aim of the paper is to define and introduce the different dimensions of green warehouses and to illustrate their importance based on literature sources by a systematic approach.

Keywords

green warehouses, green dimensions, pollution, environmental impacts, sustainability

1. Introduction

The challenges, which the world faced together with environmental problems like pollution and lack of resources, have pushed industrial organizations to pay a great attention for preserving the environment and optimizing the use of natural resources by employing green dimensions (Illés et al., 2013). Involving environmental thinking into supply chain management led to the Green Supply Chain Management (GSCM) concept (Miskolcziné Gábriel, 2017). The evaluation of environmental implications of warehousing – compared for example to transport activities – has got much less attention until now (Mesjasz-Lech, 2015), but there is a wide range of possible changes in warehouses which would reduce its environmental impacts (McKinnon et al., 2015)

In our paper, we focus on green warehouses. The energy consumption of warehouses can be significant, which leads to an increased level of carbon footprints. Warehousing costs account for 20-25% of logistics costs. As warehouses play a significant role in total cost, environmental impacts and customers' service, this formulated the main motivation to study this subject.

Greening of warehouses may result reducing operational costs and waste, as well as decreasing energy costs while maintaining productivity and efficiency. Eco-friendly warehouse dimensions can cover a wide range of solutions from the simple to complex investments.

In today's highly competitive business cycle and environmental friendly policies, companies strive for reducing costs and less damage to environment. Therefore, warehouses are among the main objectives for companies to minimize costs, efficient usage of energy, less emission of toxic gases and provide good service to customers (Lambert and Stock, 2001; Doesburg et al. 2009; Skowron-Grabowska, 2009). Therefore, it is necessary to pay attention towards improving warehouses performance especially in terms of environmental requirements.

Greening means the reduction of a product's environmental impact during its whole life cycle by keeping other essential product criteria, like performance and cost, i.e. green design means products or services with certain environmental consciousness (Gábriel, 2016; Seroka-Stolka, 2016). Green supply chain has three main issues, environmental performance, economic performance and operative performance. Environmental performance refers to the reduction of negative environmental effects, for example the reduction of waste and smaller carbon footprint (Eltayeb et al. 2011), reduction of material usage, energy and water consumption (Kumar et al. 2012). Economic performance can be measured at company level, for example in reduction of energy consumption and direct materials costs (Zhu et al. 2012); reuse of materials (Al-zaidi and Dunay, 2016), reduction of waste disposal cost or even the in the reduction of fees and penalties. Positive effects can be manifested in the increase of revenues and market share. Operational performance elements are the improved product and service quality, improved flexibility, reduced inventory and high capacity utilisation (Gábriel, 2016)

The aim of the paper is to define and introduce the different dimensions of green warehouses and to illustrate their importance based on a wide literature review by a systematic approach. This review builds the basic approach for defining the methodology of a research to be conducted in Iraq.

2. Dimensions of green warehouses

Warehouses can be defined as a large buildings used for commercial purposes (Rajuldevi et al., 2008). According to Lambert and Stock (2001), warehouses are an integral and cost effective part of supply chain management and serves as a hub for raw materials, goods-in-process, finished goods and other storage related information. The consumption of energy in warehouses can be comparatively higher which also leads to emission of carbon footprints (Doesburg et al., 2009). Warehousing costs account for 20-25% of logistics costs (TSMG, 2014). According to the World Resources Institute, commercial buildings emit 5.25 % of the total greenhouse gases (GHG) of which 65 % comes from energy

consumption. Warehousing activities contribute about 10.7% (300 megatons CO_2) of the total logistics emissions (World Economic Forum 2009). As it is shown, road freight generates the highest CO_2 load of total emissions (57,1%), ocean freight is the second, and warehouses produces the third highest CO_2 emission in the transportation and logistics industry (i.e. 10,9% of all emissions).

Sturge (2008) and Amjed and Harrison (2012) mentioned that there has been increase in promotion of warehousing facilities due to global expansion of companies and statistics also show that the increase in warehouses area has been approximately doubled between 1996 and 2008..

The abovementioned reasons underline the growing importance of implementing green policies in order to reduce cost, environmental impacts and to increase performance of warehouses. Several studies and literature reviews discussed the main dimensions of green warehouses, covering a wide range of options and dimensions.

Baker and Marchant (2015) described three stages of warehouses in order to reach sustainable level (Figure 1). The first stage is the simplest level, where green warehouse is just an energy efficient building meeting the minimum criteria (lighting, ventilation and mechanical handling equipment).
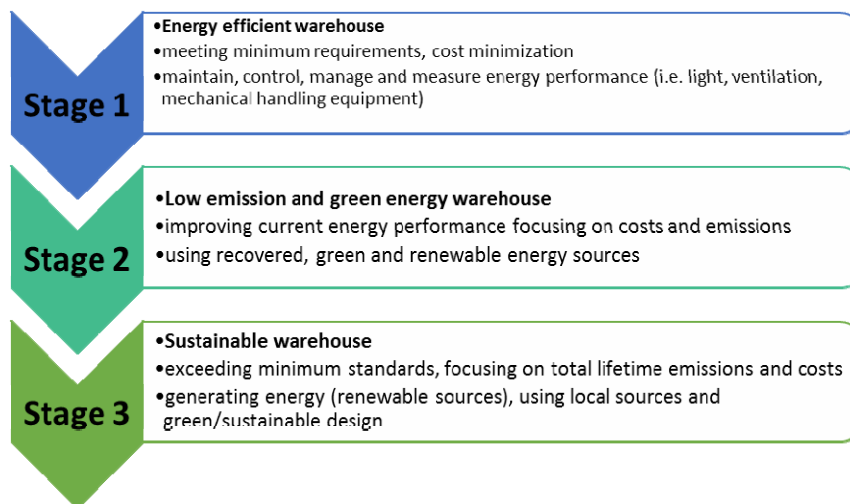
Figure 1. Stages of developing green warehouses (authors' own summary based on Baker and Marchant, 2012)

The second stage is when a warehouse is established with low-emission and using "green" energy (i.e. renewable sources of energy to decrease carbon emissions. Third stage is an advanced level, where a sustainable warehouse exceeds environmental requirements and performs beyond existing standards. At this level, managers focus on total life time emissions and the macro-level environmental issues, considering the natural environment and ecological

system. Renewable energy sources are in use: such as solar panels, winds turbines, and biomass energy. (Baker and Marchant, 2015)

As a first step of the research, the relevant literature sources were filtered to summarize the main dimensions of green – or sustainable – warehouses. Table 1 summarizes those dimensions, which were studied by more than two researchers excluding those which were studied by only one researcher. These dimensions were chosen for further explanation and will be used as the checklists in the next stage of the research.

Table 1: Dimensions of green warehouses

Authors / Dimensions	The energy and resources institute	Doesburg et al, 2009	Penny, 2009	Đukic et al, 2010	Roy, 2010	Amjed, & Harrison, 2013	Mulder, 2013	Xia & Wang, 2013	TSMG, 2014	Luu, 2016	Total
Sustainable building design and material	*	*	*		*			*	*	*	7
Heating, Ventilation and Cooling		*	*	*	*		*	*	*	*	8
Lighting system	*		*		*	*	*	*		*	7
Handling Equipment			*	*		*		*	*	*	6
Efficient water management	*	*	*			*	*				5
Waste management process	*			*		*	*	*		*	6
Green energy generation	*			*		*	*	*		*	6
Warehouse management system (WMS)				*		*		*	*		4
Future warehouse strategy						*				*	2

Source: authors' own compilation

Sustainable building design and material
Material construction and exterior design of warehouse have a significant role in reducing environmental impacts and energy consumption. Different authors (Doesburg et al., 2009; Prabhu and Dhawan, 2010; Green Economy Guide Line Manual, 2014) mentioned several considerations to be taken in account during the construction of warehouses: for example building materials (use of local materials and services, options for recycling in the future), insulation of walls and roof, glass panes that assist to reduce heat exchange and allowing to sun light pass inside and use non-toxic paint to reduce toxic small particles in the air.

Concerning warehouse design, many things have to be considered e.g. storm water, ventilation, appropriate flooring, on-site recycling and use sunlight for lighting and heating in a suitable way i.e. reduce sunlight effects in the summer (Yarra City Council, 2005; Doesburg et al., 2009). Daylight is one of the most

important lighting and heating resources in warehouses which may help reducing usage energy by reducing energy of artificial lighting up to 25%, if it is designed properly, i.e. allow winter sunlight enter into the warehouse and avoid sunlight during summer (US Department of Energy, 2002; Elsadig, 2005; Green Economy Guideline Manual, 2014). As well as, aisles and departments of warehouses have to be designed optimally to minimize time, congestion and facilitate material flow efficiently (Amjed and Harrison, 2013).

Heating, Ventilation and Cooling
Ventilation, heating and cooling has a significant importance in energy consumption which is about 10-13% of total energy consumption (E Source Companies, 2007; You, 2016 based on Madison Gas and Electric Company), and it is necessary to provide appropriate condition in place work environment.

In some times, natural ventilation systems can be used successfully by using outdoor climate which assists to reduce energy, cost and maintenance and replacement but there are some challenges e.g. difficulty in controlling high temperatures in summer and cold in winter, humidity cannot be controlled, inability to filter air and consume high amounts of energy in winter to condition the ventilation air (Engineering Guide Natural Ventilation, 2011). Therefore, using mechanical ventilation is required in some cases e.g. heating ventilation and air condition systems (HVAC). In order to obtain efficient energy in mechanical heating ventilation and air condition, it is necessary to use appropriate automatic control system which provides the service according to required dimensions, in needed time and in the necessary part of warehouse. This technology protects all equipment in warehouse from high temperature, humidity and the risk of condensation or freezing (Automatic controls in buildings, 2005). Shutting off unnecessary fan can save costs and for extra savings, the temperature should be minimized during the heating season when places are unoccupied by using automatic control or sensors (E Source Companies, 2007).

Artificial lighting system
Lighting consumes the highest rate of energy and the percentage of energy consumption varies depending on the type of warehouse and the nature of activities i.e. in the non–refrigerated warehouses, the lighting contributes to the highest energy consumption which is about 37-60% of total energy consumption (E Source Companies, 2007; SEDAC, 2011; You, 2016). There are different methods to reduce energy consumption which can save energy consumption between 30-70% of lighting energy (Cox and Graham, 2010):

Handling equipment
The movement of warehouse goods needs a range of mechanical equipment such as forklifts. The environmental effect of mechanical equipment can be eliminated by using forklifts which his engine runs on bio-diesel or hybrid fuel

combinations along with hydrogen fuel cell technology use battery-operated forklifts or works by electricity to reduce amount of emissions generated. As well as, use mechanical equipment with less noise. (Mallidis and Vlachos, 2010; TSMG, 2014)

Efficient water management
Water availability has been becoming a global issue because it is a main natural resource for ecosystem functioning and human life. To reduce water usage in the warehouses, use low-flow water fixtures or motion sensor faucets, save and use rainwater by using rain water conservation techniques and reuse grey water by using grey water systems to recycle water, thus decreasing the amount of fresh water required, and reducing the volume of wastewater produced. (The Energy and Resources Institute; Green Economy Guideline Manual, 2014)

Waste management processes
Waste management has become extremely necessary at the source because of increasing urbanization and land scarcity. Warehouses are one of the waste sources through packaging of goods. Hence, it has to be some processes to reduce waste by minimizing the amount of packaging which is used for each product, eliminating all hazardous materials of package, using package which is easy for recycling and doing recycle process onsite. These processes help to reduce cost and energy used to transport because of using less amount of package material and reducing waste going to landfills or minimize amount of material recycled (The Energy and Resources Inst; Green Economy Guideline Manual, 2014).

Green energy generation
Using renewable energy is one of the green warehouse dimensions to reduce emissions and create clean environment for instance using solar, thermal, solar photovoltaic, wind, biofuels, biomass (wood chips or other waste), geothermal resources and energy recovered from process waste such as heat from air compressors etc. (Deutsche Post AG, 2010). Using biodiesel and biogas to operate equipment is another opportunity for "greening" (Vida and Dunay, 2014).

Warehouse management system (WMS)
A warehouse management system (WMS), is a multi-tasking computer aided technological tool driven by computer application used to run day-to-day activity in any warehouse for example, from receiving of raw materials and unfinished good, stock monitoring, invoicing, logistics factors, metrics reporting, warehouse productivity and internal movements. (Palevich, 2012) WMS often uses Auto Identification and Data Capture (AIDC) technology, such as barcode scanners, mobile computers, wireless LANs (Local Area Networks) and Radio-frequency identification (RFID) to efficient control of products flow. WMS helps to run the operations effectively and efficiently by minimizing transaction error, help to maximize space utilization, reduce material handling, minimize

lead-time and gaseous emissions and inventory reduction (management) (WERC and supply chain visions, 2007; Poon et al., 2009). By adopting WMS concept, companies can help in preserving natural resources, maximize usage of energy, efficient labor productivity and costs, efficient process management and high quality customer services (Poon et al., 2009; TSMG, 2014). The importance of WMS in today's competitive scenario lies in the survival of the company in complicated circumstances, "It helps to bottlenecks, monitor current performance, perform comparative analysis, set future targets, benchmark against industry standards, perform simulations etc. Thus the warehouse future roadmap and strategic planning for achieving highest levels of economic, social and environmental performance is not possible without WMS" (Amjed and Harrison, 2013, 18).

Future warehouse strategy
If any company would like to improve itself, it has to take into account continuous improvement to its performance through for example monitor current performance, perform comparative analysis, set future targets, benchmark against industry standards, perform simulations and take green attitude into account to achieve optimal warehouse management system (Amjed and Harrison, 2013; Luu, 2016).

3. Conclusions and further research

This literature review was made for building the theoretical background of a further research to be conducted in Iraq, in order to explore how to develop Iraqi players of supply chain to be greener, to work in a more sustainable way.

The findings of this literature review are used to make checklists about green warehouse dimensions. The survey is to be conducted in three main types of warehouses of the General Company for Electrical Industries in Diyala, Iraq. The data is to be collected by using checklist, making interviews with the managers of warehouses, and doing real observations at warehouses. Data are to be analyzed through the results of checklists to find out percentage of applying and the gap size according to the results of checklists, which will give a brief assessment about the present circumstances and may give the outlines of the future applications.

References

[1] Al-Zaidi, W. A. H., Dunay, A. (2016), The role of re-use in reducing industrial costs: A case study in the general company for electrical industries, in Diyala, Iraq. Hungarian Agricultural Engineering, 29, 36-39. http://dx.doi.org/10.17676/HAE.2016.29.36

[2] Amjed, T W. and Harrison, N J. (2013), A Model for Sustainable Warehousing: From Theory to Best Practices, conference paper, Macquarie Graduate School of Management, Australia.

[3] Baker, P. and Marchant, C. (2015), Reducing the environmental impact of warehousing. In Green Logistics: Improving the environmental sustainability of logistics. McKinnon, A., Browne, M., Piecyk, M. & Whiteing, A. (eds) pp 194-226. 3rd edition. Kogan Page Limited. London

[4] Cox, S. and Graham, L (2010), Sustainability Measured: Gauging the Energy Efficiency of European Warehouses, ProLogis Research Reports, http://uli.org/wp-content/uploads/ULI-Documents/GP-Sustainability-Measured.pdf

[5] Deutsche Post AG (2010), Towards Sustainable Logistics: How Business Innovation and Green Demand Drive a Carbon-Efficient Industry http://www.dhlusa.com/content/dam/downloads/g0/logistics/green_logistics_sustainable_logistics_study_en.pdf

[6] Doesburg, R. V. Baptist, P and Heijst, W. V. (2009), Supply Chain Management Warehousing report, Capgemini Consulting is the strategy and transformation-consulting brand of Capgemini Group. https://www.uk.capgemini.com/resource-file-access/resource/pdf/tl_Warehousing_report_2009.pdf

[7] E Source Companies (2007), http://bea.touchstoneenergy.com/sites/beabea/files/PDF/Sector/Warehouses.pdf.

[8] Elsadig, A. K. (2005), Energy Efficiency in Commercial Buildings, maser thesis, Faculty of Engineering, University of Strathclyde, http://www.esru.strath.ac.uk/Documents/MSc_2004/elsadig.pdf

[9] Eltayeb, T. K., Zailani, S. and Ramayah, T. (2011), Green supply chain initiatives among certified companies in Malaysia and environmental sustainability: investigating the outcomes. Resources, Conservation and Recycling 55 (5), 495-506. http://dx.doi.org/ 10.1016/j.resconrec.2010.09.003

[10] Engineering Guide Natural Ventilation, (2011), https://www.priceindustries.com/content/uploads/assets/literature/engineering-guides/natural-ventilation-engineering-guide.pdf

[11] Gábriel, M. (2016), Green Supply Chain Management - Motivation, Methods and Expectations - in Hungarian Automotive OEMs, Theory Methodology Practice 12:(01) pp. 37-45.

[12] Green Economy Guideline Manual (2014), Iskandar Regional Development Authority (IRDA), Malaysia.

[13] Illés, B. Cs., Dunay, A., Vida, A. (2013), Position of Hungary on EU's Map of Renewable Energy Sources. In: Dermol, V.; Trunk Sirca, N.; Dakovic, G. (Eds.) Proceedings of MakeLearn International Conference 2013, 19–21 June 2013, Zadar, Croatia, 1397-1405. Bangkok; Celje; Lublin: ToKnowPress

[14] Lambert, D. M, and Stock, J. R. (2001), Strategic Logistics Management, McGraw-Hill, New York.

[15] Luu, M. (2016), Developing the implementation of green warehousing at IKEA Finland, International Business, Thesis, University of applied sciences.

[16] Mallidis, I. and Vlachos, D. (2010), A Framework for Green Supply Chain Management, 1st Olympus International Conference On Supply Chains, 1-2 October, Katerini, Greece.

[17] McKinnon, A., Browne, M., Whiteing, A. and Piecyk. (2015), Green Logistics, 3rd edition, Kogan Page, London

[18] Kumar, S., Teichman, S. and Timpernagel, T. (2012), A green supply chain is a requirement for profitability. International Journal of Production Research 50 (5), 1278–1296. http://dx.doi.org/10.1080/00207543.2011.571924

[19] Mesjasz-Lech, A. (2015), Logistic Determinants of the Freight Transport by Road Development in Poland, 17th International Conference on Transport Science, Portoroz, Slovenia

[20] Miskolcziné Gábriel, M. (2017), Complex analysis of Green Supply Chain Management in Hungarian automotive industry. Theses of doctoral (PhD) dissertation, Szent István University, Gödöllő

[21] Mulder, S. (2013), Sustainable warehousing: An empirical research at Unilever on building options and collaboration models in sustainable warehousing, master thesis, University of Twente.

[22] Palevich, R. (2012), The Lean Sustainable Supply Chain: How to Create a Green Infrastructure with Lean Technologies, Printed in the United States of America.

[23] Penny, M. N. (2009), Sustainable Supply Chain Logistics Guide, Metro Vancouver
http://www.buysmartbc.com/_Library/Resources/resource_metrovancouver_supply_chain_guide.pdf

[24] Poon, T. C., Choy, K. L., Chow, H. K. H., Lau, H. C. W., Chan, F. T. S. and Ho, K. C. (2009), A RFID casebased logistics resource management system for managing order-picking operations in warehouses, Expert Systems with Applications, Vol. 36(4), p. 8277-8301.

[25] Prabhu, P. and Dhawan, M. (2010), Green logistics, Tata Consultancy Services Limited.
http://www.tcs.com/SiteCollectionDocuments/White%20Papers/CPG_WhitePaper_Green_Logistics_08_2010.pdf

[26] Rajuldevi, M. K., Veeramachaneni, R. and Kare, S (2008), Warehousing in theory and practice: A case study at ÖoB, Clas Ohlson, Stadium, Åhlens, Master thesis, University College of Borås, School of Engineering.

[27] Roy, M. (2010), Green warehouse, Ashrae Journal, Artical American Society of Heating, Refrigerating and Air-Conditioning Engineers. file:///C:/Users/firas/Downloads/ASHRAE-D-AJ10Mar05-20100301.pdf

[28] Seroka-Stolka, O. (2016), Green Initiatives in Environmental Management of Logistics Companies. Transportation Research Procedia, Vol.: 16, pp. 483-489., DOI: 10.1016/j.trpro.2016.11.045

[29] Skowron-Grabowska, B., (2009), Performance measurement in logistics centers, Advanced Logistic systems, 3(1) p. 213-218

[30] Sturge, K. (2008), Logistics Property Today. Spring 2008 edition.

[31] Tata Strategic Management Group (TSMG) (2014), Green Logistics, Confederation of Indian industrial.
http://www.ciischooloflogistics.com/downloads/logsecrep/GreenLog.pdf

[32] The Energy and Resources Institute, Design of Green Warehouse http://www.teriin.org/upfiles/projects/ES/ES2013BS05.pdf.

[33] US Department of Energy (2002), Technology fact sheet on efficient lighting strategies.
http://www1.eere.energy.gov/buildings/publications/pdfs/building_america/26 467.pdf

[34] Vida, A., Dunay, A. (2014), Az energetikai szempontból önellátó mezőgazdasági vállalkozás ökonómai szempontú vizsgálata – különös tekintettel a biogáz-előállítás lehetőségére. Animal Welfare Ethology and Housing Systems 10:(1) pp. 32-38. (2014)

[35] World Economic Forum (2009), Supply Chain Decarbonization: The Role of Logistics and Transport in reducing Supply Chain Carbon Emissions. http://www3.weforum.org/docs/WEF_LT_SupplyChainDecarbonization_Rep ort_2009.pdf Accessed: 10 November 2016.

[36] Yarra City Council (2005), Sustainable Design Guidelines: Warehouse conversion.
file:///C:/Users/firas/Downloads/Sustainable%20Design%20Guidelines%20- %20Warehouse%20Conversions.pdf

[37] You, T. (2016), Warehousing: Understanding the fundamentals and discovering innovative technological solutions for environmentally and economically improved management, University of Applied Sciences.

[38] Zhu, Q., Sarkis, J., Lai, K (2012), Examining the effects of green supply chain management practices and their mediations on performance improvements. International Journal of Production Research 5 (50), 1377-1394

Lean supply chain management practices in iraqi mineral water producing factories

A. DUNAY[1], F. A. SHABAN[2]

[1]Department of Business Economics and Management,
Faculty of Economics and Social Sciences, Szent István University
Páter K. u. 1., Gödöllő, H-2100, Hungary
[2] Amedi Technical Institute, Duhok Polytechnic University
Duhok 42001 , Kurdistan region, Iraq

Abstract

The main purpose of the study is to examine availability of Lean Supply Chain Practices in mineral water producing factories in Dohuk province, Iraq. The correct determination of the situation of supply chains of the investigated factories will show us the most important challenges faced when applying Lean Supply Chain Management practices. The survey was prepared through field visits and personal interviews with managers of factories. The checklist method was used as a main tool for data collection, and through certain statistical procedures, the reality of the efficient supply chain management practices and the challenges of their application in the investigated factories were identified.

Keywords

Lean Supply Chain, mineral water industry, Supply Chain Management, Iraq

1. Introduction

The 21st century is the most challenging for operation management in different organizations; advanced technology has generated advanced information systems that have contributed to the development of means of communication, transportation and logistics, and makes industries faster and more efficient. Competition challenges and government legislations increased the pressure on organizations to adopt modern conceptions in their practices. Today's world has turned to the apply Lean Supply Chain Management (LSCM) as the modern frontier in contemporary organizations and guarantees the way to remain competitive due to its ability to provide products with high quality and reduce waste in all activities (Hezbon, 2016). LSCM is a possible strategy that organizations can utilize to coordinate themselves internally or with other organizations, to attain efficiency, eliminate waste and create value in products (Daud and Zailani, 2011). Borac et al. (2010) explained this interest to the LSCM as it avoids all parties involved in the supply chain, from manufacturers, distributors, suppliers, wholesalers, and service providers from the extreme

pressures on them to reduce costs and time and to achieve the balance of inventory levels to meet the requirements of their customers constantly. Therefore, LSCM has emerged as an efficient management approach that helps organizations to provide better value to the customer by responding efficiently to their requirements and needs and to achieve competitive advantage (Sezen and Erdogan, 2009).

Womack and Jones (2003), mentioned that Japanese at Toyota used the Lean concept at the beginning of the 19th century and used it basically in production processes called the Toyota Production System. The word "Muda" in Japanese means waste, which is one of the most important words that managers of Japanese organizations are afraid of. It means any activity that consumes resources without adding value. Some authors mentioned that Japanese considered that Lean thinking is the best solution to solve the waste problem, and the concept can be used with supply chains (Vajna and Tangl, 2017; Womack and Jones, 2003). Slack et al. (2010) and Tangl and Vajna (2016) asserts that the concepts, thoughts and techniques of Lean concepts can be applied to all components of supply chain, although they are described as applicable to individual activities and processes but can be applied to supply chain as well.

Johansson (2010) defined LSCM as a network of activities through which products flow seamlessly through supply chain to provide value-added to customers by meeting their requirements with no waste and errors along the chain. While Kovac (2013) defined LSCM as a set of interconnected organizations that contribute to the flow of materials from their supply sources to their beneficiaries and at the same time, reduce costs and waste through the adoption of the drawdown system. Nowakowska-Grunt (2008) highlighted the role of lean management in logistics infrastructure of enterprises, while Ulewicz and Kuceba (2016) identified the main problems of implementing Lean concept in the SME sector.

2. Principles and practices of lscm

The change from a traditional supply chain to Lean requires application and adherence of Lean principles that will be implemented through a set of practices to achieve improvements in supply chain and organization. These practices support a set of techniques which ultimately contribute to generate Lean activities along in supply chain (Yala, 2016). Authors frequently emphasized that there is a difference between principles, practices and techniques and tried to separate them from each other. However, because of the linkage between the three terms, it is difficult to separate from each other, especially practices and techniques. Many writers use practices and techniques interchangeably in their studies (Ugochukwu, 2012).

The Lean principles, practices and techniques were able to make organizations more flexible, efficient and competitive. The benefits obtained from the concept stimulated managers to adopt in the entire supply chain including suppliers, distributors, producers, customers and all stakeholders, which necessitated

improvement of the internal organization's business environment. Logically, we cannot apply the concept without having lean suppliers to ensure the success of the application process. Behrouzi and Wong (2011) and Afonso and Cabrita (2015) have worked to address these requirements (principles, practices, and techniques). Their opinion show that the difference between Lean principles, practices and techniques are existing, but they are interdependent and complementary to one another. If the organization wants to apply them, it must be apply gradually, because we cannot have lean practices or lean techniques without a principle. Mainly, there is adherence to the principles first and then converted to a set of practices and then use appropriate techniques.

Many authors have addressed the principles of the LSCM and have confirmed what Womack and Jones (2003) are first formulated and defined it with five principles.

Table 1. LSCM practices

Authors	LSCM practices
Daud and Zailani (2011)	Demand management, Standard, Waste Management, Organizational Behavior.
Ugochukwu (2012)	Sources information about customer needs, Value chain analysis and end customer focus, Value chain analysis , Waste reduction , System Organization , Strong and effective relationship , Waste reduction , Production of exact customer needs only when needed, Strong and effective relationship , Problem search , Problem solving.
Mutheke (2014)	Demand management, Standard, Waste Management.
Farah (2015)	Demand management, Standard, Waste Management, Behavior change.
Rahman, et al. (2016)	Customer and staff participation, Suppliers' Relationship, continuous improvement, Eliminate waste, 5S.
Onyango (2016)	Sources of information about customer needs, Value flow analysis, Eliminate waste, relationships with customers and suppliers, Find the problem and resolve the problem, 5S.
Yala (2016)	Demand management, standard, waste minimization, organizational behavior, collaboration across the organization.
Hezbon (2016)	Total Quality Management, Demand Management, Continuous Improvement, Business Excellence.
Tortorella, et al. (2017)	Relationships with customers and suppliers, Logistics Management, Waste Management, Continuous Improvement, Commitment of top management.
Abdullah and Jabr (2017)	Cultural change, Operations' Standard, Industrial' Standard, Relationship with suppliers, Eliminate waste.

Source: Authors' own summary

The authors who agreed with this proposition are Bicheno and Holweg (2009); Johansson (2010); Ugochukwu (2012) and Kumar et al. (2015). The five principles are: value determination from the point of view of the customer, value flow and continuous value flow, depend on withdrawal system and the perfection

in work. In relation to LSCM practices, Daud and Zailani (2011) note that the authors described LSCM practices as "common practices, good practices, best practices" and there was no agreement between the authors on these practices. Table 1 illustrates the views of some authors on LSCM practices.

Demand management is focusing on the concept, that product demand is a feature of the LSCM strategy, so managing it properly avoids organization waste and overwork, a negotiable final product, and the accuracy of these signals may enrich the need to predict (Ventana Research, 2007).

Elimination of waste: The philosophy of Lean includes the elimination of all types of waste and applied in the LSCM for this purpose, and the waste is defined as any activity which does not add value. Studies show that only 5% of the total production time is directly consumed to add value, (95%) of the remaining time of production add costs to the goods or service, this percentage shows the percentage of hidden waste within the various operations, whether in the product or service (Slack et al., 2010). Proper diagnosis of waste is the first step to eliminate it. Most writers agree that there are seven types of waste: Farah (2015) and Lotfi (2015) mentioned overproduction, waiting time, transportation, excess operations, storage, movement, defects.

Standardization: It is an important practice of LSCM and an integral part of the Total Quality Management System is to make the activities of supply chain consistent and frequent by providing a consistent and acceptable approach by all the partners in the chain, and working to unify all processes or activities related to the performance of the series.

Standard operations of supply chain activities reduce or eliminate duplication of processes or activities that do not add value to the organization and customers, starting from the entry of raw materials to the delivery of products to customers (Abdullah and Jabr, 2017). The standardization of the process allows continuous and smooth flow of activities across the supply chain, reducing complexity, it is a continuous movement of information and raw materials received from suppliers regularly (Illés and Szuda, 2015).

Relationship with suppliers: LSCM's philosophy of the modern suppliers is different from that of the previous suppliers. The relationship was characterized by distrust and competition to maximize profits at the expense of the other party. LSCM now encourages cooperation and partnership through which many of the ideas can be achieved such as withdrew system, JIT system, reduce costs and eliminate waste, and LSCM contributes to strengthening cooperation with suppliers through the participation of suppliers in the design and development of the organization's products, motivating and encouraging them to improve themselves as partners and part of the LSCM, thus exchanging information and making contacts continuously between them (Ugochukwu, 2012).

Customer relationship: The relationship with customers refers to a set of activities or practices aimed to identify customer needs and his current and expected wishes, and carrying out all procedures to manage the customer complaint, and provide products to him at low cost and appropriate quality, and to build long relations with him to reach the satisfaction level. According to Onyango (2016), obtaining information from customers and building relationships with

them contributes greatly to identify their needs and accurately reducing the waste resulting from providing wrong or undesirable products, and assuring that a good understanding of customer requirements contributes to the adoption of correct practices, building and developing a lean supply chain, so that reliance on assumptions, forecasting and prediction may lead to incorrect results.

3. Material and methods

The research problem was to answer the following question: Can the practices of lean supply chain be applied in mineral water factories in Duhok Governorate? For data collection, on-the-spot visits were conducted in three factories in Duhok governorate. Interviews were conducted with factory managers to determine the nature of their supply chains. Checklist method was used as a main tool for data collection. Methodology described by Babu (2016) and Zaman (2012) were used in formulating the checklist paragraphs of this study. Triple scale was used in checklists to diagnose LSCM practices. The weights of the scale were distributed in descending order from the highest weight to the lowest weight: Applied = 2, Applied to some extent = 1, Not Applied = 0.

To test the research question, the study used the following methods:
1. Calculating the approximate rate of the extent of conformity by the following equation:

$$\text{Weighted Mean} = \frac{\sum Wf}{\sum f} \quad \text{where W= weight; f= frequency} \quad (1)$$

2. Calculating the extent of conformity (corresponding with instructions) through the following equation:

$$\text{The percentage of application} = \frac{\text{Weighted Mean}}{2} *100 \quad (2)$$

3. Calculating the size of the gap through the following equation:

$$\text{The size of the gap} = 1 - \text{Percentage of the extent of application} \quad (3)$$

4. Research results

This part of the study shows the diagnosis results of LSCM practices at Mazi, Gara, and Zalal factories for mineral water production in Duhok / Iraqi Kurdistan Region. Table 2 summarizes the checklist questions prepared to determine the LSC practices of factories and the results of the survey, to what extent they are matching with LSCM practices to identify percentage of match and the gap as shown below.

Table 2. Diagnosis results of LSCM practices in the surveyed companies

Practices		Questions (checklist)	Mazi			Gara			Zalal		
			2	1	0	2	1	0	2	1	0
Demand Management	1	Factory manages demand and invests time and money in achieving it.	✓				✓		✓		
	2	Factory uses appropriate demand management techniques such as forecast and withdrew system.		✓			✓			✓	
	3	Factory connects its customers' requests to all parties in the supply chain.	✓			✓				✓	
	4	Demand management in our Factory is accurate and there has never been an increase in production over the required supply.	✓				✓			✓	
Waste Management	5	Factory seeks to eliminate all kinds of waste in the supply chain.	✓			✓			✓		
	6	Factory was able to determine all kinds of waste in the supply chain.	✓			✓			✓		
	7	Factory uses appropriate techniques to treat waste during supply chains such as JIT, 5S, and withdrew system.		✓			✓			✓	
	8	Factory promotes continuous improvement as base for eliminating waste.		✓			✓		✓		
Standardization	9	Factory uses standard processes (production, transport and storage) during its supply chains.	✓			✓			✓		
	10	The techniques used by the factory help in simplifying the operation of their supply chains.	✓				✓			✓	
	11	The factory uses raw materials and standard spare parts in its products, especially in packaging process.	✓			✓			✓		
	12	The factory encourages quality control activities throughout the supply chain.	✓				✓			✓	
Relationship with Customers	13	Factory seeks to build long term relationships with its suppliers.		✓			✓			✓	
	14	Factory deals with a few suppliers.	✓			✓			✓		
	15	Factory deals with suppliers based on standards of trust and common interest not on price basis.	✓			✓			✓		
	16	Our suppliers have high flexibility to process orders without any delay.	✓			✓				✓	
Relationship with Suppliers	17	Factory seeks to build long-term relationships with its customers.	✓			✓			✓		
	18	Factory uses appropriate tools and techniques to manage its relationship with its customers.		✓			✓			✓	
	19	We have ongoing contacts with customers and use them to address issues (delivery, waiting, quality).	✓				✓		✓		
	20	Factory seeks to know the needs of customer and determine the value of it and handling of complaints to achieve customer satisfaction.	✓				✓		✓		
		Weights	2	1	0	2	1	0	2	1	0
		Frequencies rate (responses)	15	5	0	9	11	0	11	9	0
		Weighted result	30	5	0	18	11	0	22	9	0
		Weighted Mean	1.7			1.4			1.5		
		Corresponding with the instructions (%)	85			70			75		
		The size of the gap (%)	15			30			25		

The results of Table 2 indicate that the investigated factories obtained varying percentages in the application of the LSCM practices. Mazi obtained the highest percentage of matching which is (85%) while the gap reached (15%). Zalal factory obtained a similar percentage of (75%) size gap (25%), and the lowest percentage of matching is Gara Factory by matching (70%) with (30%) of gap size. We noted that the percentages of match with LSCM practices are high and 70% is the lowest in all investigated factories. Many authors note that the accepted compliance ratio is 66.6 in administrative studies (Sulaiman, 2002).

The answer to the research question 'Can Lean Supply Chain Management practices be applied to the mineral water factories in Duhok Governorate?' is yes, these practices are applicable based on the experiences of the examined factories.

The high ratios to conform to the LSCM practices of the investigated factories represent strengths through the following actual practices:
- Care of factories to eliminate waste and identify all types of waste.
- The nature of mineral water production processes using standard processes.
- Having strong relationships with sales agents.
- Dealing with a few suppliers and the base of dealing is trust and respect, not price.

While the size of the gap refers to weaknesses which can be considered obstacles in some practices:
- Inability to confirm actual demand, resulting in excess production, storage and excess costs.
- Lack of full awareness of techniques that can be used with each practice of LSCM.
- Although few suppliers are dealt with suppliers are contracted for periods not to exceed one year due to unstable political and economic conditions in the area.

Conclusions

This study is an attempt to determine the extent of the ability of some mineral water production factories in Duhok governorate/ Kurdistan Region of Iraq to adopt LSCM practices by identifying the reality of their actual practices. The study illustrated possibility of applying LSCM practices to achieve a higher ratio of (66.6), which is acceptable in administrative studies, although there are some weaknesses or obstacles such as lack of knowledge of actual demand in the future, difficulty of long term contracts with suppliers and lack of knowledge of techniques to be used with each practice of LSCM practices.

The results of this study can be applied at all other mineral water factories working in the Iraqi Kurdistan Region due to similar production processes and supply chains and similarity of external environment in which they operate. This study suggests more emphasis on those practices that have not been applied and which have been weaknesses, and try to determine appropriate methods to

address them through conducting studies to determine the causes and methods of treatment.

References

[1] Abdullah, A. and Jabr, Q. (2017), Adoption of lean supply chain practices in improving the organization's response to its customers. Tikrit Journal for Administration & Economics Sciences (2) 38, pp. 10-39.

[2] Afonso, H. and Cabrita, R (2015), Developing a lean supply chain performance framework in a SME: A perspective based on the balanced scorecard. Elsevier Procedia Engineering 131 (2015) 270 – 279.

[3] Babu, O. F. (2016), Lean Supply Chain Management performance and organization performance of Cement Manufacturing Companies in Kenya: A case study of Bamburi Cement. Master thesis, School of Business, University of Nairobi

[4] Behrouzi, F. and Wong, K. (2011), An investigation and identification of lean supply chain performance measures in the automotive SMEs. Scientific Research and Essays Vol. 6(24), pp. 5239-5252.

[5] Bicheno, J. and Holweg, M. (2009), The Lean Toolbox: The essential guide to lean transformation. 4th ed. Buckingham: PICSIE Books.

[6] Borac N., Milovanovic G. and Andjelkovic A. (2010), Lean Production and Six Sigma Quality in Lean Supply Chain Management. Ministry of Science and Technological Development of the Republic of Serbia

[7] Daud, A. and Zailani, S. (2011), Lean Supply Chain Practices and Performance in the Context of Malaysia . www.intechopen.com

[8] Farah, M. (2015), Lean Supply Chain Management Practices and organization performance in the public water sector in Kenya. Master thesis, School of Business, University of Nairobi

[9] Hezbon, K. O. (2016), Lean Supply Chain Management and Operational Performance of Almasi Beverages Company limited . Master thesis, School of Business, University of Nairobi

[10] Illés, B. Cs. and Szuda, Cs. (2015), Quality in manufacturing - is a management tool? In: Dunay (ed.) Proceedings of the 5th International Conference on Management 2015. Szent István University Publishing House, Gödöllő, pp. 126-129.
http://dx.doi.org/10.17626/dBEM.ICoM.P00.2015.p023

[11] Johansson, E. (2010), Can lean be mean? A study of negative consequences of lean in supply chains. Master's Thesis in Business Administration, Blekinge School of Management

[12] Kovac, M. (2013), Lean Supply Chain Management. Transfer innovation. Milan.Kovac@tuke.sk

[13] Kumar, R., Kumar, V. and Singh, S. (2015), Managing the Utility of Manufacturing Process Facilities through Lean Supply Chain. ADR Journals; 2(1): 13-23.

[14] Lotfi, M. (2015), Disentangling Resilience, Agility and Leanness: Conceptual Development and Empirical Analysis. (Unpublished Doctoral thesis, City University London)

[15] Mutheke, M. L. (2014), Lean Supply Chain Practices and Supply Chain responsiveness among Vegetable oil processing Firm in Kenya. Master thesis, School of Business, University of Nairobi

[16] Nowakowska-Grunt, J. (2008), Impact of Lean Management on Logistics Infrastructure in Enterprises. Advanced Logistic systems, 2(1), 71-74.

[17] Onyango, S. A. (2016), Lean Supply Chain Management Practices and Business performance of the state corporation in the Ministry of Health. Master thesis, School of Business, University of Nairobi, Kenya

[18] Rahman, A., Ismail, N. and Ariffin, Z. (2016), From Green to Lean: Firms' Waste Management Practices and Their Impacts on Business Performance. Pertanika J. Soc. Sci. & Hum. 24(S) pp. 29-46.

[19] Sezen, B. and Erdogan, S. (2009), Lean Philosophy in strategic Supply Chain Management and Value Creating. Journal of Global Strategic Management Vol.3. No.1.68-73.

[20] Slack, N. C. and Johnston, R. (2010), Operation Management. Sixth Edition, prentice Hall

[21] Sulaiman, H. (2002), Total Quality in the Evaluation of University Performance. Master thesis, Faculty of Administration and Economics, University of Mosul, Iraq

[22] Tangl, A. and Vajna, I. (2016), Lean-Kaizen Tools for the Accounting System and the Decision Making Process. In: Bylok and Tangl (eds.): The role of management functions in successful enterprise performance. Agroinform, Budapest, pp. 159-170. DOI: 10.18515/dBEM.M2016.n01.ch14

[23] Tortorella, G. L., Miorando, R. F. and Fries, C. E. (2017), Lean Supply Chain: empirical research on practices and performance. Proceedings of the International Conference on Industrial Engineering and Operations Management Rabat, Morocco, April 11-13, 2017.

[24] Ugochukwu, P. (2012), Lean in the supply chain: research and practice. Master Thesis, Department of Management and Engineering, Linkoping University

[25] Ulewicz, R. and Kuceba, R. (2016), Identification of Problems of Implementation of Lean Concept in the SME Sector. Economics and Management 8(1), pp.19-25. DOI: 10.1515/emj-2016-0002

[26] Vajna, I. and Tangl, A. (2017), The Lean effect of the 5S and standard work development in different automated machine process standardization. pp. 67-74. In Illés et al. (eds): Management and Organization: Concepts, Tools and Applications. Pearson, Harlow. DOI: 10.18515/dBEM.M2017.n02.ch06

[27] Ventana Research (2007), Strategies to Run a Lean Supply Chain. www.ventanaresearch.com

[28] Womack, J. and Jones, D. (2003), Lean Thinking; Banish waste and create wealth in your Corporation. Simon and Schuster, New York, NY 10020

[29] Yala, J. O. (2016), Lean Supply Chain Management Performance Practices and Operation Performance of the Manufacturing Firm in Kenya. Master thesis, School of Business, University of Nairobi

[30] Zaman, K. A. (2012), A Fuzzy TOPSIS Based Multi Criteria Performance Measurement Model for Lean Supply Chain. Master thesis, Science & Engineering Faculty Queensland University of Technology (QUT) Brisbane, Australia

Overview of the theories of integration into other cultures

I. RUDNÁK, K. BAJKAI-TÓTH, Y. WANG

Head of Department, Associate Professor, Trainer-Consultant,
Institute Deputy Director of Communications and Relations
Department of Communication Science, Social Sciences and Teacher Training Institute
Faculty of Economics and Social Sciences, Szent Istvan University

Keywords

multiculturalism, culture shock, competencies,

1. Introduction

Culture shock is a very real experience for many people who move to another country. Anyone who has lived or studied or even travelled extensively in another country has tasted and lived through some level of culture shock. At the time it may feel more like homesickness, but what most people who haven't undergone any kind of adaptation program don't know are the stages one goes through when adjusting to a new language, country and culture.

When comes to a totally new environment, people always must face unpredictable shock and pressure. From this thinking, anthropologists first began to study the issue about cultural adaptation firstly. In this process, there exists many influential cultural adaption theories.

2. Trans-cultural adaption research in early stage

In the earlier time of twentieth century, Park (1923) and Stonequist (1937) has deepen the conclusion that sojourner who were between two cultural boundaries which may cause by intermarried, or because they were born and live in different place, can be claiming to belong to both cultures. Park argues that marginalization may lead to psychological conflict, which may conduct to a double personality, or even personality disorder. Stonequist argues that marginalization has both sociological and psychological attributes: sociological attributes contain immigration factors, racial (biology) distinctions and advantages of culture and inferior culture with the same place. At the same time, Tsung-Kao Yieh (1934) made a deep study on a series of questions about the cultural adaptation among Chinese graduate students in American universities. These scholars are pioneers in cross-cultural adaptation.

In 1936, American Anthropological Society assigned Robert Redfield, Ralph Linton and Melville Herskovits (1936) to be responsible for a cross-cultural

adaptation research. After one year's efforts, the group finish a report and give a clear definition of cross-culture adaption: cross-culture adaption is a kind of phenomenon that some group or two sides change its way due to a continual and direct contact among different cultural group. The report also categorizes different topics and areas of cross-cultural adaptation research, laying the foundation for this research.

3. Classical linear theory model

Culture adaption means when people come from different culture background live with each other, the change of culture model may bring to them. Although this phenomenon has existed for a long time since ancient time, however, a systematic and scientific research only started at the beginning of 20 century. Since that, cultural transaction has been developed rapidly. Many researchers had made great devotion in cross-cultural adaption research, and promoted a big number of theoretical model. For example, the U-curve hypothesis which is put forwards by Lysgaard (1955). Oberg's culture shock model (1960) Adler's cultural transition model (1975), culture assimilation (Gordon, 2008). All these theories are support the basic phases of culture transaction: Honeymoon period, crisis period and adaption period. For example, such as Park (1929), Yieh (1934), Stonequist (1935). In 1936, American anthropologist Redfield, Linton and Herskovits published an important thesis and first defined the concept of culture adaption, and relevant research topic, research method, which may lay the foundation for further culture adaption research. After the World War II ,with more and more people choose to live or study abroad. It helped put forwards the culture adaption research in some degree. Especially the U-curve hypothesis which is promoted by S. Lysgaard. The process of cultural adaptation appears to be a U-curve based on the different satisfaction of acculturation (from high to low, and then to high again). Except for U-curve hypothesis, if sojourners return to motherland, they will also go through a similar process of cultural adaptation. Moreover, Gullahorn (1962) extended to U Curve Hypothesis "double U Curve Hypothesis", or it can also be called "W-curve hypothesis". Gullahorn and his wife focus on the study of the U-curve hypothesis, and put forwards a new version on the base of that---the W-curve assumption. This W-curve hypothesis describes the culture adaption problem when people come back to their motherland after a long time stay abroad. In fact, most people will suffer culture shock when they back to their country, and this kind of shock can be called as "reverse culture shock". This theory can explain the shock phenomenon the dwellers back to their country.

The U-curve hypothesis echoes with culture shock theory which is put forward by Oberg. In fact, when Oberg first come Brazil, as the new comer, he found a general phenomenon about the culture adaption symptom and a series of specific behaviour and attitude towards new life and environment. And on behalf of this, Oberg put forward this theoretical assumption. This hypothesis is a kind

of echo of another theory culture shock hypothesis. He is famous for putting the "culture shock" conception into all circumstance for people who live in another country. In 1960, Oberg thinks, "Culture shock might be called a normal acculturation disease of people who have been suddenly transplanted abroad. Like most ailments, it has its own symptoms and cure." From the opinion of view, the whole culture adaption procedure can be divided into three phases: initial adjustment, crisis, regained adjustment. And the whole phases can have combined as a U curve on behalf of degree of culture adaption.

Gordon thinks the process of culture assimilation can be divided into seven types, and those types can be used to explain the whole process of how the foreigners adapt American society. The types can be shown in chart 1.

Table 1. Gordon's types

Assimilation Type	Specific performance
Cultural/Behaviour assimilation	Learning to accept typical characteristics of mainstream culture
Structural assimilation	Establish formal relationship with mainstream community members
Identity assimilation	Have sense of belonging for the mainstream culture
Intermarriage assimilation	Get married with local people
Accepting attitudes assimilation	Take no prejudice towards mainstream culture and mainstream group
Accepting behaviour assimilation	Do not have prejudice
Civility assimilation	Do not have value or power conflict with mainstream society

Gordon thinks cultural or behaviour assimilation will appear at first time, but other types may not show up later which are shown in the chart. In contract, Structural assimilation may lead to other kind assimilation.

Adler's (1975) cultural transition model is another version of U-curve model, which detailed separate it into 5 phases: contact, disintegration, reintegration, autonomy, and independence. The five phases may happen one by one, and the bound between two phases is vague and is gradually moving from one to another, which means one phase can't change into another phase immediately.

All theoretical models which mentioned above are characterized by different phases of cross-cultural transaction, belonging to linear analysis, but it is not enough to fully explain the complexity of cross-cultural transaction totally. This kind of models simplify the process of cross-cultural transaction, and only focus on the cultural transformation for individuals, but ignoring the individual's impact on culture.

4. Classical non-linear theory model

John W. Berry (1980) put forwards a trans-culture adaption model. According to different attitude of cultural sojourners, cross-culture adaption can be divided into the following 4 kinds:

Table 2. Berry's model

	Keep initial cultural identity (YES)	Keep initial cultural identity (NO)
Keep good relationship with local community (YES)	Integration	Assimilation
Keep good relationship with local community (NO)	Isolation/Rejection	Marginalization

Berry's "cross-cultural adaptation model" is based on the degree of keeping culture, which means the degree of how an individual attaches importance to and the degree that they willing to hold the original cultural identity and to what extent access to the culture of the place of residence. Moreover, the principle of cultural retention can be introduced as follows: "Cross-cultural adaptation model" to establish the basis of the two questions:
  – Are you willing to maintain initial cultural identity and cultural identity?
  – Are you willing to establish and maintain a good relationship with local community?

According to John W. Berry's cross-cultural adaptation model, it suggests that travellers can choose to accept residential culture or not, and maintain or abandon the original cultural identity. The model belongs to the two-dimensional model, focusing on the two-dimension influence between the occupant and the guest culture. In addition, Berry put forward the theory of "cultural adaptation pressure" about psychological problems that may arise from occupants (Berry, 1990: 247). The degree of cultural adaptation is influenced by the number of adaptation experiences and the source of stress, but the three are probabilistic rather than inevitable (Berry, 1990: 247). The pressure of cultural adaptation is only possible companion in the process of cultural adaptation (Berry, 1990: 252).

As mentioned above, cultural adaptation problem is a kind of state, but it can also be understood as a process (Ward, 1996: 124). Ward founded the "Cultural Adaptation Process Model" to summarize the process of cultural adaptation and its various dimensions. (Figure 1.)

This is a systematic induction and synthesis of existing cross-cultural adaptation theory models. After combining theory with reality, it can be applied widely. For example, students who are enrolled in foreign universities have the need to accept culturally appropriate targeted training, which can be combined

with this model. But it also cannot say that the model has the best universality, because it is difficult to be falsified, at the same time, it is also difficult to be confirmed.
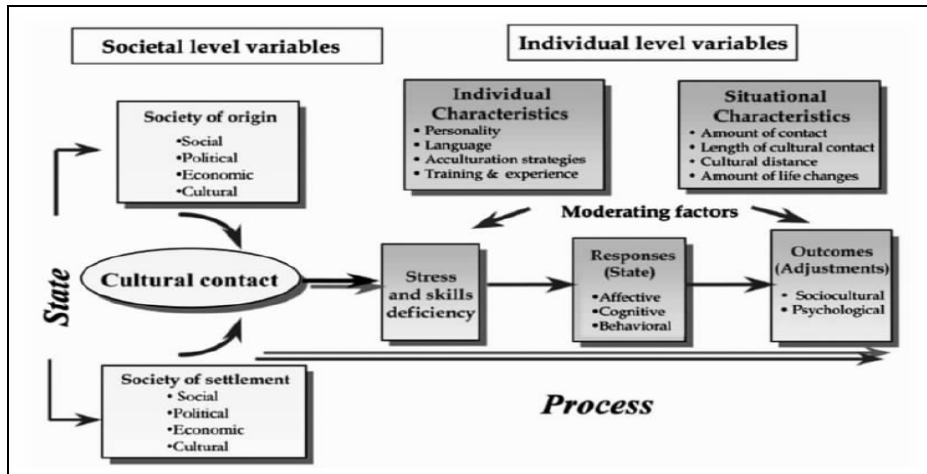

Figure 1. Ward's model

5. Analysis of current situation and influencing factor

Spradley and Philips (1972) identified 33 life events to explain the internal structure of cross-cultural adaption, which includes food, language, recreation, pace of life, and the degree of love and kindness. Furnham and Bochner (1986) take the difficulties which brought by the social changes into account, and to assess sojourners' cultural adaption by difficulties which may lead by the local environment or the change of social situation lead by contacting with local people. For example, how to deal with close relationships, how to treat the assessment by local people of different social status, how to establish friendship, participation in public events, handling of general events (such as taking local public transport and eating at restaurants) and so on. Due to the complexity and diversity of the internal structure of social and cultural adaptation, it has not yet formed a unified structure. However, many studies have shown that the general socio-cultural adaptation structure will contain some common factors, such as diet, language, communication, communication, cultural awareness.

The previous studies show that the factors which may influence the process of social and cultural adaptation mainly include: the time of contacting a new culture; the knowledge of a new culture; the recognition of the host country; the interaction with the host people; the cultural distance and the cultural interpenetration model; language and communication skills; the number and quality of contact with the people of the host country; interpersonal network; foreign travel experience; whether permanent residence; cross-cultural training.

Among all these influencing factors, the most widely studied variables are nationality, language proficiency, and existing cross-cultural experiences.

- **Nationality**: According to previous studies, it's shown that the farther the cultural distance, the more difficult the socio-cultural adaptation would be. In another word, cultural or racial similarity is positively related to better socio-cultural adaptation. Therefore, the cultural distance has become an important variable in culture study.
- **Language level**: A report shows that the correlation among international member's language level, the frequency of social interactions, and support from host country is positively related. A lower language levels may indicate a more difficult cultural adaptation challenge. Correspondingly, the language barriers often become an obstacle for social interaction between foreigners and their host country.
- **Time**: It takes time to obtain the cultural capital of the host country. The longer a foreigner lives in a host country, the better language and social skills will be, so that it has more help to get support from social and network.
- **Social interaction**: Social interaction with local people is a key variable that affects socio-cultural adaptation. Bochner (1982) put up with an interpersonal model which can explain the importance of social interaction. He thinks international students always rely on different social relationships depends on different purposes, and good relations with the local people are particularly effective for cultural studies.
- **Psychological adaptation**: In addition to social interaction, socio-cultural adaptation is also related to psychological adaptation. On the one hand, the interaction between foreigners and local people is positively related to their satisfaction. On the other hand, the lack of social support has a significant negative impact on the psychological well-being of international students.

Seeing cultural diversity as an opportunity rather than as a threat obviously has intellectual, emotional, and moral appeal. The challenge is to have the willingness to confront our own assumptions, to question them, and to hold on the essential ones out of a sense of conviction rather than fear of something different.

Cross-cultural recommendations may sound like little more than common sense but it takes considerable robustness, openness, and effort to see to it that common sense prevails.

References

[1] Adler, Peter. 1975. "The Transitional Experience: An Alternative View of Culture Shock." Journal of Humanistic Psychology 15, 4:13–23.

[2] Berry, J.W. (1980) Acculturation as varieties of adaptation. In A. Padilla (Ed.), Acculturation: Theory, models and some new findings (pp. 9–25). Boulder, CO: Westview.

[3] Berry, J.W. (1990 Psychology of acculturation. In J. Berman (Ed.), Cross-cultural perspectives: Nebraska Symposium on motivation (vol. 37, pp. 201–34). Lincoln, NE: University of Nebraska Press.

[4] Bochner, S. (1982) The social psychology of cross-cultural relations. In Cultures in contact: Studies in cross-cultural interaction. ed. S. Bochner, 5–44. Oxford: Pergamon

[5] Furnham, A., and S. Bochner. (1986) Culture shock: Psychological reactions to unfamiliar environment. London: Methuen. Gudykunst, W.B. 1983a. Tow

[6] Gordon, Milton (2008) Assimilation in Native and Immigrant groups, special editor, Andres Suarez, Seminar presented June 9, 2008, London, Ontario

[7] Gullahorn, J.R., & Gullahorn, J.E. (1962). An extension of the u-curve hypothesis. Journal of Social Issues, 3, 33-47

[8] Lysgaard, S. (1955) Adjustment in a foreign society: Norwegian Fulbright grantees visiting the United States. International Social Science Bulletin, 7, 45-51.

[9] Oberg, K. (1960). Culture shock: Adjustment to new cultural environment. Practical Anthropologist, 7, 177-182.

[10] Park, Robert E. [1923] 1950. "Negro Race Consciousness as Reflected in Race Literature." Pp. 284–300 in *Race and Culture, Essays in the Sociology of Contemporary Man*, edited by E. C. Hughes, C. S. Johnson, J. Masuoka, R. Redfield, and L. Wirth. Glencoe, IL: Free Press.

[11] Redfield R, Linton R, Herskovits MJ. Memorandum for the Study of Acculturation. American Anthropologist. 1936;38(1):149–152.

[12] Spradley, James and Philips, Mark (1972) Culture and Stress: A Quantitative Analysis. American Antropologist

[13] Stonequist, Everett V. [1937] 1965. *The Marginal Man: A Study in Personality and Culture Conflict*. New York: Russell & Russell.

[14] Ward, C. (1996). Acculturation. In D. Landis & R. Bhagat (Eds.), Handbook of intercultural training (2nd ed., pp. 124–47). Thousand Oaks, CA: Sage

[15] Yieh, Tsung-Kao [1934] The Adjustment Problems of Chinese Graduate Students in American Universities. Chicago University Press

Multiple linear regression based model for the temperature of the upper, undisturbed part of a solar storage

R. KICSINY

Department of Mathematics, Institute of Environmental Systems,
Faculty of Mechanical Engineering, Szent István University
Páter K. u. 1., Gödöllő, H-2100, Hungary

Abstract

Developing mathematical models for describing the temperature of solar storage tanks is of great importance for the practice, since the storage tank stores and provides the solar heat directly, in the form of hot water, for the consumer. In this study, a new, general and easy-to-apply multiple linear regression based model, called LR model, is proposed to predict the temperature at the upper, undisturbed part of solar storages. This model is likely one of the simplest linear black-box type models, which can still describe the transient changes of the upper temperature with a satisfactory precision. Comparing measured and simulated data on a real solar storage, the validation and the efficiency of the LR model is presented. The generality and the simple applicability of the model are also mentioned along with future research proposals.

Keywords

solar storage, upper temperature, mathematical modelling, black-box model, multiple linear regression

1. Introduction

Developing mathematical models for describing temperatures of solar storage tanks is of great importance for the practice, since these elements are unavoidable in any solar heating systems, where some heat should be stored in the form of hot fluid. There are two main categories of mathematical models for solar storages: physically-based models (or white-box models), which describe exact physical laws (on the basis of theory) and black-box models, which represent empirical correlations (based on experiences or measurements).

The difficulties of the exact physically-based modelling caused by the complex/complicated physical phenomena, like the effect of the inlet fluid flow on the thermal stratification (Meyer et al., 2000), can be often overcome by means of the empirical black-box models. The most frequent black-box model type may be the artificial neural network (ANN) in thermal engineering applications. Kalogirou et al. (1999) predict the useful heat extracted from a

solar heating system and the temperature increase of the stored water with an ANN with a modelling error of 7-10%. This can be stated appropriate accuracy for such systems (Kalogirou, 2000). An ANN is worked out in (Géczy-Víg and Farkas, 2010) to model the temperatures of the layers in a storage tank for domestic hot water. In general, ANNs are rather arduous to apply because of the so-called training (or learning) process used for identification. For example, 30 943 data sets were used in (Géczy-Víg and Farkas, 2010) in a version of the trainings (identification) while only 2997 in the validation. Furthermore, many different back-propagation algorithms needed for training processes are available. The selection of the right one along with the proper number of layers and neurons, forming the ANN model itself, requires high experience and expertise of the user. The convergence of the training algorithm indicating the end of a training session may be also time-consuming.

Because of the above problems on arduousness, complexity and time consumption, the present work aims at establishing a simple and general but still precise black-box model, which can be used fast and easily for a wide range of storage tanks. The model is based on a well-known method of mathematical statistics, namely, the multiple linear regression (MLR). Based on studies in the literature, MLR is a missing black-box modelling technique in the field of storage tanks despite of its linear algebraic simplicity. MLR-based models have been worked out in recent works for other working components of solar heating systems, namely, for solar collectors (Kicsiny, 2016) and for pipes (Kicsiny, 2017). As proposing a new MLR-based model to predict the temperature of the upper part of a solar storage, called *LR model* in short, the present study can be considered as the continuation of these works.

The reason for the upper part is modelled in this work is that this part is less disturbed by the inlet flows to the storage (caused by the consumption load and the pump of the heating loop), and, accordingly, easier to model. Basically, a simple model, like the LR model, can be expected to describe relatively simple, undisturbed cases more efficiently.

2. LR model

Fig. 1 shows the general scheme of the studied solar storage.

The storage tank can be heated up through a heating loop, within which the fluid enters the storage with temperature T_{in} and leaves it with T_{out}. A pump circulates the fluid in the heating loop with 0 or a prefixed constant flow rate value v according to on/off pump operation. Sometimes a consumer discharges some fluid from the storage with the flow rate v_{load}.

All time dependent variables T_{in}, $T_{s,up}$, v and v_{load} are measured periodically according to a time period Δt.

Because of the bounded propagation speed of physical effects and the bounded speed of measurements, the inputs of the LR model are $T_{in}(t-\tau)$,

$v_{load}(t-\tau)$ and $T_{s,up}(t-\tau)$ with respect to the output (which is the modelled value of $T_{s,up}(t)$) at the current time t. Here τ is the time delay with respect to the effects of the inlets (more particularly T_{in} and v_{load}) to the interior of the storage tank. Clearly, the previously detected value of the temperature in the upper part of the storage (called simply *storage temperature* below), as some initial value of the model, has also essential effect on its current value $T_{s,up}(t)$. For simplicity, $T_{s,up}(t-\tau)$ is taken as this previous temperature to be considered in the model.

Figure 1. Scheme of the solar storage
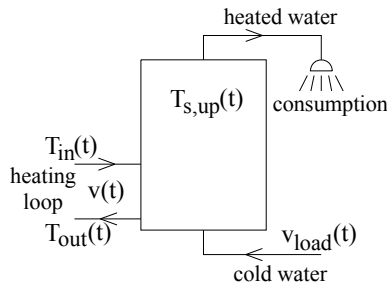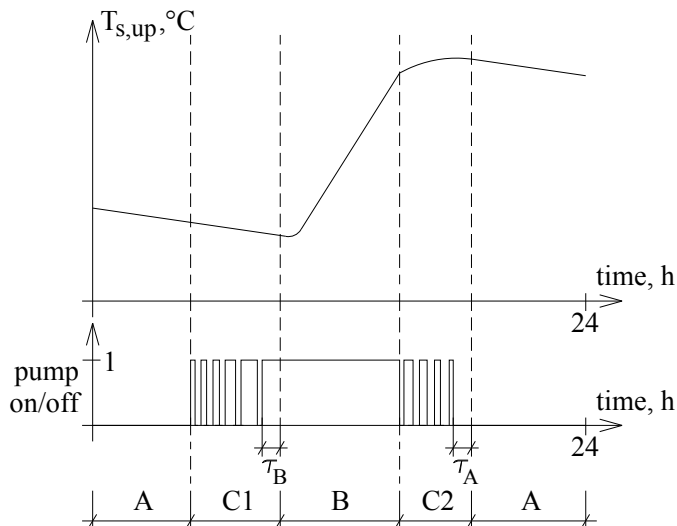

Figre 2. Upper storage temperature and pump operation on a typical day

Considering the storage tank as a black-box, it can be admitted that distinct sub-models as parts of the LR model (as a black-box model) should be identified for significantly different operating conditions. More particularly, the storage tank behaves absolutely different if the pump is on ($v>0$) or off ($v=0$)

permanently. Namely, under the same initial storage temperature, $T_{s,up}$ basically increases if the pump is on and decreases if the pump is off. Even, the effect of T_{in} can be neglected in case of permanently switched off pump, since there is no fluid flow into the storage from the heating loop. Considering a typical day, when the temperature increase of $T_{s,up}$ is significant (and the consumption load is not extremely high), four different operating cases should be distinguished according to Fig. 2.

Cases A and *B* correspond to permanently switched off and switched on pump, respectively, while *Case C1* and *C2* correspond to frequent switch-offs and -ons. Since the storage temperature basically increases before the solar noon and decreases after it, it seems practical to divide *Case C* into two parts accordingly. The detailed specification of each *Case* can be found below (see also Fig. 2).

Case A: The pump is switched off permanently. This *Case* consists of the time period from the beginning of the day to the first switch-on of the pump and all such periods, which start at a time when the pump has been (permanently) switched off for exactly τ_A time and stops either at the time of the next switch-on or at the end of the day.

Case B: The pump is switched on permanently. This *Case* consists of all such periods, which start at a time when the pump has been (permanently) switched on for exactly τ_B time and stops at the next switch-off.

Case C1: Time periods besides *Cases A* and *B* before the solar noon.

Case C2: Time periods besides *Cases A* and *B* after the solar noon.

Remark: τ_A is the time which should be passed after a switch-off to go on with *Case A*. More particularly, τ_A is the time which is generally enough for the pump to become permanently off (and not alternating), and, this behaviour is considered as the characteristic feature of *Case A*. Similarly, τ_B is the time which should be passed after a switch-on to go on with *Case B*. More particularly, τ_B is the time which is generally enough for the pump to become permanently on (and not alternating), and, this behaviour is considered as the characteristic feature of *Case B*.

For the best possible modelling precision, distinct sub-models based on MLR are worked out for each operating case. In the sub-models of *Cases B*, *C1* and *C2*, T_{in} is among the inputs, since there is some fluid flow into the storage tank from the heating loop in accordance with the permanently or intermittently switched on pump. In the sub-model of *Case A, T_{in}* is neglected according to the permanently switched off pump.

The LR model is composed of Eqs. (1A), (1B), (1C1) and (1C2), which are simple linear algebraic relations representing the corresponding sub-models of the separate operating cases.

Case A:

$$T_{s,up,\mathrm{mod}}(t) = c_{load,A}v_{load}(t-\tau) + c_{s,up,A}T_{s,up}(t-\tau) \tag{1A}$$

Case B:

$$T_{s,up,\mathrm{mod}}(t) = c_{in,B}T_{in}(t-\tau) + c_{load,B}v_{load}(t-\tau) + c_{s,up,B}T_{s,up}(t-\tau) \tag{1B}$$

Case C1:

$$T_{s,up,\mathrm{mod}}(t) = c_{in,C1}T_{in}(t-\tau) + c_{load,C1}v_{load}(t-\tau) + c_{s,up,C1}T_{s,up}(t-\tau) \tag{1C1}$$

Case C2:

$$T_{s,up,\mathrm{mod}}(t) = c_{in,C2}T_{in}(t-\tau) + c_{load,C2}v_{load}(t-\tau) + c_{s,up,C2}T_{s,up}(t-\tau) \tag{1C2}$$

$c_{load,A}$, $c_{s,up,A}$, $c_{in,B}$, $c_{load,B}$, $c_{s,up,B}$, $c_{in,C1}$, $c_{load,C1}$, $c_{s,up,C1}$, $c_{in,C2}$, $c_{load,C2}$, $c_{s,up,C2}$, are constant parameters to be identified.

3. Identification and validation

In this section, the LR model (Eqs. (1A), (1B), (1C1) and (1C2)) is applied to a real storage tank for identification and validation. The calculations needed have been done in the Matlab software (Etter et al., 2004).

In the identification, $T_{s,up,meas}(t-\tau)$ is used as $T_{s,up}(t-\tau)$. During the validation of the already identified LR model, the previously modelled value $T_{s,up,\mathrm{mod}}(t-\tau)$ is used as $T_{s,up}(t-\tau)$ when modelling $T_{s,up}(t)$. Measured $T_{in}(t-\tau)$ and $v_{load}(t-\tau)$ values are available both during the identification and the validation. According to the specification of Δt, the measurements happen at times $t = 0, \Delta t, 2\Delta t, 3\Delta t,...$ Practically, the modelled value of $T_{s,up}$ (that is $T_{s,up,\mathrm{mod}}$) is determined in the LR model also at times $t = 0, \Delta t, 2\Delta t, 3\Delta t,...$ Furthermore, for simplicity, $\tau = \Delta t$ is assumed in the LR model. *Case A* holds and $T_{s,up}(t-\tau) = T_{s,up,meas}(0)$ is used as measured initial condition in Eq. (1A) at $t = \tau$ (at the beginning of the day).

The real storage tank, which is to be modelled, is the solar storage of a measured solar heating system (Farkas et al., 2000) installed at the Szent István University (SZIU) in Gödöllő, Hungary. This storage will be called below *SZIU storage* in short. The SZIU storage contains preheated domestic water for a kindergarten at the campus of the university. The heat is transferred from a solar

collector field into the SZIU storage by means of a heating loop equipped with a pump working in on/off operation. The measurements are carried out once a minute, that is, $\Delta t = 1$ min. The volume of the SZIU storage is 2 m³. Based on observations, τ_A and τ_B can be set 10 min. These and other important parameter values can be found in Table 1.

Table 1. Parameter values of the LR model and the SZIU storage

Δt, s	60
τ, s	60
τ_A, s	600
τ_B, s	600
$c_{in,B}$, -	0.0049
$c_{in,C1}$, -	-0.000096
$c_{in,C2}$, -	0.0011
$c_{load,A}$, Ksm⁻³	37.7445
$c_{load,B}$, Ksm⁻³	31.0834
$c_{load,C1}$, Ksm⁻³	13.3407
$c_{load,C2}$, Ksm⁻³	29.4138
$c_{s,up,A}$, -	0.9999
$c_{s,up,B}$, -	0.9952
$c_{s,up,C1}$, -	1.0000
$c_{s,up,C2}$, -	0.9989

The following indices (corresponding to the currently investigated day) are used in this paper for the evaluation. The average of error is the time average of $\left(T_{s,up,\mathrm{mod}} - T_{s,up,meas}\right)$, the average of absolute error is the time average of the absolute value $\left|T_{s,up,\mathrm{mod}} - T_{s,up,meas}\right|$. The average of absolute error is determined also in % dividing it by the (positive) difference between the maximal and minimal value of $T_{s,up,meas}$.

Identification
The measured data of four days have been selected for the identification in such a way that they cover a wide range of possible operating conditions of a selected season (summer). Two days (8th June, 2012; 28th June, 2012) are with relatively

high consumption load (more than 1000 litres) and two ones (24th June, 2012; 2nd July, 2012) are with relatively low consumption load (less than 200 litres). Based on many computer experiments (not detailed here), such four days proved to be enough for the identified model to have a rather good accuracy. For the sake of practice, these four days have been selected from the first third of the summer. In this way, the already identified model can be conveniently used in the remained two summer months. (To apply the model for the whole year, the identification could be carried out easily for each season separately for maximal yearly precision).

Four independent standard MLR routines have been applied based on the measured data of each separate operating case (*Cases A*, *B*, *C1* and *C2*) of the LR model to identify parameters $c_{load,A}$, $c_{s,up,A}$, $c_{in,B}$, $c_{load,B}$, $c_{s,up,B}$, $c_{in,C1}$, $c_{load,C1}$, $c_{s,up,C1}$, $c_{in,C2}$, $c_{load,C2}$, $c_{s,up,C2}$ in Eqs. (1A), (1B), (1C1) and (1C2) in the LR model. The standard MLR routine (based on least squares method) is well-known and available in most statistical and spreadsheet programs (SPSS, Excel, etc.), so it is not detailed here. The identified parameters of the LR model can be seen in Table 1.

Table 2 contains the average of error and the average of absolute error values for a selected day (2nd July, 2012) of the identification (with the already identified LR model). The average of absolute error value is presented in proportion to the positive difference between the daily maximal and minimal measured storage temperature values as well (in %). The mean of these % values relating to all of the four days of the identification can be also seen in Table 2 (2.6 %).

Table 2. Average of error and average of absolute error values with the LR model

Identification	2nd July	Average of error	0.08 °C
		Average of absolute error	0.11 °C; 1.5%
	Mean % value for the whole identification (four days)	Average of absolute error	2.6%
Validation	3rd August	Average of error	0.15 °C
		Average of absolute error	0.15 °C; 2.6%
	Mean % value for the whole validation (3rd July – 31st August)	Average of absolute error	7.7%

Fig. 3 compares the modelled and measured storage temperatures of the LR model for a selected day (2nd July, 2012) of the identification. The operating state of the pump is also shown in the figure.
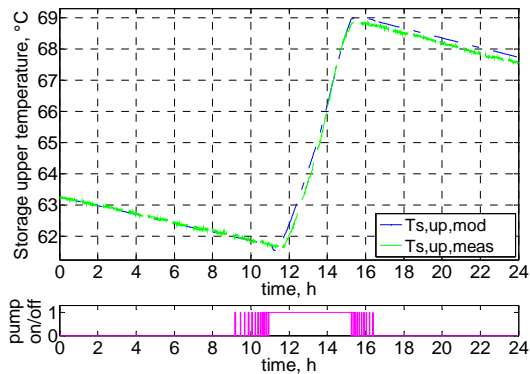
Figure 3. Modelled $T_{s,up,\mathrm{mod}}$ and measured $T_{s,up,meas}$ upper storage

temperatures on 2nd July 2012

Validation

In the validation, the LR model is applied with the corresponding measured inputs of the remaining two summer months. More precisely, one input of the model is changed in comparison with the inputs of the identification, namely, the modelled value $T_{s,up,\mathrm{mod}}(t-\tau)$ is used as $T_{s,up}(t-\tau)$ in the LR model (1A), (1B), (1C1) and (1C2) (not $T_{s,up,meas}(t-\tau)$). The modelled days are from 3rd July, 2012 to 31st August, 2012, which means 56 days for the validation according to minor technical interruptions in the operation.
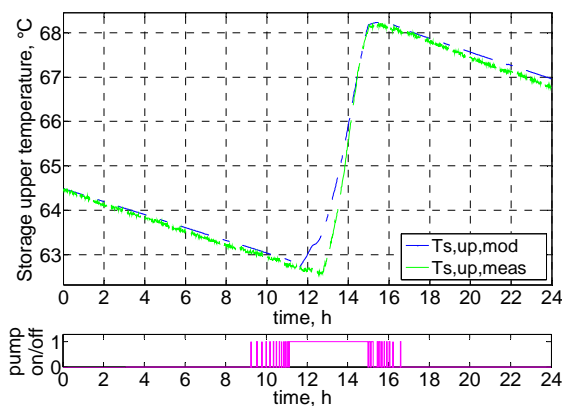

Figre 4. Modelled $T_{s,up,\mathrm{mod}}$ and measured $T_{s,up,meas}$ upper storage

temperatures on 3rd August 2012

The modelled and measured storage temperatures are compared and evaluated. Table 2 contains the average of error and the average of absolute error

values for a selected day (3rd August, 2012) of the validation. The average of absolute error value is presented in proportion to the positive difference between the daily maximal and minimal measured storage temperature values as well (in %). The mean of these % values relating to the whole modelled time period 3rd July – 31st August is also presented in Table 2 (7.7%).

Fig. 4 compares the modelled and measured storage temperatures of the LR model for a selected day 3rd August, 2012) of the validation. The operating state of the pump is also shown in the figure.

Conclusion

Based on the validation, it can be stated that the temperature in the upper (undisturbed) part of a solar storage can be modelled rather precisely with the LR model (with an error of 7.7%) in view of the general solar engineering aims (studying the thermal processes and developing solar storage tanks).

Because of the simple linear algebraic relations of the LR model, the computational demand is low, which may make it ideal for model-based controls. Even, this model is likely one of the simplest black-box models still describing the transient changes of the upper storage temperature with a satisfactory precision. The advantages of the simple usability and low computational demand can be seen especially in comparison with other black-box models, e.g. the often used ANN models, which have essentially the same precision.

Future research may deal with modelling the lower part of a solar storage, which is more disturbed by the inlet flows to the storage (caused by the consumption load and the pump of the heating loop), and, accordingly, more difficult to model. Also, the already existing MLR-based models of separate working components (worked out in (Kicsiny, 2016; 2017) and the present study) may be connected in the future to form an easy-to-use and, hopefully, precise MLR-based model for complete solar heating systems.

Nomenclature

t: time, s;

T_{in}:   inlet temperature of the solar storage from the heating loop, °C;

T_{out}:   outlet temperature of the solar storage to the heating loop, °C;

$T_{s,up}$:   temperature of the upper part of the solar storage, °C;

$T_{s,up,meas}$: measured temperature of the upper part of the solar storage, °C;

$T_{s,up,mod}$: modelled temperature of the upper part of the solar storage, °C;

v: volumetric flow rate of the heating loop, m^3/s;

v_{load}:   volumetric flow rate of the heating loop, m^3/s;

Δt :   time period between successive measurements, s;

τ :   time delay with respect to the effects of the inlets to (the upper part of) the storage tank, s;

τ_A :   time lag before Case A in the LR model, s;

τ_B :   time lag before Case B in the LR model, s

Acknowledgements

References

[1] Etter, D.M., Kuncicky, D., Moore, H. (2004), Introduction to MATLAB 7, Springer

[2] Farkas, I., Buzás, J., Lágymányosi, A., Kalmár, I., Kaboldy, E., Nagy, L. (2000), A combined solar hot water system for the use of swimming pool and kindergarten operation, Energy and the environment, Vol. I. /ed. by B. Frankovic/, Croatian Solar Energy Association, Opatija, 2000., pp. 81-88.

[3] Géczy-Víg, P., Farkas, I. (2010), Neural network modelling of thermal stratification in a solar DHW storage, Solar Energy, Vol. 84, pp. 801-806.

[4] Kalogirou, S.A., Panteliou, S., Dentsoras, A. (1999), Modelling of solar domestic water heating systems using artificial neural networks, Solar Energy, Vol. 65, No. 6, pp. 335-342.

[5] Kalogirou, S.A. (2000), Applications of artificial neural-networks for energy systems, Applied Energy, Vol. 67, pp. 17-35.

[6] Kicsiny, R. (2016), Improved multiple linear regression based models for solar collectors, Renewable Energy, Vol. 91, pp. 224–232.

[7] Kicsiny, R. (2017), Grey-box model for pipe temperature based on linear regression, International Journal of Heat and Mass Transfer, Vol. 107, pp. 13–20.

[8] Meyer, J.P., Raubenheimer, P.J.A., Kruger, E. (2000), The influence of return loop flow rate on stratification in a vertical hot water storage tank connected to a heat pump water heater, Heat Transfer Engineering, Vol. 21, No. 2, pp. 67-73.

Mathematical modelling of a solar air collector

A. F. A. ELBARGHTHI, J. BUZÁS

Department of Physics and Process Control, Szent István University
Páter K. u. 1., Gödöllő, H-2100, Hungary

Abstract

A mathematical model of double pass solar air collector and solution procedures were investigated under forced convection mode. The theoretical efficiency from the outlet air temperature obtained composed of steady state form solution show a reasonable agreement linked with the experimental results. The accuracy of the mathematical model has less than 1% uncertainty. A detailed collector thermal performance includes the theoretical useful heat gain under different mass flow rate were presented. The optimum air mass flow rates were simulated with different solar radiation, inlet, and ambient air temperatures. The results are very beneficial for investigating and designing more modern and complex solar air collectors.

Keywords

solar energy, thermo-hydraulic efficiency, heat gain, air mass flow, simulation

1. Introduction

The Sun as an infinite source of energy cannot be overemphasized, it is one of the cleanest energy especially nowadays where the global attention is on climate change mitigation. Solar energy therefore, plays a significant role as an unlimited renewable energy resource. Despite the attenuation, the total amount of solar energy emitted by the Sun into the earth's surface is approximately equal to $1.8*10^{14}$ kW which is intercepted (Thirugnanasambandam et al., 2010). According to Tchinda, (2009) the supply of hot air for space heating, is one of the most potential applications of solar energy which is to provide the comfortable environment especially using active systems that often demonstrated better performance than their passive counterparts and deliver more heat per square meter of collector. The efficiency of active heating space growths significantly with radiation from 100 to 500 W/m^2. Whereas, for wind velocity from 0 to 5 m/s, the efficiency decreases sharply (Dragicevic et al., 2015). The air mass flow rates in the active solar air heating is the main sensitive factor which can affect the process of heat transfer and adequate the efficiency of the collector (Zelger et al., 1999). Choudhury et al., (1988) detailed a theoretical parametric analysis of air heater to provide hot air for agricultural use. The results illustrate that to obtain higher air temperature, lower air mass

flow rate via the air heater and longer air channel is desirable. It was observed that the efficiency of flat-plate solar air collector improves with increasing air flow rates due to an enhanced heat transfer to the air flow while temperature difference of fluid decreases (Alta et al., 2010; Gao et al., 2011). Omojaro and Aldabbagh (2010) examined the single and double pass solar air heaters and concluded that the efficiency increases in case of double pass with 7% to 19.4% at the same air mass flow than that in the single pass. A mathematical model was investigated to solve results for every element of the collector in a steady state form by using a matrix inversion method with some algebraic rearrangements (Fudholi, 2011; Fudholi et al., 2012; Fudholi et al., 2013b).

2. Material and methodology

The double pass solar air collector designed and manufactured at the laboratory of Institute for Environmental Engineering Systems, Faculty of Mechanical Engineering, Szent István University, Hungary. The size of the collector is 500 mm wide and 1250 mm long. The collector was mainly made from wood and the back side has 20 mm thickness of polystyrene insulation layer. A transparent plastic type Guttagliss Hobbyglas with high transparency is used at the front having 4 mm thickness. The absorber has (1210 mm x 460 mm) and 1.2 mm thickness made from copper type C 110 and painted in black matt. There are two overlapping air flow channels in a single flow air with double pass. The air inlet to the collector passes through the upper absorber surface with 6.38 cm depth then goes along the lower absorber channel via holes to pass through a 35 mm x 160 mm rectangular cross section path with 3.5 cm depth in seven parallel baffles to the outlet. Fig. 1 illustrates the schematic of the designed solar air collector.
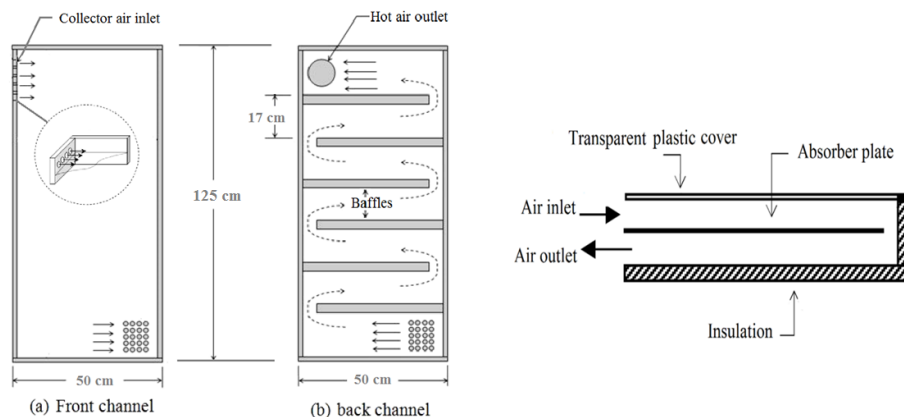

Figure 1. Schematic of the double pass solar
air collector

3. Theoretical analysis

The mathematical model of the double pass solar air collector under forced convection approach is obtained. The heat transfer coefficients of the collector are shown in Fig. 2. The analysis was simplified by some assumptions as following (Fudholi et al., 2012): (i) The collector performance and all convective heat transfer coefficients are steady state (ii) Flowing air is equal and constant (iii) Thermal conductivity of absorber is constant (iv) The useful heat gain to the air is uniform along the length of the collector.
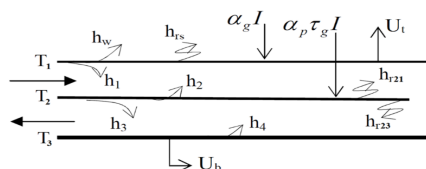

Figre 2. Schematic of heat transfer coefficients

In steady state, the performance of a flat-plate solar collector is described by an energy balance that indicates the distribution of incident solar energy into useful energy gain and thermal losses. The steady state energy balance equations from Fig. 2 can then be written as following:

At the transparent plastic cover (T_1):

$$\alpha_g I + h_{r21}(T_2 - T_1) + h_1(T_{f1} - T_1) = U_t(T_1 - T_a) \tag{1}$$

For the upper air flow channel at (T_{f1}):

$$h_2(T_2 - T_{f1}) = h_1(T_{f1} - T_1) + Q_1 \tag{2}$$

For the absorber plate at (T_2):

$$\alpha_p \tau_g I = h_3(T_2 - T_{f2}) + h_2(T_2 - T_{f1}) + h_{r23}(T_2 - T_3) + h_{r21}(T_2 - T_1) \tag{3}$$

For the lower air flow channel at (T_{f2}):

$$h_3(T_2 - T_{f2}) = h_4(T_{f2} - T_3) + Q_2 \tag{4}$$

For the back insulation plate at (T_3):

$$h_4(T_{f2} - T_3) + h_{r23}(T_2 - T_3) = U_b(T_3 - T_a) \tag{5}$$

Heat balance along flow direction (Ong, 1995):

$$Q_1 = 2\dot{m}C\left(T_{f1} - T_{f1,i}\right)/(W_1 L_1) \tag{6}$$

$$Q_2 = 2\dot{m}C\left(T_{f2} - T_{f2,i}\right)/(W_2 L_2) \tag{7}$$

Air temperature is changing linearly along short collector less than 10 m (Fudholi et al., 2013a). The mean air temperature then equal to the arithmetic mean:

$$T_f = \left(T_{f,o} + T_{f,i}\right)/2 \tag{8}$$

The solar radiation heat flux has been absorbed by the transparent plastic cover surface and the absorber plate surface per unit area [W/m^2] S_1 and S_2 respectively are:

$$S_1 = \alpha_g I \tag{9}$$

$$S_2 = \alpha_p \tau_g I \tag{10}$$

Substitute equations 6 to 10 into the first five equations and make some algebraic arrangements then 5 x 5 matrix will obtained as following:

$$
\begin{bmatrix}
h_1 + h_{r21} + U_t & -h_1 & -h_{r21} & 0 & 0 \\
h_1 & -\left(h_1 + h_2 + \dfrac{2\dot{m}C}{W_1 L_1}\right) & h_2 & 0 & 0 \\
-h_{r21} & -h_2 & (h_2 + h_3 + h_{r21} + h_{r23}) & -h_3 & -h_{r23} \\
0 & \dfrac{4\dot{m}C}{W_1 L_1} & h_3 & -\left(h_3 + h_4 + \dfrac{2\dot{m}C}{W_2 L_2}\right) & h_4 \\
0 & 0 & -h_{r23} & -h_4 & (h_{r23} + U_b + h_4)
\end{bmatrix}
\times
\begin{bmatrix}
T_1 \\ T_{f1} \\ T_2 \\ T_{f2} \\ T_3
\end{bmatrix}
=
\begin{bmatrix}
U_t T_a + S_1 \\[4pt]
-\dfrac{2\dot{m}C}{W_1 L_1} T_i \\[4pt]
S_2 \\[4pt]
\dfrac{2\dot{m}C}{W_2 L_2} T_i \\[4pt]
U_b T_a
\end{bmatrix}
$$

The matrices can be displayed as [$\underline{A}$] [$\underline{T}$] = [$\underline{B}$]. The mean temperature vector was determined by matrix inversion [$\underline{T}$] = [$\underline{A}$]$^{-1}$ [$\underline{B}$] which based on Matlab software. The initial guessed mean temperature of the air stream, the plastic cover, the absorber and the insulation were substituted with all the input collector parameters. The sky temperature and the wind convection heat transfer coefficient are then calculated. Heat transfer characteristics (HTCs) of the collector was determined and represents the value of coefficients (U_t and U_b). New temperatures are determined then each new temperature compared with the corresponding initially-guessed one. The residual of the outlet temperature was set to be 0.01. All solutions were reached at the iteration number 6. At the end of the iteration, the program calculates the outlet temperatures, the useful energy gain and the efficiency as well. The heat transfer coefficients are calculated as following:

The convection heat transfer coefficient due to wind is (Fudholi et al., 2013b):

$$h_w = 2.8 + 3.3 V_w \tag{11}$$

The radiation heat transfer coefficients (Fudholi, 2011; Karim et al., 2014):

$$h_{r21} = \frac{\sigma(T_2^2 + T_1^2)(T_2 + T_1)}{\frac{1}{\varepsilon_p} + \frac{1}{\varepsilon_g} - 1} \tag{12}$$

$$h_{r23} = \frac{\sigma(T_2^2 + T_3^2)(T_2 + T_3)}{\frac{1}{\varepsilon_p} + \frac{1}{\varepsilon_b} - 1} \tag{13}$$

$$h_{rs} = \frac{\sigma \varepsilon_g (T_1 + T_s)(T_1^2 + T_s^2)(T_1 - T_s)}{(T_1 - T_a)} \tag{14}$$

Where σ is Stefan-Boltzmann constant 5.67 x 10^{-8} W/m^{2}K^4, T_s is the sky temperature equal to 0.0552 $T_a^{1.5}$.

Overall top heat transfer coefficient U_t and conduction heat transfer coefficient loss from bottom surface U_b can be obtained as (Ong, 1995):

$$U_t = h_w + h_{rs} \tag{15}$$

$$U_b = \frac{1}{i = \sum_{1}^{n}(x_{bi}/k_{bi}) + \frac{1}{h_w}} \tag{16}$$

The convective heat transfer coefficients are determined by (Njomo and Daguenet, 2006):

$$h = \frac{k}{D_h} Nu \tag{17}$$

Where D_h is the hydraulic equivalence diameter. N_u is Nusselt number which depends on the flow inside the channel. The physical properties of the air as the fluid media are assumed to vary linearly with the temperature (Fudholi, 2011). The solar collection efficiency is determined by:

$$\eta = \frac{\dot{m}C(T_o - T_i)}{WLI} \tag{18}$$

The thermo-hydraulic efficiency (η_{th}) expresses the net energy gain over the total energy which received from the sun. It is used to evaluate the thermal performance of the collector as folowing (Sun et al., 2016):

$$\eta_{th} = (Q_u - P_{fan})/(I * A_P) \tag{19}$$

Where P_{fan} is the useful output power given by the fan, Q_u is the useful thermal output power, I is the solar radiation intensity and A_p is the frontal area solar collector.

Table 1. Relevant parameters used for numerical calculations

Relevant parameters	α_g	α_p	ε_g	ε_p	ε_b	τ_g
value	0.1	0.95	0.8	0.9	0.9	0.93

4. Results analysis and discussion

The thermal inertia of the collector was presented in Fig. 3. The mass flow rates (ṁ) and the solar intensity plays significant roles to provide the value of the collected heat. ṁ was varied over the technical range of interest $0.006 \leq \dot{m} \leq 0.019$ kg/s. Table 2 illustrates the hourly useful heat gained from the collecter with the hourly solar radiation. Increasing ṁ, increasing the usefull heat gain and parallel increasing the instantaneous collector efficiency.

(a) ṁ=0.006 kg/s

(b) ṁ=0.0091 kg/s

(c) ṁ=0.0125 kg/s
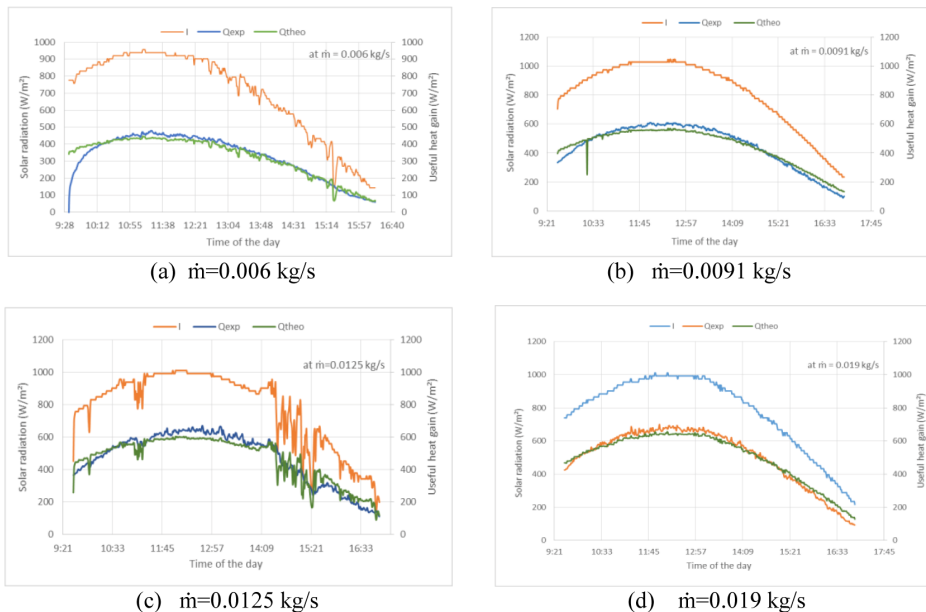
(d) ṁ=0.019 kg/s

Figure 3. Experiment and theoritical useful heat gain from the collector

The measurement and the theoretical results have a reasonable agreement respecting the fluctuating of the solar radiation intensity at the day time.

However, the developed Matlab code tested using the same boundary conditions that recorded at the experiment (Sun et al., 2016). The computation was repeated under five different conditions. The efficiency then calculated from the useful heat gain and the collector outlet temperatures and compared with the theoratical result to validate the code accuracy. There were some practical uncertainties during the measurements in addition to the assumptions at the theoretical modelling part. The comparable results have reasonable agreement supporting the validity of the theoretical model used with less than 1% error as shown in Fig. 4. Moreover, to test the collector performance and the optimum ṁ the thermo-hydraulic efficiency (η_{th}) has to be characterized. η_{th} reachs 62% at 1000 W/m^2 solar radiation from the sinulation results. Fig. 5 (a) and (b) shows slightly differences at (η_{th}) when ambient and inlet air temperatures are equal and whereas in Fig. 5 (c) and (d) at constant inlet air temperature the (η_{th}) values are considerable when ambient air temperatures are changing. However, (η_{th}) was increased up to a specific value where ṁ of the designed collector reach the optimum value and then start to decrease with further increasing at ṁ. The optimum ṁ for the collector equals around 0.02 kg/s at solar radiation higher than 700 W/m^2. To detail the collector optimal working region, 3D plot was graphed in Fig. 6 to illustrate the highest (η_{th}) that this collector can reach and the optimum ṁ. In addition, the collector is insufficient to use at low radiation because of the high losses.
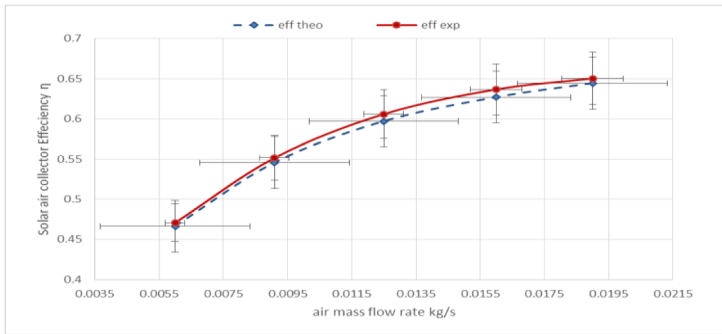

Figre 4. Comparison of experimental and
theoretical results

Table 2. Collector hourly solar radiation and useful heat
gain with the efficiency

measuring day mass flow rate [kg/s]	0.006	0.0091	0.0125	0.016	0.019
hourly solar radiation [MJ/m^2]	16.99	21.89	20.87	21.04	20.89
hourly useful heat [MJ/m^2]	7.99	12.07	12.65	13.39	13.59
hourly efficiency of the collector %	47.06	55.15	60.59	63.66	65.03

(a) I=1000 W/m^2 (b) I=700 W/m^2
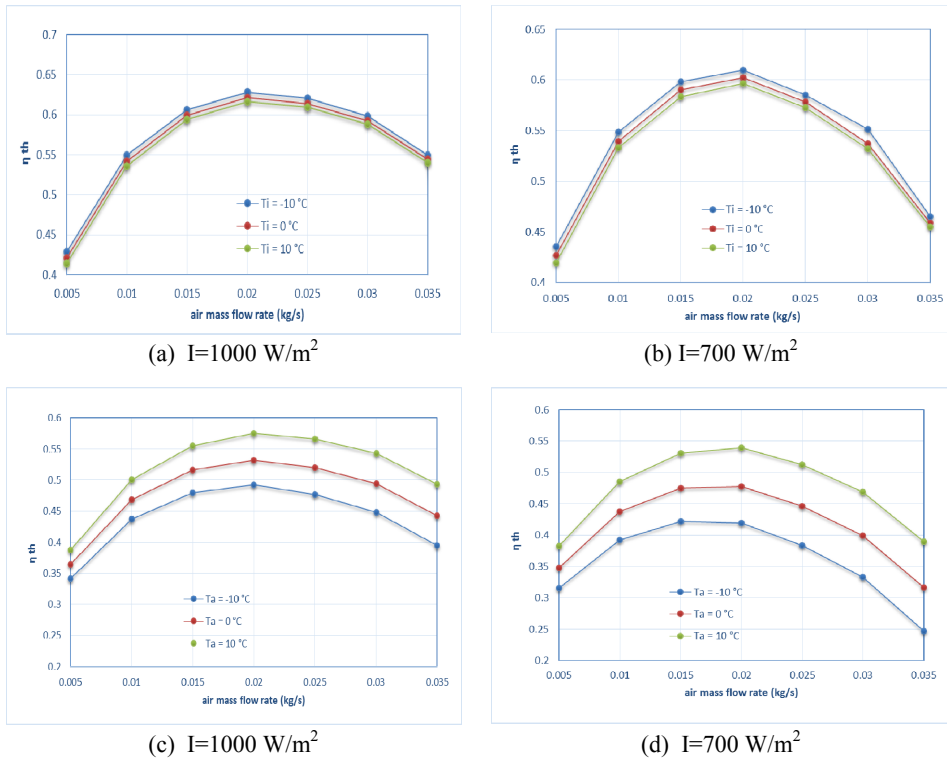

(c) I=1000 W/m^2 (d) I=700 W/m^2

Figre 5. Variation of thermo-hydraulic efficiency at T_i=21 ^{o}C
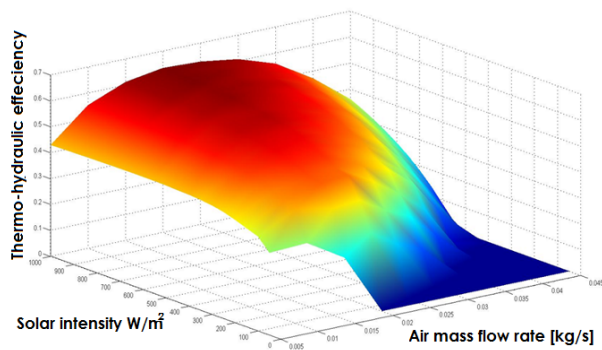

Figure 6. 3D plot for the collector thermo-hydraulic efficiency

Conclusions

In this paper, a mathematical model for double pass solar air collector has been developed under forced convection mode to evaluate the collector performance and examined its operation efficiency. The accuracy of the theoretical results is

validated and compared with experiments. The collector working environments can be predicted specially at winter time for instance in space heating and drying or any linked applications. The maximum thermo-hydrolic efficiency of the collector obtained and introduced at different mass flow rate along with solar intensity. The optimum air mass flow rate for this collector was 0.02 kg/s. The maximum thermo-hydrolic efficiency of the collector obtained is 62% at 1000 W/m^2 solar radiation. As a matter of fact the efficiency of the collector is strongly dependent on the air mass flow rate.

Nomenclature

h	heat transfer coefficient	$(W/m^2\ ^oC)$	*Subscripts*	
k	thermal conductivity	$(W/m\ ^oC)$	a	ambient
L	length of the collector	(m)	b	back plate
$\dot{m}$	mass flow rate	(kg/s)	f	fluid
U_b	overall heat transfer coefficient	$(W/m^2\ ^oC)$	g	glass
U_t	top heat loss coefficient	$(W/m^2\ ^oC)$	i	inlet
V	wind velocity	(m/s)	o	outlet
W	width of the collector	(m)	p	plate
Greek letters			r	radiative
α	absorptivity		s	sky
ε	emissivity		t	insulation
τ	transmissivity		w	wind

References

[1] Alta D., E. Bilgili, C. Ertekin and O. Yaldiz (2010), Experimental investigation of three different solar air heaters: Energy and exergy analyses, Applied Energy, 87 (10), pp. 2953–2973.

[2] Choudhury C., S. L. Andersen and J. Rekstad (1988), A solar air heater for low temperature applications, Solar Energy, 40 (4), pp. 335–343.

[3] Dragicevic S. M., M. R. Lambic, J. M. Radosavljevic and M. T. Raos (2015), Estimating the Effects of Environmental Conditions on Active Solar Wall Air Heating System Efficiency, Journal of Energy Engineering, 141 (3), 04014008.

[4] Fudholi A. (2011), Thermal Efficiency of Double Pass Solar Collector with Longitudinal Fins Absorbers, American Journal of Applied Sciences, 8 (3), pp. 254–260.

[5] Fudholi A., M. H. Ruslan, L. C. Haw, S. Mat, M. Y. Othman, A. Zaharim and K. Sopian, (2012), Mathematical Model of Double-Pass Solar Air Collector with Longitudinal Fins, Recent Advances in Fluid Mechanics, Heat & Mass Transfer and Biology, pp. 114–120.

[6] Fudholi, A., K. Sopian, M. H. Ruslan and M. Y. Othman (2013a), Performance and cost benefits analysis of double-pass solar collector with and without fins, Energy Conversion and Management, 76, pp. 8–19.

[7] Fudholi A., M. H. Ruslan, M. Y. Othman and K. Sopian (2013b), Mathematical Model of Double-Pass Solar Air Collector, Solar Energy Research Institute. MALAYSIA. ISBN: 978-1-61804-175-3

[8] Gao L., H. Bai and X. Fang (2011), Experimental study of solar air heating system based on unglazed transpired collector, In 5th International Conference on Energy Sustainability, pp. 7–10.

[9] Karim M. A., E. Perez and Z. M. Amin (2014), Mathematical modelling of counter flow v-grove solar air collector, Renewable Energy, 67, pp. 192–201.

[10] Njomo D., and M. Daguenet (2006), Sensitivity analysis of thermal performances of flat plate solar air heaters, Heat and Mass Transfer, 42 (12), pp. 1065–1081.

[11] Omojaro A. P., and L. B. Y. Aldabbagh (2010), Experimental performance of single and double pass solar air heater with fins and steel wire mesh as absorber, Applied Energy, 87 (12), pp. 3759–3765.

[12] Ong, K. S. (1995), Thermal performance of solar air heaters: mathematical model and solution procedure, Solar Energy, 55 (2), pp. 93–109.

[13] Sun C., Y. Liu, C. Duan, Y. Zheng, H. Chang and S. Shu (2016), A mathematical model to investigate on the thermal performance of a flat plate solar air collector and its experimental verification, Energy Conversion and Management, 115, pp. 43–51.

[14] Tchinda, R. (2009), A review of the mathematical models for predicting solar air heaters systems, Renewable and Sustainable Energy Reviews, 13 (8), pp. 1734–1759.

[15] Thirugnanasambandam M., S. Iniyan and R. Goic (2010), A review of solar thermal technologies, Renewable and Sustainable Energy Reviews, 14 (1), pp. 312–322.

[16] Zelger T., M. Bruck and C. Muss (1999), Solar air systems, Austrian Ministry of Science and Transport, Vienna, p. 6.

Investigation of finned solar air collector performance for drying purposes

Maytham A. Al-NEAMA, I. FARKAS

Mechanical Engineering Doctoral School, Szent István University,
Gödöllő, Hungary Páter K. u. 1. Gödöllő, H-2100, Hungary

Abstract

In this paper, the effects of collector absorbing surface increasing on the thermal performance of flat plate solar collector with forced air circulation investigated. For that, two absorbers are tested: un-finned and finned double-pass solar collector. These collectors are tested experimentally for 5 hours of 25th of August 2017 in Szent Istvan university laboratory in Gödöllő city. The experimental results showed that the increasing of absorbing surface area by extended surfaces plays the main factor to increase solar collector performance. The maximum value of useful heat of finned collector more than 600 W compared with un-finned collector with about 504W maximum useful heat. The thermal efficiency increased by 7.7% with using finnes (buffers).

Keywords

solar, collector, performance, finned absorber, dryer

1. Introduction

The utilization of solar energy becomes more important in the last decades especially in the agriculture products drying. At the same time, the quality control and quality preservation technology becomes also important technologies for processing of agricultural products than before. The Traditional application and very widely used product preservation is the drying process. Solar drying technology has many features upon the traditional dry technologies, it is low cost process and clean. In the past, the Agricultural and other products have been dried by the direct sun and wind in the open air for thousands of years.

According to the brief review for many literatures, the performance of drying process depend mainly on the performance of solar collector. And the improvement of solar collector will improve the dryer work also. But, some products do not need for high air temperature because it will damage such as fish, meats, etc. So the control on the process parameters, air temperature, moister content for air and product and air speed very important.

Solar air collectors are classified broadly into two types: bare plate and cover plate solar air heaters. The bare plate solar air heaters consist simply of an air duct, the upper surface of which operates as the solar-energy absorber plate and

the back surface insulated. For covered-plate solar air-heating collectors, to reduce upward heat losses from solar air heaters a transparent cover materials above and usually parallel to the absorber plate are used of one or more (Ekechukwu and Norton, 1999). The effects of design parameters of the solar heater such as the length, width, gap spacing between the absorber plate and glass cover, mass flow rate and thickness and type of the storage material (sand, granite and water) on the outlet and average temperatures of the flowing air are studied. The study obtained that thermal performance of the solar air heater with using storage materials was higher than that without storage. The optimum thickness of the storage material layer was about 12 cm and found to be convenient for drying different agriculture products (Aboul-Enein et al., 2000). Madhlopa et al. (2002) studied a solar dryer system had composite absorber plate systems on the principles of psychometric. The dryer consists of a flat plate solar collector, absorber plate approved with wire mesh, glass cover, chimney and insulated drying chamber. The drying chamber and solar collector box were made from wood sheets. The solar collector was connected to a drying chamber for product dehumidification.

The performance of evacuated-tube solar collectors had been investigated experimentally under eastern Mediterranean climatic conditions. The experiments were carried out during the period of November to January (winter conditions), at days where the sky was almost clear with some little clouds scattered (Hayek et al., 2011). The productivity of flat plate solar collector had been estimated by Mammadov (2012). The performance of solar collectors under low temperature conditions measured and simulated. The experimental results showed that for temperatures below ambient and for cases without irradiance, unglazed collectors performed better than glazed ones, with considerable heat gains from condensation and frost. Due to their design, glazed collectors are not suitable to operate at temperatures below the dew point as condensation and frost conditions might lead to deterioration of materials, compromising the reliability and durability of this type of collector (Bunea et al., 2012). A parabolic trough collector was tested under the climatic condition of Aliero Town, Kebbi State, Nigeria to see the effect of meteorological parameters on the performance of the system. The experimental results obtained lowest daily average ambient temperature of 37.2 $^{\circ}$C was recorded at 1.30m/s daily average wind speed while efficiency has its peak value of 8.36%. It is therefore, indicates that efficiency and wind speed has positive correlation and negatively correlated with ambient temperature (Umar et al., 2014. Wind flow around a cylindrical trough solar collector had been investigated numerically. Ambient temperature was assumed to be constant at 300 K and for specific geometries different meshing methods and boundary conditions were used in various runs. Validation was done by comparing the simulation results for a horizontal collector with empirical data (Shojaee et al., 2015).

In this paper, the effects of collector absorbing surface increasing and its shape on the thermal performance of flat plate solar collector with forced air circulation. The collectors are connected with drying chamber by insulated ducts.

2. Experimantal setup

To achieve the goals of this paper, a double air-pass solar air collector had been constructed. Solar collector external dimensions are 120×50×15 cm length, width and thickness respectively. The external cases of collector is made from wood sheets and bars with different thicknesses with dimensions. For study purpose, two absorbing surfaces are made from copper sheet with 1.5 mm thickness and thermal conductivity 385 W/mK (see Fig. 1). To enhance these surfaces (increase absorptivity and decrease reflectivity) a black matt paint used to coat copper absorbing surfaces. A polystyrene material with thermal conductivity 0.038 W/mK is used as back insulation. Back insulation thickness is 2 cm and dimensions are 120×50 cm length and width respectively. A transparent glass cover fixed on the top edges of the collector wood case and thermal insulation at the bottom base side of the wooden case. A 4 mm thickness plastic glass sheet used to cover solar collector, to decrease the heat energy losses between absorber plate and the ambient.
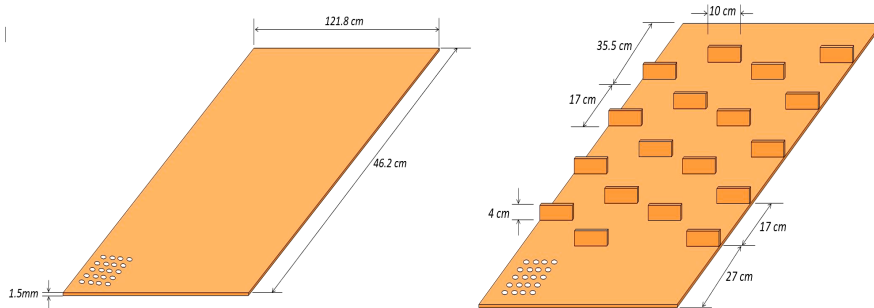

Figure 1. Finned and un-finned copper absorbing surfaces

The first absorber is flat absorber (un-finned) with dimensions 46.2×121.8 cm, while second absorber had made with the same dimensions of first surface with horizontal fins to increase its area of surface. 18 buffers (fins) are attached to the absorber with dimensions 10×4 cm length and width respectively. Fins function is increasing air streams length with the absorber surface to improve the useful heat transfer to the air. The space between every two buffers is 17 m. Areas of air heater inlet, exit and second channel entrance are the same, to avoid pressure reduction through solar collector. The solar system is energized by the sun's rays (solar radiation energy) passing through the solar heater (collector) glazing cover. The trapping of the solar radiation (short waves) is enhanced by the inside surfaces of the solar collector that were painted black to change it to heat energy (long waves). Then, the heat energy will transfer from the black absorber plate to the air which passing inside the collector by convection. The air recirculated from first to second air channel through 25 holes, which made on the absorber. Second air channel designed with using many wood buffers, which

fixed on back surface of solar collector. The remaining space between the absorber plate and glass cover represents the upper air flow channel with 50 mm height. Air circulates through the solar collector, air inline blower in air duct between solar heaters and surrounding has been used. The suction and discharge of blower is bigger than ducts with 10.5 cm diameter. The blower works with 12 V and 270 CFM.

It is important in the solar air collector components arrangements, tight any air leakage because the leakage of air will effect on the performance of the solar collector (especially air temperature) and decrease its thermal efficiency. According to Duffie and Beckman (2013) flat-plate solar collector tilted in a way that it receives maximum solar radiation during the day, and to be perpendicular with solar radiation rays at noon. The best stationary orientation is due south in the northern hemisphere and due north in southern hemisphere. Therefore, the two solar air heaters in this work are oriented facing south line and tilted at 45° to the horizontal according to the solar chart for Budapest region (Budapest 47.5^o N, 19.05^o E).

In these experiments, k-type thermocouples, digital thermometer, solar power meter and hot wire anemometer are used to measure system parameters. All of these instruments are calibrated in the rage of drying system performance before using them. Actually, the experiments are carried out on different days in July 2017 in the laboratory of mechanical engineering department of Szent Istvan University in Gödöllő.

3. Solar air collector model

Heat energy balance of the absorbing surface is obtained by equating the total radiation which gained from the sun rays through glass cover with transmittance (τ) to the total heat loosed from the absorber plate of the solar air collector. Therefore,

Solar radiation energy per unit area = useful heat +heat losses+ reflected radiation losses.

If τ is the transmittance of the glass cover sheet, I is the total solar radiation incident on the top surface of the solar air heater and A_c is the area of absorber plate, then mathematically the solar radiation per unit area will be:

Solar radiation per unit area = τ I A$_c$.

The solar radiation (Global) represents three components; beam or direct radiation, diffuse and ground reflected radiation. Experimentally, radiation had measured by calibrated solar sensor. Theoretically, Global solar radiation can be calculated according to the location and the time. For the reflected radiation losses from the solar collector, a mathematical expression can be given by the following:

$$\text{Reflected radiation losses} = \rho \, \tau \, I \, A_c.$$

Where ρ is the reflectivity of the absorbing surface. By the Substitution total solar radiation and reflected radiation losses expressions in the general energy balance equation for the absorbing surface, will get:

$$\tau \, I \, A_c = \text{useful heat} + \text{heat losses} + \rho \, \tau \, I \, A_c.$$

The summation of absorptivity, reflectivity and transmissivity of any surface equal one. The transmissivity of absorbing surface is zero. The useful heat energy, which gained from solar heater is: (Duffie & Beckman, 2013)

$$\text{Useful heat} = (\alpha\tau) \, I \, A_c - \text{heat losses}.$$

The above expression represents the energy balance equation for the absorbing surface. For this study, it is very important to estimate air temperature rise thorough solar heater. The change of air temperature through it depend on how much energy which absorbed (collected) by the absorbing surface. So the above energy balance is not enough useful to show the behaviour of air temperature.

In the direction of air stream, the inlet fresh air to the heater had carried some sensible heat which depends on its mass flow rate m_a and temperature $T_{c,i}$. The same for the outlet air, it had caught the heat from stored absorber plate energy by convection. Then, air had left the solar heater with the same mass flow rate and new temperature equal to $T_{c,o}$. By considering the heat energy content for inlet and outlet air, the final energy balance for the air solar heater will be:

$$\text{Useful heat} = (\alpha\tau) \, I \, A_c - \text{heat losses} + \text{inlet air heat content} - \text{outlet air heat content.}$$

Mathematically:

$$\frac{dT_{c,o}}{dt} = \frac{1}{M \, C_p}\Big[(\alpha\tau) \, I \, A_c - U \, A_c \, (T_c - T_\infty) + m_a C_p \, T_{c,i} - m^o C_p \, T_{c,o}\Big] \tag{1}$$

where M in Eq. (1) represents mass of air inside collector duct in (kg), T_∞ is the temperature of ambient air in (K), T_c is the average temperature of the absorber plate in (K), C_p is an air specific heat at constant pressure in (J/kgK), $\tau\alpha$ is called transmittance-absorptance product for glazed collector, for black colour absorber plate about 0.87. U represents the total energy losses from the flat plate solar collector in (W/m^{2}K) (Anderson et. al., 2009)

4. Results and discussion

In this part, the conditions of solar collector inlet, outlet and absorbing surface temperatures with the time of experiments are obtained. Also, the amount of heat which collected (useful) from solar radiation. The thermal efficiency of two types of

collectors had been obtained for these collectors. The velocity of air through solar collector is 2.5 m/s with 1.2 kg/m^3 density and 1000 J/kgK a specific heat at constant pressure. The duct which used to circulate air has 0.00635 m^2 diameter.

A trapezoidal rule has been used to calculate the amount of hourly and daily solar radiation and daily hourly useful energy. Trapezoidal rule is a method of numerical integration and can be defined as follow (Scheid, 1968). Fig. 2a and Fig. 3a show the variation of surrounding, average absorbing surface, inlet and exit temperature of solar collector for 5 hours of 25th of August 2017. As shown, air inlet and ambient temperature are approximately the same with very small difference. At the beginning of experiment, temperature difference very small up to low solar radiation and low temperature. The highest value of collector temperature differences for three collectors were between 13:40 and 14:40 that is because the radiation was at maximum values. Fins increased the area of absorber and it works as an air buffers. These buffers allow to air to still more time in collector duct, that is mean would heat more. The other function of these buffers is to trouble air flow streams, that is mean more friction forces generate between air and absorber.
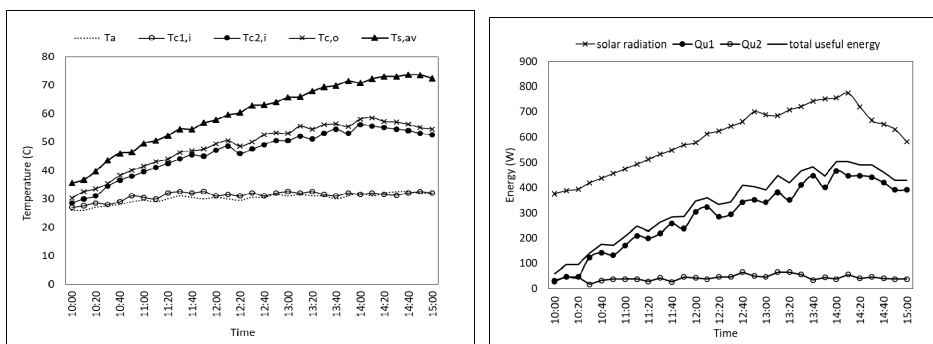

Figure 2. Performance of un-finned solar air collector with time of experiment
(a) Variation of inlet, outlet, absorber temperatures and ambient temperature
(b) First pass, second pass and total useful heat energy with solar radiation
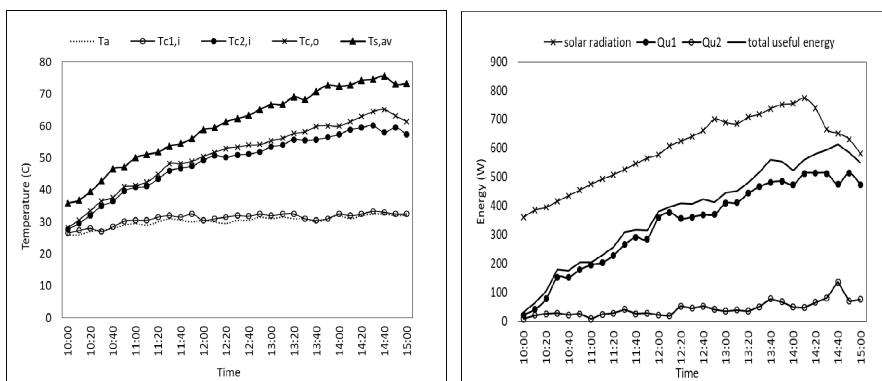

Figure 3. Performance of finned solar air collector with time of experiment
(a) Variation of inlet, outlet, absorber temperatures and ambient temperature
(b) First pass, second pass and total useful heat energy with solar radiation

Fig. 2b and Fig. 3b show useful heat curve which gained from solar collectors and solar radiation intensity after multiplying it by absorber area during 5 hours of experiments day. There are two components of useful heat, first from upper pass and second from the lower pass. As shown, the amount of total useful heat is the summation of two components of gains. In the first pass, lower channel worked as insulation. The outlet temperature of upper pass represent inlet temperature of lower pass. The effects of fins is very clear, where the maximum value of gained heat more than 600 W compared with un-finned collector with about 504W maximum useful heat. Actually, the increasing of absorbing surface area plays the main factor to increase solar collector performance. As explained before, also the turbulence flow of air will cause more friction forces.

Fig. 4 and Fig. 5 show daily useful heat, solar radiation and thermal efficiency which calculated by using numerical integration method. The thermal efficiency increased by 7.7% with using horizontal finnes to increase absorbing surface area. Actually this improvement was very acceptable compared with the costs of solar collector manufacturing.
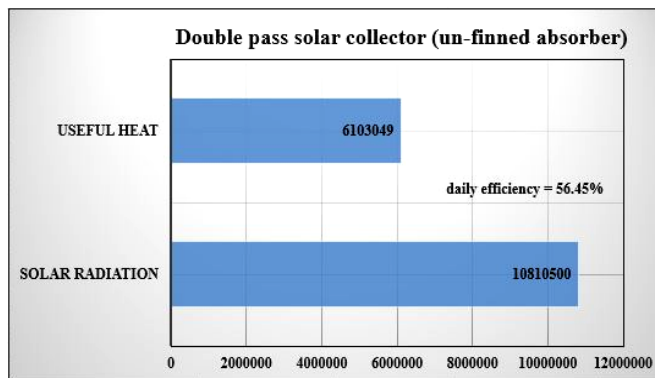

Figure 4. Daily total useful heat energy and daily solar radiation
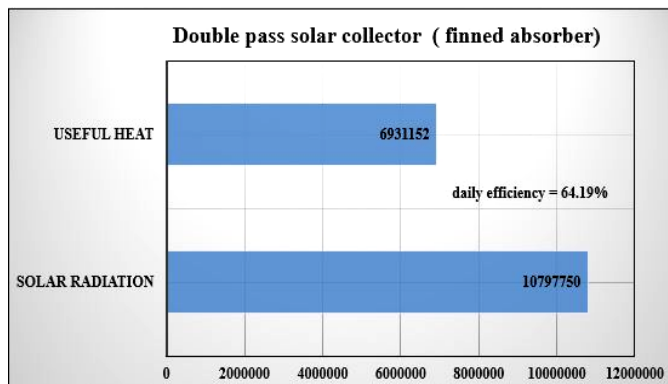of un-finned solar air collector.

Figure 5. Daily total useful heat energy and daily solar
radiation of finned solar air collector.

Conclusions

From the paper, many conclusions were deduced. The effects of fins was very clear. The maximum value of gained heat more than 600 W compared with un-finned collector with about 504 W maximum useful heat. The improvement of absorbing surface area by providing surfaces plays the main factor to increase solar collector performance due to flow turbulence of air. The daily efficiences of finned and un-finned collectors are 56.45% and 64.19% respectively. The thermal efficiency of collector increased by 7.7% with using finnes to increase absorbing surface area. From side of economic vesibility, the improvement was very acceptable compared with the costs of solar collector manufacturing.

Nomenclature

A	surface area	m^2
C_p	air specific heat at constant pressure	J/KgK
I	total solar radiation	W/m^2
M	air mass	Kg
m^o	air mass flowrate	Kg/s
Q_u	useful heat energy	W
T	temperature	K
U	overall heat loss coefficient	W/m^2 K

Greek letters

α	Absorptivity	----
P	reflectivity	----
τ	Transmittance	----

Subscripts

a	air	i	inlet
av	average	o	outlet
c	collector	s	surface

Acknowledgements

References

[1] Aboul-Enein, S., El-Sebaii, A.A., Ramadan, M.R.I. and El-Gohary, H.G. (2000), Parametric study of a solar air heater with and without thermal storage

for solar drying applications. Renewable Energy Journal, Vol. 21, pp. 505–522.

[2] Anderson,T., Duke, M. and Carson, J. (2009), Performance of colored solar collectors. The First International Conference on Applied Energy (ICAE09), January 5-7, 2009, Hong Kong, p. 8.

[3] Bunea, M., Eicher, S., Hildbrand, C., Bony, J., Perers, B. and Citherlet, S. (2012). Performance of solar collectors under low temperature conditions: Measurements and simulations results. CD-ROM Proceedings, EuroSun 2012, ISES-Europe Solar Conference, Rijeka, Croatia, September 18-20, 2012, p. 8.

[4] Duffie, J. and Beckman, W. (2013), Solar Engineering of Thermal Processes. Fourth edition. John Wiley & Sons. New Jersey. USA.

[5] Ekechukwu, O. and Norton, B. (1999), Review of solar-energy drying Systems II: an overview solar drying technology. Energy Conversion and Management Journal, Vol. 40, pp. 615-655.

[6] Mammadov, F.F. (2012), Estimation of flat plate solar collector productivity, International Journal on Technical and Physical Problems of Engineering, Vol. 4, pp. 35-40.

[7] Hayek, M., Assaf, J. and Lteif, W. (2011), Experimental investigation of the performance of evacuated-tube solar collectors under eastern mediterranean climatic conditions, Energy Procedia, Vol. 6, pp. 618–626.

[8] Madhlopa A., Jones S.A. and Saka J., (2002), A Solar Air Heater with Composite-Absorber Systems for Food Dehydration, Renewable Energy Journal, Vol. 27, pp. 27–37.

[9] Scheid, F. (1968), Numerical analysis. First edition. McGraw-Hill Book Company.

[10] Shojaee, S.M.N., Moradian, M.A. and Mashhoodi, M. (2015), Numerical investigation of wind flow around a cylindrical trough solar collector. Journal of Power and Energy Engineering, Vol. **3**, pp. 1-10.

[11] Umar, S., Kangiwa. U.M., Garba, M.M. and Yahya H.N. (2014), Effects of atmospheric variables on the performances of parabolic trough concentrating collector. American Journal of Energy Engineering, Vol. 2(1), pp. 23-26.

Experiments with phase change materials

P. VÍG

Department of Physics and Process Control, Szent István University
Páter K. u. 1., Gödöllő, H-2100, Hungary

Abstract

The thermal storage based on phase change materials (PCM) is a novel method. The recent work examines the thermal properties of Glauber's salt mixture for heat storage utilization. Outlines the studies are to stabilize the melting point of Glauber's salt, to present the measurements for the determination of the specific heat, melting point and the latent heat of the several mixtures containing different proportions Glauber's salt and sodium chloride and to examine the thermal inertia of the samples dependence of the sample sizes.

Keywords

PCM, Glauber's salt, salt mixture, melting point**,** thermal storage

1. Introduction

Nowadays, the role of the energy in our life is essential, as well as the issue of efficient energy storage both for electricity and heat. For storing the heat, coming directly from the environment, generated directly or with the help of an active heat generating device, (e.g. solar collector), there are various options. Long-time used method is the sensible heat storage (e.g. storing in hot water), which has two disadvantages: relatively low energy density and the useable temperature varies.

The thermal storage based on PCM is a relatively new method, where the latent heat can be used for tempering purposes. When the environment has higher temperatures than the melting point, the material melts and during the melting the PCM gathers heat from the environment, and when the temperature drops below the melting point the process returns, the material solidifies, and gives heat to its environment. If the PCM surrounds a given space the result of heat storage is that the fluctuations of the outside temperature is attenuated for the internal temperature. Thus, the energy needed to provide the constant temperature can be efficiently reduced with usage of PCM which change phase in the required temperature.

The PCMs can be classified into three major groups (Fig.1): aqueous solutions of salts (with below 0 °C melting point), paraffin and salt hydrate mixtures (the two latest with a melting point above 0 °C). Salt hydrate mixtures has the highest latent heat, therefore they can be used most effectively to tempering at around of their melting point (Árokszállási, 2012).
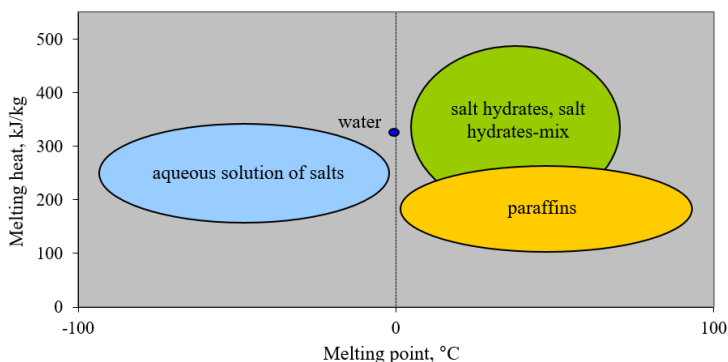
Figure 1. PCMs between -100 and 100 ^{o}C temperature range

Main application areas of PCMs are follows: in *construction industry*: tempering buildings (drywall, concrete, plaster); in *textile industry*: intelligent textiles; in *computer technics* as phase change memory; in *transport*: materials require a constant temperature, cooling vest, engine preheating. Research and application areas are growing on the topic.

The long-term objective of the research is to contribute to the costs reduction of crop storage by using aqueous solutions of salts for tempering purposes. Therefore as the first step among the various types of PCMs, the present work studies the Glauber's salt mixtures (Fig. 2).

Figure 2. Glauber's salt in anahydrate and decahydrate (melted and solid) form

This material first was studied and used for the storage of solar energy by Mária Telkes (Telkes, 1980), who was a pioneer in solar energy engineering. The usage of this salt as heat storage material was forced into the background because the high hysteresis of this material overheating and its reaction with its reservoir. With the development of material sciences the study of the usefulness of the Glauber's salt for tempering has been re-emphasized (Cabeza et al, 2011, Jiang and Tie, 2017).

Thermal properties of pure Glaubert's salt (Na_2SO_4 x $10H_2O$) are follows:

Melting point: 32.4 °C,
Melting heat: 240-254 kJ/kg
Heat conductivity: 0,544 W/mK
Density: 1485 kg/m^3

Readily available, unattractive after installation, relative inexpensive (the price of pharmacy quality is much higher but for this use the chemical quality is sufficiently pure, the price is 0.5 EUR/kg) are the advantages of usage Glauber's salt.

For the fixation of melting point and reduction the super-cooling hysteresis several methods may be used, e.g. Gök et al. (2006) used gelatin gel or solved the problem by using borax (which is salt, also), well mixed and dissolved (Garg et. al, 1985; Garcia-Romero et al, 2012). In my work, the latter method was also used to stabilize the melting point by adding 5% borax to the Glauber's salt.

The present study aimed to investigate the possibility of reducing the melting point of Glauber's salt with using Glauber's salt - sodium chloride mixture, determination the thermal properties (specific heat, melting point, heat of fusion) of this mixtures and to determine the thermal inertia (time constant) dependence of the mixture size.

2. Measurements

The measurements were elaborated in the Laboratory of the Department of Physics and Process Control, Szent István University, Gödöllő, Hungary. The masses were measured by a digital scale with 0.001 g accuracy, the temperatures were measured by thermocouples. The heat capacity of the used calorimeter was measured and converted to water equivalent (v = 6 g). For the parallel measurements (measuring rate was 2 seconds in each channel) and recording data a computer was used with an ADAM module (Fig. 3). To set the Glauber's salt dose in anahydrate form, 5% borax and the appropriate proportions of salt and distilled water were mixed. The resulting samples were placed in small, sealed sachets (Fig. 4).

Figure 3. Used equipment: scale, calorimeter, thermocouples,
ADAM module

Figre 4. The preparation of samples for measurements

In this form the temperature change of the mixtures can be effectively measured by thermocouples. Fig. 5 shows a sample prepared for measurement and the temperature of it as the function of time (8 g Na_2SO_4, 4 g salt, 10.14 g H_2O, 1.16 g borax) and the temperature of the cooling water in the calorimeter. The figure shows that the super-cooling, which in case of pure Glauber's salt is up to 15 ^oC, has been decreased with 2 degrees with the addition borax.
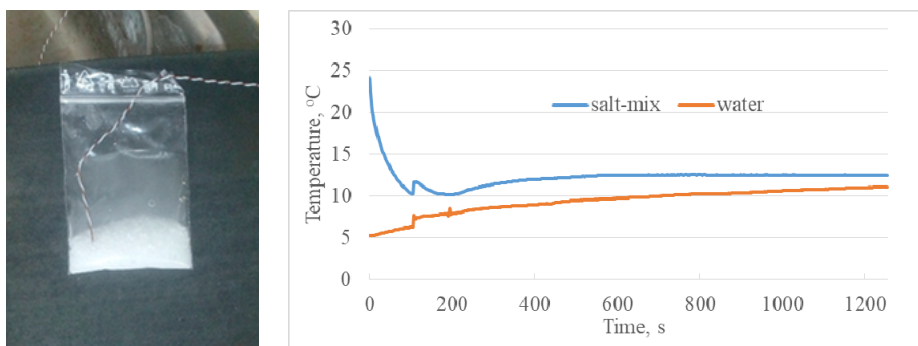

Figre 5. A sample and a measurement result

In the calorimeter 120 g of water and, the sample (with known mass) has been taken and the temperature of the water and the sample were recorded in every 2 second during the process.

3. Calculations

The equation of calorimetry (1) was the base for the evaluation of the measurement data:

$$Q_{up} = Q_{down} \tag{1}$$

From this equation, first the average specific heat in solid state and in liquid state were determined by separate measurements (with solid state and later on melted salt mixture) by the 2nd and 3rd equations,

$$c_s*m_{salt}*\ \Delta t_s = c_{w*}(m_w+v)_*\Delta t_w \tag{2}$$
$$c_l*m_{salt}*\ \Delta t_l = c_{w*}(m_w+v)_*\Delta t_w \tag{3}$$

and the latent heat can be calculated from equation (4):

$$c_s*m_{salt}*\ \Delta t_s\ +L_*m_{salt}+c_l*m_{salt}*\ \Delta t_l = c_{w*}(m_w+v)_*\Delta t_w \tag{4}$$

4. Results

1. Melting point dependence of the salt content of the mixture
The different vegetables and fruits have different optimal storage temperatures. For most of the fresh foods the optimal storage temperature is between 0-5 °C in the refrigerators, but there are many exceptions. For apple, citrus, melon, cucumber and potatoes the ideal storage temperature is between 7 and 10 °C, for bananas it is between 12 and 14 °C, and in case of tomato this value is 16 °C.

If the phase change of Glauber's salt mixture we would like to utilize for vegetables, fruits storage, it is necessary to reduce the melting point. By increasing the salt content the melting point is decreased. The mixture containing only borax and Glauber's salt has a 30.34 °C melting point. The melting point dependence of this mixture on the salt ratio is shown in Fig. 6.
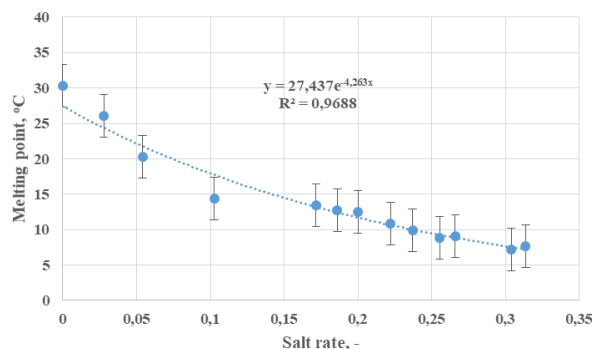

Figure 6. Dependence of melting point on salt concentration

In case of salt rate between 10 and 35% the melting point is between 7 and 15°C, so, it can be used for storage. During the calculation of the results 12.6% of relative error can be determined on the base of the error propagation law.

2. Specific heat and latent heat of the mixtures
For applying these mixtures the examination of how the addition salt affects the thermodynamic parameters is required. A left graph of Fig.7 shows a cooling process in liquid state (temperatures of mixture and water in calorimeter; salt

rate is 8.23%), and the right graph shows these temperatures in the solid state (this mixture contain only borax and Glauber's salt). Fig. 8 shows an example for the phase change of the mixture (mixture containing 23.7% salt).
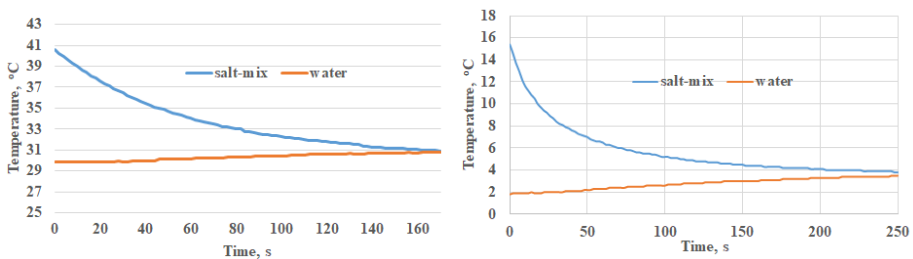

Figure 7. Examples for cooling in liquid and solid-state
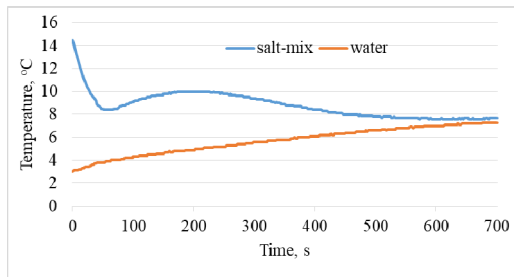

Figre 8. Example for phase change thermal behavior of mixture

The data of similar graphs gave the basics for determining the specific and latent heats. Fig. 9 shows the specific heats of mixtures in the liquid state.
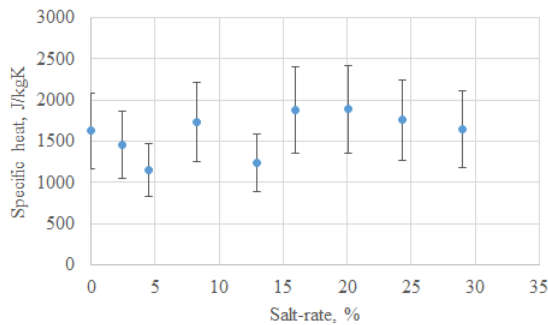

Figure 9. Specific heats vs salt rate

The specific heat values do not show significant difference if changing the ratio of salt. The values are lower than the specific heat of pure water. On the

basic of the measurement data the mixtures can be characterized by with average specific heat, and the melting heat values are between 94-140 kJ/kg. The results accuracy are 32%.

The determination of solid specific heat and melting heat with water bath is more difficult in case of larger samples. The part of sample which are in contact with the water bath reacts quickly to the temperature change while the inside parts of the sample follow this change more slowly. Therefore difficult to isolate the heat generated from the cooling of already solidified parts and the phase changing parts.

3. Dose optimization

The mixtures have poor thermal conductivity, so to define an optimal size is reasonable. Conditions for the optimal size: low thermal inertia and good encapsulation. The examination was performed for a mixture with a melting point around 8-10°C, which could be suitable for storing several vegetables, fruits. The temperature change of samples against the time during a heating and cooling is shown in Fig. 10. The samples containing different quantity from the mixture, they were put into the water bath together and their temperatures were measured in parallel.
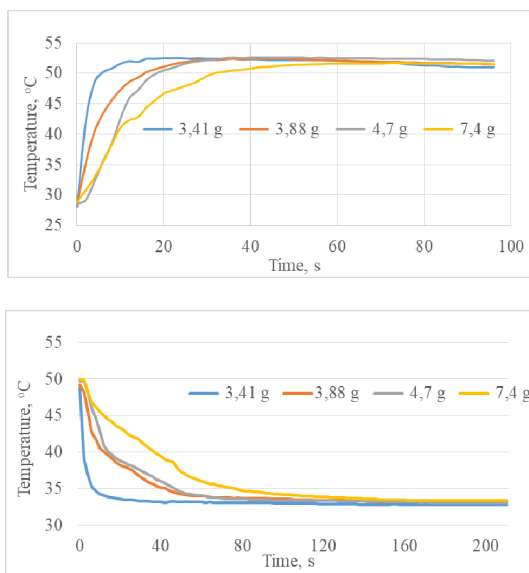

Figre 10. Thermal behavior of samples with different mass
for the optimal size determination

Fig. 11 shows the calculated time constants.

It can be observed that smaller samples have a shorter time constant, as expected, but may also be read from the graph that about 3 g of this mixture can be efficiently used for tempering.
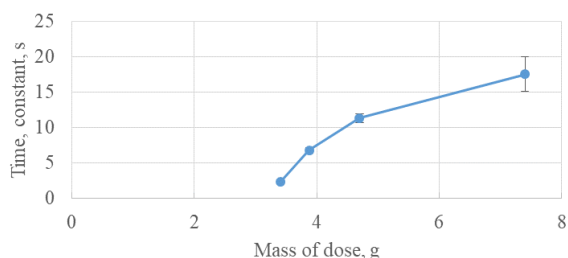
Figre 11. Time constants depending on the mass of dose

Conclusions

During the work, the melting points of the Glauber's salt-mixtures were determined as a function of the salt rate. It can be said that the melting point can be shifted to the desired lower temperature value by adding salt to the Glauber's salt, but the thermal parameters of these samples are less favorable than the pure Glauber's salt.

If the samples appear in smaller portions, the thermal inertia decreases, so thinking about encapsulation it is worth. The more accurate determination of the specific and melting heat values, the development the details of encapsulation and the analysis of the effectiveness of the application mixtures are the next tasks.

The results of the work can be used in building energetics for storing at special temperatures, for example to reduce the energy consumption of a fruit and vegetable storage process.

Nomenclature

c	specific heat	$Jkg^{-1}K^{-1}$
L	melting heat	Jkg^{-1}
m	mass	kg
Q	heat	J
v	water equivalent of the heat capacity of calorimeter	kg
Δt	temperature change	^{o}C

Subscripts

up	absorbed
down	emitted
w	water
salt	sample
l	liquid state
s	solid state

References

[1] Cabeza, L.F., Castell, A., Barreneche, C., Garcia, A., Fernandez, A.I. (2011), Materials used as PCM in thermal energy storage in buildings: A review, Renewable and Sustainable Energy Reviews, Vol. 15, Issue 3, pp. 1675-1695.

[2] García-Romero, A., Diarce, G., Ibarretxe, J., Urresti, A., Sala, J.M. (2012), Influence of the experimental conditions on the subcooling of Glauber's salt when used as PCM, Solar Energy Materials and Solar Cells, Vol. 102, pp. 189-195.

[3] Garg, H.P., Mullick, S.C., Bhargava, V.K (1985), Solar Thermal Energy Storage, Reidel Publishing Company, Boston

[4] Gök, Ö., Yilmaz, Ö., Paksoy H.Ö. (2006), Stabilization of Glauber's salt for latent heat storage, Proceedings of the 10th International Conference on Thermal Energy Storage, Ecostock 2006 Conference, Stockton University, New Jersey, USA

[5] Jiang, Z., Tie, S. (2017), Preparation and thermal properties of Glauber's salt-based phase-change materials for Qinghai–Tibet Plateau solar greenhouses, International Journal of Modern Physics B, Vol. 31, pp. 16-19.

[6] Ryu, H.W., Woo, S.W., Shin, B.C., Kim, S.D. (1992), Prevention of supercooling and stabilization of inorganic salt hydrates as latent heat storage materials, Solar energy materials and solar cells, Elsevier

[7] Saito, A., Okawa, S., Shintani, T. Iwamoto, R. (2001), On the heat removal characteristics and the analytical model of a thermal energy storage capsule using gelled Glauber's salt as the PCM, International Journal of Heat and Mass Transfer, Vol. 44, Issue 24, pp. 4693-4701.

[8] Telkes, M. (1980), Thermal energy storage in salt hydrates, Solar Energy Materials, Vol. 2, Issue 4, pp. 381-393.

Experiences with transparent pv module system

I. KOCSÁNY, I. SERES, I. FARKAS

Department of Physics and Process Control, Szent István University

Páter K. u. 1., Gödöllő, H-2100, Hungary

Abstract

Beside the existing educational photovoltaic systems, a new PV system was designed and constructed in the campus of the Szent István University, Gödöllő. The feature of the newly developed system is, that it consists of transparent photovoltaic modules, and it makes possible for plants to live below the PV modules (they can get enough light). In the paper the reasons of the selection of the location, and some detail of the construction together with the significant data of the system is presented. Based on the first operational data some analysis and comparison with the existing PV systems, based on different PV technology is shown, as well.

Keywords

Solar energy, photovoltaic module, energy production, spectral dependence, installation

1. Introduction

The Department of Physics and Process Control, Institute of Environmental Systems, Szent István University, Gödöllő, has a lot of different research topic connected to the renewable energy sources, and among them mainly to the solar energy. The research areas extend from the passive utilization of the solar energy (e.g. transparent wall insulation), through the solar drying to the examination of the different solar collectors. However these topics are important, nowadays the photovoltaic technology gets more and more important. In this field different research areas were investigated by the staff and the students of the department, for example analysis was made on the comparison of the energy production of the different PV technologies, or measurement were carried out on the spectral dependence of PV modules (Seres, 2014).

Nowadays two main types of photovoltaic module technology are widespread, the thin layer and the polycrystalline technologies. However our Department has numerous modules of each technologies to carry on research on them, a new PV system with new transparent type of PV modules were installed at the Gödöllő campus of the Szent István University. The system consist of transparent modules, which can be interested for special applications, where plants can live under the PV system, e.g. the modules can transmit enough light for the plants. This technology can be interested e.g. for greenhouses, where the transparent

modules are transporting enough light for the plants, and produce enough electricity to the operation of the electric devices.

The system was installed in front of the Aula building of the Campus above the plants of the air wells in the main staircase (Fig. 1).

Figure 1. The installed system in front of the Aula building of the campus

2. Technical parameters

As the installation has educational and research purposes, the power of the system was not the main criteria during the development. During the planning different brands were analyzed, finally the transparent modules of the Solarwatt Company were chosen. The system has the nominal power of 3,3 kWp, and consist of 2 x 10 pieces of Solarwatt Vision transparent modules (10 modules in each side in symmetrical distribution). The main characteristics of the modules can be seen in Tab. 1.

Table 1. The main technical data of the installed modules

Type of the collector modules	SolarWatt Vision 36M Glass
Technology	Monocrystalline
Covering material	Partly tempered high transparent float glass, 4 mm
Mechanical ratings	Applied load up to 6000 Pa
L x W x H / mass	1550 mm x 710 mm x 9 mm / 25 kg
No of cells	36 pieces
Transparency	20 %
Bypass diodes	2
Open Circuit Voltage	23.4 V
Short Cut Current	9 A
Nominal Voltage (under STC)	19.2 V
Nominal current (under STC)	8.7 A
Nominal power /module	165 Wp
Maximal system voltage	1000 V

The picture of the installed module type can be seen in Fig. 2.

Figure 2. The picture of the SolarWatt Vision 36M Glass module

However this location is not ideal for the system, as the PV modules face to almost west (a bit oriented to south), we decided to use this site instead of the flat roof of some buildings, for the visibility of the system. The other PV systems of the Department, a smaller 1 kWp stand alone system in the solar lab, a 10 kWp grid connected system in the top of the student hostel building, (Seres, 2006) are located far from the eyes of the students, and as they are dangerous areas, the students can visit them just under supervision in special cases. But we think, that the new technologies, e.g. the solar energy utilization will wide spread if only the new generation get accustomed to it, so if they meet every day with these devices. This was the main reason, that despite the location is not ideal for the maximal energy production, the busy and popular staircase of the main entrance of the Aula was chosen. The orientation of the developed system can be seen in Fig. 3.

Figure 3. The orientation of the staircase and the system (~ west)

3. The location and the construction

The system was constructed by one of the partner company of the Department. As the chosen location was the the air wells in the main staircase of the building, where plants were growing, it was a requirement, that the support system of the PV modules has to be hidden. Finally it was solved by screwing the holders of the support system onto the concrete walls of the wells, behind the plants, so now it is mainly invisible. For the ideal operation of a PV system the inclination angle (the angle of the module plane to the horizontal) is important, as well, but in our case we had to use the inclination angle of the staircase for the proper vision. That means, that the inclination angle of the system is lower, than the ideal inclination angle in Hungary.

Fortunately, below the staircase there is a closed yard, where the inverter of the system could be installed close enough, but safe from the meteorological effects (from the rain). From the inverter a direct line goes with the AC energy to the power grid centre of the building, about 20 m far. The produced energy is fed to the electric grid of the building.

4. Measurements and results

The energy production of the system is solved by a smart inverter, where the inverter collects not just the system size power data, but each module is measured separate. The measurement data are saved in every 15 minutes (12 minutes averages), and it can be read out in daily, weekly, monthly and yearly base. However the inverter producer provide free internet based service for storing the measured data, for safety reasons an own data logger computer was set up, and a software was constructed to read out and store the operational data locally, as well. The actual energy production data are shown for the interesting student as well, through a large monitor in the buffet of the faculty (Fig. 4.)
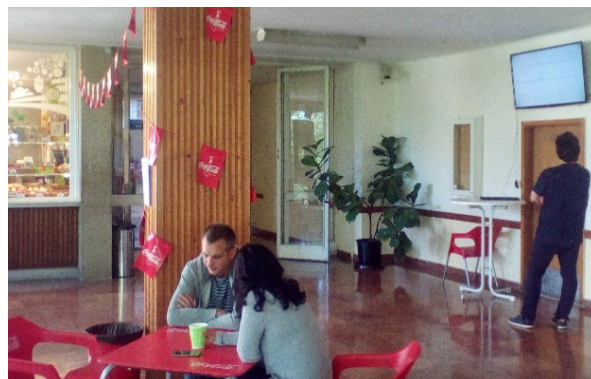

Figure 4. Informing screen about the operation
in the faculty buffet

After the first period of operation, enough data were collected to start to analyze the operation of the system. The energy production of the system for the first whole month of its operation, for July, 2017 can be seen in Fig.5. (daily distribution).
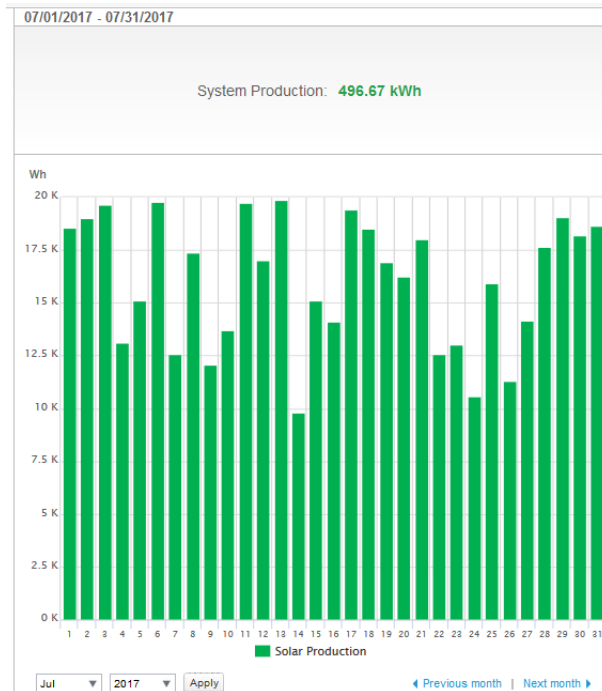

Figure 5. The daily distribution of the energy production in July, 2017
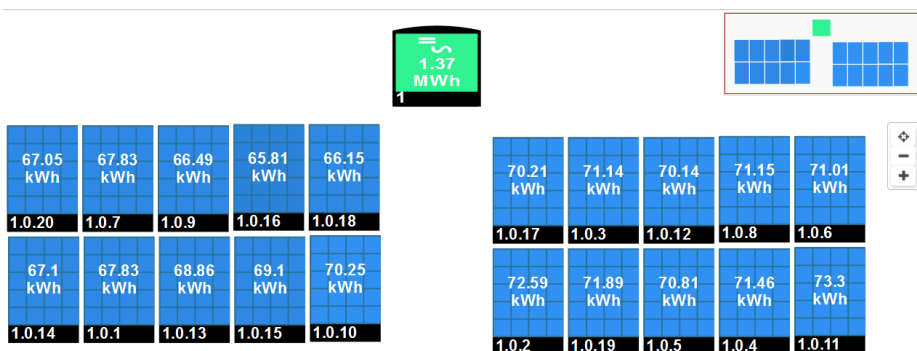

Figure 6. Energy production of the different modules

Another very useful option of the data logger, that not just the system production, but the production of the separate modules can be analyzed, as well.

For example in Fig. 6 the total (yearly) energy production of the modules in the physical layout can be studied.

From the data, it can be seen, that however the modules are theoretically identical, their energy production differs by about 10 %. The reason of the difference can be the different shading, before sunset the left side of the system get some shading, while the right part get it later. The differences inside the two blocks hopefully are originated just from stochastic effects (e.g. small clouds), and will be equalized during longer time.

5. Comparison the new system to the existing ones

During the analysis of the system production the measured energy values can be compared to the energy production of the other PV systems, operated by the Department. The comparison is made between the polycrystalline ASE modules, the amorphous silicon DS modules and the transparent (TRA) systems.

In Fig. 7 the energy production distribution is given for the first few days of operation
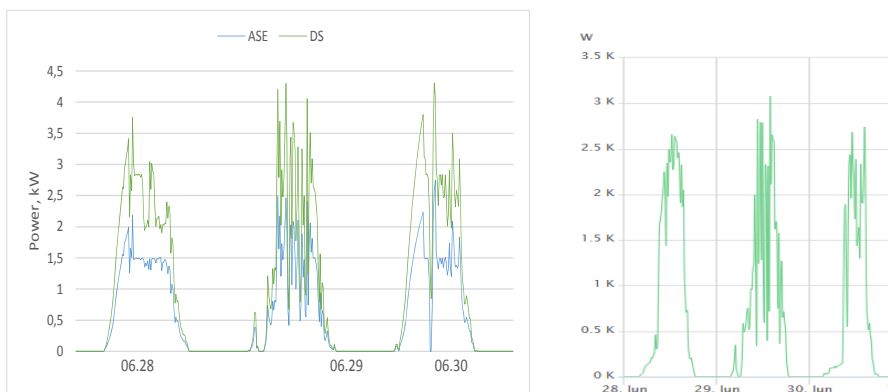
Figure 7. Power distribution of the ASE, DS and TRA systems

The different shape of the graphs originates from the different orientation (the ASE and DS systems has south orientation, the TAR has west). For the comparison the specific energy production (the energy production divided by the nominal power of the system (3.5 kWp for the ASE, 3.1 kWp for the DS and 3.3 kWp for the transparent -TRA) is used.

The energy production data of the first days of the operation (kWh):

day	ASE	DS átlag	TRA
06.28	15.09	10.28	16.565
06.29	12.53	8.73	15.5
06.30	14.79	11.35	13.542

The specific energy production for the same days (kWh/kWp):

day	ASE	DS átlag	TRA
06.28	4.31	3.32	5.02
06.29	3.58	2.82	4.70
06.30	4.23	3.66	4.10

From these data it can be seen, that the newly developed system in spite of the not ideal orientation produces higher specific energy than the other type of PV modules.

Conclusions

In the paper the setup of a 3.3 kWp grid connected PV system is shown, which was build up with transparent PV modules. During the work the reasons for the selection of the location, the technical details of the installed systems and the first operational data are presented.
From these data it can be concluded, that in spite of the not ideal orientation of the system, its specific energy production is higher, than the specific energy production of the other installed systems in the campus.

References

[1] Seres I, Farkas I, Kocsis L: Development of a 10 kWp photovoltaic system - installation and operational results, In: Burek S, Hutchins MG, Lockhart Ball H, Abrahamson S (szerk.) EuroSun 2006 : European solar conference. Glasgow, UK, 2006.06.27-2006.06.30. Abingdon: The Solar Energy Society, 2006. pp. 1-6. (ISBN:0904963731)

[2] I Seres, I kocsány, I Farkas: Spectral dependence of different PV module technologies, MECHANICAL ENGINEERING LETTERS: R AND D: RESEARCH AND DEVELOPMENT 11: pp. 116-123. (2014)

[3] K.E.Park, G.H.Kang, H.I.Kim,, G.J.Yu,,J.T.Kim: Analysis of thermal and electrical performance of semi-transparent photovoltaic (PV) module, Energy, Volume 35, Issue 6, Pp. 2681-2687 (2010)

[4] https://www.solarwatt.de/-/media/website-de/pm/datenblaetter/module/data-sheet-36m-l-glass-de.pdf

A simulink library for solar energy applications

J. TÓTH, I. FARKAS

Department of Physics and Process Control, Szent István University
Páter K. u. 1., Gödöllő, H-2100, Hungary

Abstract

This paper deals with the creation of a development environment for block-oriented modelling of the solar thermal systems. The library block contains 6 initial modules as collectors, controllers, storages, pipes, dryers and chimneys. Recently, two main components, e.g. the collector and the controller units of this system were elaborated and presented. The possible application of the developed blocks was also demonstrated along with the detailed description of the model and its parameter identification, validation and simulation issues.

Keywords

solar thermal, development environment, MATLAB, simulation, validation.

1. Introduction

The development of solar systems is highly speeded up in the recent years. Quite a lot of experiments were made and a lot of prototype systems were built. It is fact, that it is expensive to build a real physical system to do experiments. With the aid of the computer assisted modelling methods, however, such costs can be reduced. The algorithms developed so far were created for a specific task and they not provide too much flexibility.

In this study, the main focus of this development is the solar thermal systems. These systems can be divided into several main tasks which are: collection of the energy, storage of the energy, circulation of the working fluid, controlling the working fluid. Beside such main tasks other components are also play role in the working process, for example the pipes and the expansion tank.

The above mentioned tasks can be modelled separately, and this way the entire system became a collection of individual models linked together. The advantage of this approach is that one can find accurate mathematical models of the parts of a solar thermal system (Stuckmann, 2008), but the implementation of a complex mathematical model can be complicated in the wrong environment. There were attempts to create a development system in the past (Farkas et al., 1997), due to the technical limitations remained in an early stage.

There are working solutions, which use the same approach for design. For example ithe TRNSYS software (Kyn et al., 2013; TRNSYS, 2009) or the Polysun software (Lacoste et al. 2010). The reputation of such softwere shows the potetial in

this field and a need for a reliable slution for educational intent. The commercial software are proven-to-work, and they are used mainly by the designers.

The MATLAB + Simulink software package, made by MathWorks, is an ideal choice for the base of this environment. Ordinary differential equations, which are the most obvious descriptors of these devices, can be solved with these programs by long-time tested, proven-to-work numerical methods (Ashino et al., 2000). The Simulink is a block-oriented modelling tool for simulations and it supports all the necessary basic element for a more complex system, such as a solar energy device.

This paper is dealing with these platforms. The purpose is to presents the creation of a development environment for solar systems, where one can make unique devices based on a set of predefined building blocks.

2. Block-oriented modelling approach

The block-oriented modelling approach is a modelling technique, where the model is divided into "blocks". A block is basically a function with input and output variables and the model is the relation of the blocks. The main advantages of this modelling are the visual representation and modularity. A model can be viewed as a "wiring diagram" and it gives a good intuition on the underlying mechanisms. The modularity plays role, when the changing of a model means changing of some of its blocks. In this paper a block-oriented development environment will be presented, which is a Simulink library, a collection of solar thermal energy related models.

The modularity was the main aspect during the design of the library. The main goal of this development to create an easy-to-expand library/environment, so one can make additional modules depending on the task.
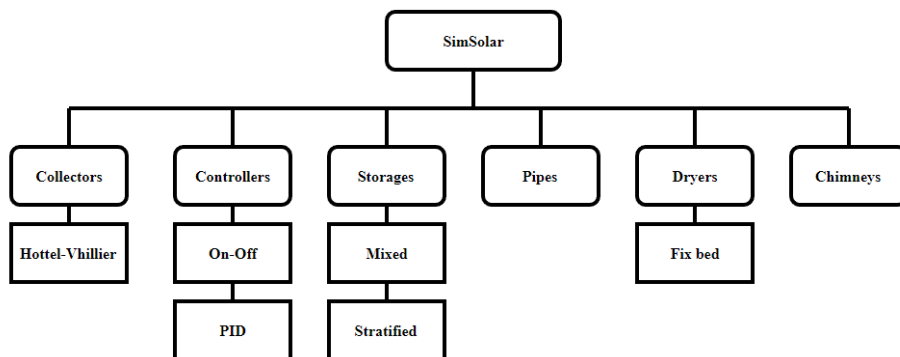

Figure 1. Architecture of the library blocks

The main modules of the system are shown in Fig. 1. These are the planned modules, and because of the design of the system, can be added later with ease.

The library will contain 6 initial modules: collectors, controllers, storages, pipes, dryers and chimneys. Each module contains several models that fall into the category of the module.

3. Developing a solar collector model

In this section a development of the Hottel-Vhillier (H-V) model and its possible application is described.

H-V model
In this paper a collector model (Hottel-Vhillier) and a controller (On-Off) will be presented. The first step was to create a simple collector model. For this we used the Hottel-Vhillier model (Farkas, 1999), as follows:

$$T(x,\tau) = T_w(\tau) + \frac{I(\tau)}{k_{aw}} + \left(T_{in}(\tau) - T_w(\tau) - \frac{I(\tau)}{k_{aw}} \right) \exp\left(-\frac{k_{mw}wx}{c_m \dot{m}} \right). \quad (1)$$

This model is simple enough to build and perfect for testing the capabilities of this environment. The following figure (Fig. 2) shows the implementation of the model.
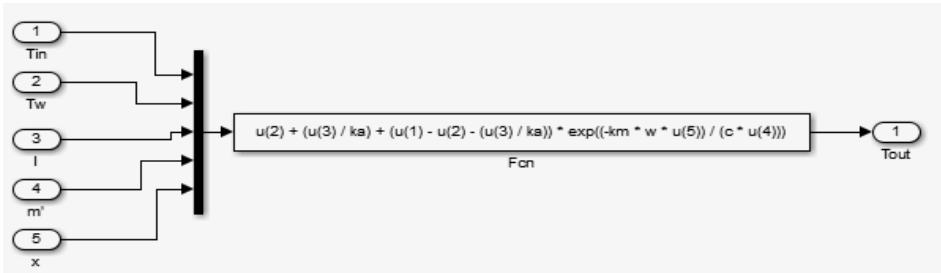

Figure 2. Simulink implementation of the Hottel-Vhillier model

Application of the H-V model
The next step was to identify then verify the developed model. Previously measured data has been used for this purpose. The data were for a specific collector, where the length and the width of the device, the k_{aw}, k_{mw} coefficients and the specific heat of the working fluid are the parameters of the model, these constants should be changed if one wants to simulate a different device.

The temperature of the input working fluid and the mass flow rate of the pump are system specific values.

The environmental effects are the global radiation and the environmental temperature, these values change over time and the purpose of the simulation to calculate the output of the system given these inputs.

The system, used in the identification/validation process, has the following parameters:
 – width of the collector: 0.95 m,
 – length of the collector: 1.91 m,
 – mass flow of the pump: 0.057 kgs^{-1},
 – working fluid: water.

The Figs 3-4 show the measured input variables used for identification of the Hottel-Vhillier model.
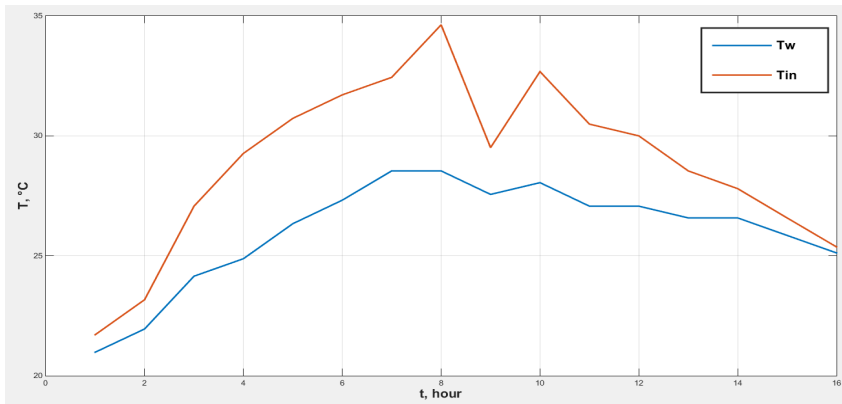
Figure 3. Measured temperature data
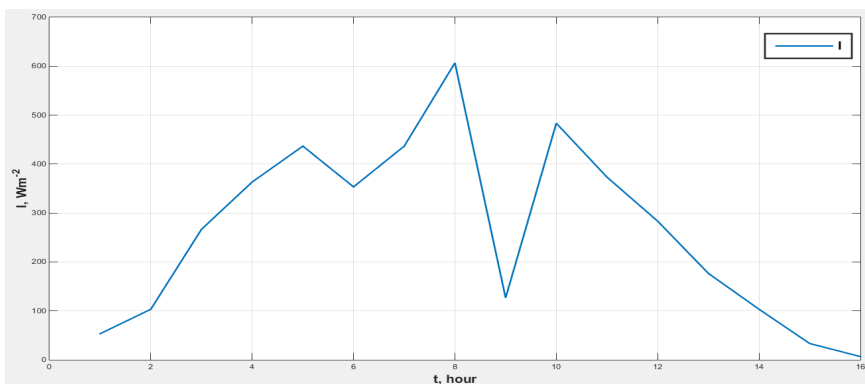
Figure 4. Measured radiation data

A subsystem from the block model in Fig. 2 was created with the option of changing the parameters, so the handling of the block became much easier.

In the identification task means to find the k_{aw} and k_{mw} coefficients, because these parameters most of the cases are not given by the collector manufacturers and also hard to measure. With the measured output temperature this task is possible through a minimalization process which is available within the MATLAB + Simulink system.

During the validation process a different set of measured data was used to calculate the difference between the measurements and the simulation results of the model with the properly identified parameters. After the simulations the accuracy of the model, the correlation between the data sets and the correlation coefficient can be specified which measure the goodness of the model and, based on these, the model was certainly valid. After all, the model is ready to carry on simulations on it with the identified coefficients.

The already mentioned subsystem of the collector is designed in such a way that the user can easily enter the necessary constant values for the device, as it can be seen in Fig. 5. The first results of a simulation are shown in Fig. 6. Based on the results, it can be ensured that the model is right an the environment is capable of developing other parts of a solar thermal system.
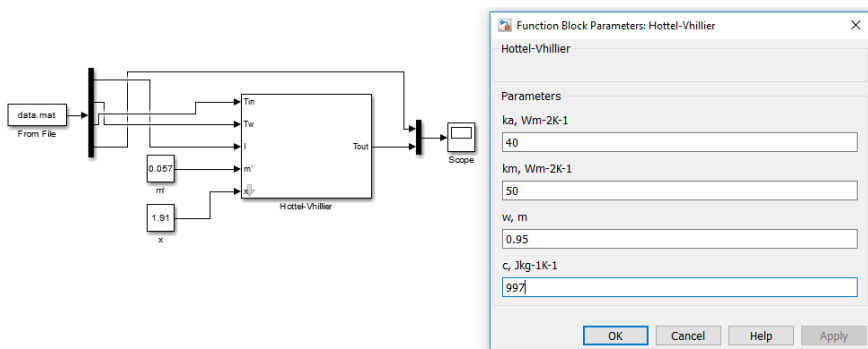

Figure 5. Input parameter layout of the collector model
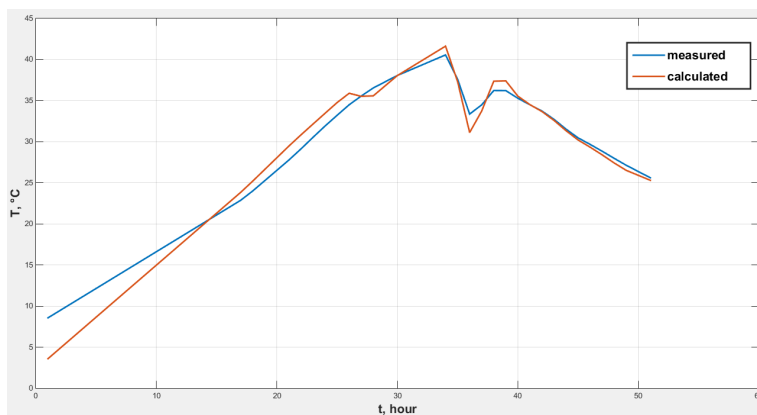

Figure 6. Result of the simulation and the measured data

4. Developing of the controller model

In this section a development of an On-Off controller model and its possible application arrangement are described.

On-Off controller

With the properly working collector model described before, the controller part of a solar thermal system was implemented.

For the controlling device, an on-off controller was chosen. It has a binary controlling algorithm, because there are only two possible outputs, usually a low and a high-level signal. Simulink system has got a built-in block with the same behavior, it's the Relay block. That was actually used for the modelling of the controller operation.

Application of the On-Off controller

For the previously verified model a sine wave generator was used, with the properly picked gain for the periodically changing input radiation and environmental temperature. The input temperature was set to constant 20 °C and the set point was 22 °C with 3 °C hysteresis.

The controlled parameter of the system was the mass flow rate of the pump. The implemented model, which works in a proper way, is shown in Fig. 7.
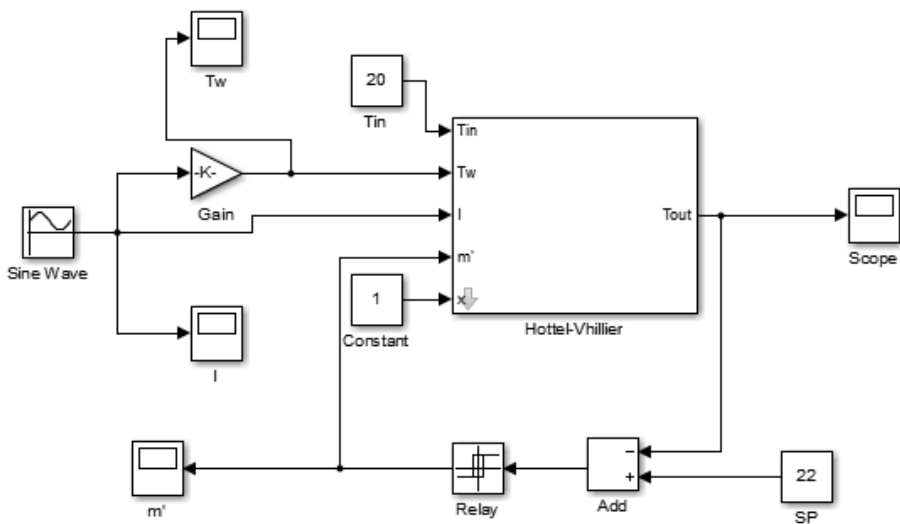
Figure 7. Collector with a controller unit

Conclusions

A block-oriented modelling environment based on the MATLAB + Simulink system was elaborated for the use of solar thermal applications.

First, a solar thermal collector model was created. That model was identified and validated for a given example using the measured data.

The verified collector model was also used to control the solar thermal system. Accordingly, another important module of the library was created and tested, which is the controller unit.

The further development will be the creation of the new modules, e.g. storage, and the creation of the more sophisticated version of the already existing ones.

Nomenclature

c	specific heat	$Jkg^{-1}K^{-1}$
I	solar radiation	Wm^{-2}
k	parameter of the heat transfer	$Wm^{-2}K^{-1}$
ṁ	mass flow of the working fluid	kgs^{-1}
T	temperature	K
w	width of the collector	m
x	length co-ordinate	m

Greek letters

τ	time	s

Subscripts

a	absorber
in	input
m	working fluid
w	environmental

Acknowledgements

References

[1] Ashino, R., Nagase, M., Vaillancourt, R. (2000), Behind and Beyond the MATLAB ODE Suite, CRM-2651

[2] Kyn, M., Urban, M. (2013), TRNSYS Software Model of Solar System with Long-Term Storage, Advanced Materials Research Vol. 649, pp. 303-306.

[3] Lacoste, B., Wolf, A., Witzig, A., Marklin, A. (2010), Polysun: PV, Wind and Power-Heat Cogeneration in one Design Tool, Proceedings of the 5th European PV-Hybrid and Mini-Grid Conference, pp. 1-8.

[4] Farkas, I. (1999), Computer simulation, p. 45.

[5] Farkas, I., Bíró, A., Buzás, J. (1997), Climate control in a solar operated laboratory greenhouse, Mathematical and control applications in agriculture and horticulture, IFAC Workshop, Hannover, Germany, pp. 43-48.

[6] Struckmann, F. (2008), Analysis of a flat-plate solar collector, Project Report, 2008 MVK160 Heat and Mass Transport, Lund, Sweden

[7] TRNSYS Manual, 2009, Vol 1.
http://web.mit.edu/parmstr/Public/Documentation/01-GettingStarted.pdf, [downloaded: 2017.09.29.]

Symmetry analysis of incommensurate condensed matter systems by symmetry theory of Q1D systems

Cs. MÉSZÁROS[1], Á. BÁLINT[2]

[1]Department of Physics and Process Control, Szent István University
Páter K. u. 1., Gödöllő, H-2103, Hungary
[2]Institute of Environmental Engineering
Óbuda University, Doberdó u. 6. H-1034 Budapest, Hungary

Abstract

The detailed experimental and theoretical research of basic structural characteristics of carbon nano-tubes plays a role of increasing importance in the condensed matter physics. The symmetry analysis of these properties of such materials represents a crucial part of these investigations. Within them, research activities connected to possible applications in solar cells became very significant. In the present study, we demonstrate some possible and promising techniques of the same modelling methods relevant for chain-type molecular systems, which may contribute to understanding and increase of the energy transformation efficiency in solar energetics.

Keywords

incommensurate structures, line groups, collective elementary excitations, solar elements

1. Introduction

One of the basic problems of the contemporary condensed matter physics is, that the classical crystallographic symmetry theories cannot cover the factically existing (experimentally confidently proven) structure symmetries of all the correlated condensed matter systems, which are e.g. nevertheless able to scatter X-rays, neutrons or electrons coherently. Some earlier studies about applications of the theory of line groups (which are the exact symmetries of the quasi-one-dimensional (Q1D) discrete systems) were mainly related to structural investigation of polymers e.g. (Vainshtein, 1966), (Elliott, 1969). Despite of these very succesful experimental application areas, the abstract theory of line groups, as well as the representation theory of its have also been further improved and elaborated in detail many years later (Vujičić et al., 1977). The technique of line groups has also become very succesful in the detailed analyses and interpretation of the basic structural-, and various-type physical properties of

carbon-nanotubes (Barros et al., 2006), (Damnjanović and Milošević, 2010). This relatively new research domain of the condensed matter physics may play a decisive role in the future solar energetics, too. In the present concise study, a new approach for solving of problems emanating from the structure descriptions indicated above will be presented, based on some well-established methods of the group representation theory, widely applied in the most generalized description of transformation groups, too. It is also an intention of ours to apply the projective representations (such types of representations of classical crystallographic point-, and space groups have been well-established mathematical tools in different areas of molecular-, and crystal physics from both macroscopic and microscopic points of view for decades e.g. (Birman, 1974), (Hamermesh, 1989)) of line groups in our forthcoming later studies in a completely novel manner for describing incommensurately modulated crystals, despite of the fact, that the complete systems of projective representations of line groups are (at least according to our knowledge) still absent in the literature about symmetries of Q1D systems. Therefore, it may be stated with confidence, that the representation theory of symmetry groups of the discrete infinite chain-type systems still belongs to the completely open areas of the contemporary algebra. In our forthcoming discussion, we will limit ourselves to applications of mathematical methods from this area, which have already been established as very effective tools at evaluating very different types of experimental results. Among them, the symmetry analysis methods reviewed in this paper have particularly successfully been applied at evaluations of spectroscopy results of very different types of chain-type condensed matter systems.

2. Some basic elements of the contemporary line group theory

According to the definition, the complete set of symmetry transformations leaving invariant a *Q1D* system belongs to one of the (discrete) infinitely many line groups, which are gathered into 13 families (Vujičić et al., 1977), (Barros et al., 2006), (Damnjanović and Milošević, 2010). The irreducible representation $D^{(\mu)}(\underline{L})$, of a full line group $\underline{L}$ can be obtained from the irreducible representation of symmetry group (i.e. point group) of the motif (monomer) itself $D^{(\nu)}(\underline{P})$, by use of the induction technique (elaborated within frame of the general group representation theory and widely applied in different areas of the contemporary solid state physics for decades e.g. (Streitwolf, 1967), (Birman, 1974)), usually denoted by $D^{(\mu)}(\underline{L}) = D^{(\nu)}(\underline{P}) \uparrow \underline{L}$). For the most basic - type line group Ln_p, the relevant irreducible representation matrix expression is:

$$_k A_m \left(C_n^s \left| Fr\left(\frac{sp}{n}\right) + T \right. \right) \equiv e^{ims\alpha} \cdot e^{ik\left[Fr(sp/n)+T\right]_a^{\Gamma}},$$

(1)

where $\overset{1}{a}$ is the generating element of the subgroup of pure and integer translations of $\underline{L}$ (i.e. symmetry transformations, which interconnect the motifs being arranged regularly along the main axis of the infinite, discrete chain-type system under investigation) and the symbol $Fr(\xi)$ denotes the fractional part of a quantity „ξ", and the product factor corresponding to the purely orthogonal part (i.e. point group transformation) of the line group is given by:

$$g \equiv C_n^s \Rightarrow A_m\left(C_n^s\right) = e^{ims\alpha}, 0 \le s \le (n-1), \alpha = \frac{2\pi}{n}. \tag{2}$$

Therefore, if we consider the most basic line group, which may be assigned to discrete helical systems: $Ln_p = (n/r) \otimes C_q^a$ (i.e. which is given as a direct product of the group of generalized translations (n/r) and the (cyclic discrete rotational) point group C_q^a), the following general form of the irreducible representation of its may be derived:

$$_k A_m\left(\left(C_n^r\big|n\right)C_q^s\right) \equiv e^{ikt\zeta}e^{imsa}, k \in \left(-\frac{\pi}{\zeta}, +\frac{\pi}{\zeta}\right], \tag{3}$$

where ζ denotes the distance between nearest-neighbour scattering centres in a helical system, while k is a wave-vector, whose possible allowed values according to the Born-Kármán cyclic boundary conditions relevant for Q1D systems denote the nonequivalent irreducible representations of the subgroup of generalized translations (n/r).

3. Connections of the symmetry theory of the infinite discrete chain-type systems with some earlier algebraic formalisms

In this section we will represent the essential result of the present study on the base of the general symmetry methods described in (Vujičić et al., 1977), based on the well-known method of group extensions formally described by sequences of homomorphisms of groups and their subgroups. The main motivation for this further refinement of the abstract algebraic part of the recently existing variant of the general line group theory is, that the infinite correlated systems, which may be characterized by (at least:) two, or even more translationally invariant subsystems may be treated in a very general manner. Accordingly, if a line group L is composed from line groups L_1 and L_2 (in the sense of the generalized semi-direct product (Vujičić et al., 1977) of them) which have the same translational subgroup T, its relevant point group P is in relation $P = P_1 \wedge P_2$ with

the point groups of the constituent line groups. Then, the following condition (explained by point group elements „R" and basic fractional translations „v") must be satisfied:

$$v_2 + R_2 v_1 - R'v_2 = v' + t, t = 0, \pm 1, \pm 2, \ldots \tag{4}$$

where $\left(R_1 \middle| v_1\right)$ and $\left(R_2 \middle| v_2\right)$ are any coset representatives in L_1 and L_2, respectively and the relation $R' = R_2 R_1 R_2^{-1}$ is also valid. Furthermore, if we compare this condition with the one emanating from the general treatment of basic properties of the unimodular group in two dimensions (i.e. characterized by three (continuously varying) parameters), defined by use of the elementary linear transformation formulae $\hat{g}_a x = x' = a_1 x + a_2, \hat{g}_b x' = x'' = b_1 x + b_2$, it is possible to define e.g. (Hamermesh, 1989) the one-dimensional projective group represented by

$$\zeta \to \frac{a_1 \zeta + a_2}{b_1 \zeta + b_2}. \tag{5}$$

Then, the relevant most general conjugate transformation $g_a g_b g_a^{-1}$ from the unimodular group is realized by

$$a_1 x + a_2 b_1 - a_1 b_2 = x' - b_2. \tag{6}$$

Although the simultaneous application of the formulae (4-6) may explain the essential symmetry features of two different translationally invariant (with translational invariance in the same direction, but with generating elements, which cannot be interrelated with integer numbers) *Q1D* systems, this possible connection has not been applied in detail in the case of incommensurately modulated condensed materials. Finally, as a closing remark of this section, it must be emphasized here, that the generalized variant of (5) serves as a genuine mathematical basis (e.g. (Hamermesh, 1989), pp. 459) for creating the projective representations of the discrete groups discussed here, too.

5. Symmetry analysis of raman-type collective elementary excitations in incommensurate systems

In the present section a novel-type application of representations of line groups will be proposed for obtaining selection rules relevant for collective elementary excitations at Raman-type scattering processes. Besides, the same types of descriptions of the collective elementary excitations in molecular crystals (i.e.

excitons (Agranovich, 2009)) may also lead to remarkable new results. In order to sketch this programme, we start here from the basic group-theoretical relation relevant for analysis of the possible quantum-mechanical transitions from given initial („i") to allowed final („f") states of atoms, molecules, crystals (Streitwolf, 1967), (Hamermesh, 1989):

$$D_i^+(G) \otimes D^{pv}(G) \otimes D_f(G) \ni D^{(1)}(G), \tag{7}$$

where the upper index „+" refers to an adjoint representation of G, and $D^{(1)}(G)$ is the unit representation of the same group. For the sake of simplicity, it will also be assumed here, that all representations of the group G in (7) are already irreducible representations. Then, using the relevant character functions, the above presented well-known method for selection rules will directly lead to the following important relation, realized by explicit use of the character functions (Streitwolf, 1967):

$$n = \frac{1}{|\underline{P}|} \sum_{\alpha \in \underline{P}} \chi_{\vec{k}_1'}^* \left(a_0^{'-1} a a_0'\right) \chi_{\vec{k}_1''}'' \left(a_0^{''-1} a a_0''\right) \chi_{\vec{k}_1} \left(a_0^{-1} a a_0\right), \tag{8}$$

where the coset-representatives have the form $a \equiv \left(\alpha | \vec{v}_\alpha\right)$ and $\underline{P} = \underline{P}_{\alpha_0' \vec{k}_1'} \cap \underline{P}_{\alpha_0 \vec{k}_1''} \cap \underline{P}_{\alpha_0 \vec{k}_1}$. Then, for the allowed quantum-mechanical transitions in the given systems possessing translational invariance, too, according to the formulae (7) and (8), the following selection rules must also be satisfied:

$$-\alpha_0' \vec{k}_1' + \alpha_0'' \vec{k}_1'' + \alpha_0 \vec{k}_1 = \vec{K}, \tag{9}$$

where, as usual, the vector $\vec{K}$ is composed by linear combinations from the basic reciprocal lattice vectors with integer coefficients. In order to apply the same description method to incommensurately modulated crystals, the relevant specific characteristics of line groups must also be taken into account (Kirschner and Mészáros, 2001). Then, the relevant selection rules (in the sense of the relation (9)) can be written as

$$\Delta k \equiv k_f - k_i = k + \frac{2j\pi}{\zeta}, (j \in \mathbb{Z}), \tag{10}$$

and

$$\Delta m \equiv m_f - m_i = m + zq, (z \in \mathbb{Z}), \tag{11}$$

i.e. beyond the usually applied selection rules (10) emanating from the conservation of quasi-impulse in a given, translationally invariant discrete system, the selection rules (11) related to conservation of the quasi-angular momenta in the same type of (Q1D) condensed matter systems must also be taken into account.

Conclusions

The selection rules relevant for discrete infinite Q1D systems must be incorporated into the quantum-statistical formalism of excitons propagating through molecular crystals.

By taking into account the well-known structural properties of carbon-nanotubes, and other not strictly - crystallographic type condensed matter systems, which are able to scatter incoming electromagnetic waves and particle beams coherently, it is necessary to extend the whole above-discussed formalism to quasi-two-dimensional (Q2D) (i.e.: layer-type-) discrete systems, too.

References

[1] Agranovich, V., (2009), Excitations in Organic Solids, International Series of Monographs on Physics, University Press, Oxford

[2] Barros, E. B., Jorio, A., Samsonidze, G.G., Capaz, R.B., Souza Filho, A.G., Mendes Filho, J., Dresselhaus. G. and Dresselhaus, M.S. (2006), Review on the symmetry-related properties of carbon nanotubes, Physics Reports, Vol. 431(6), pp. 261-302.

[3] Birman, J.-L. (1974), Theory of Crystal Space Groups and Infra-Red and Raman Lattice Processes of Insulating Crystals, Springer-Verlag, Berlin-Heidelberg-New York

[4] Damnjanović, M. and Milošević, I. (2010), Line Groups in Physics (Theory and Applications to Nanotubes and Polymers), Springer-Verlag, Berlin-Heidelberg

[5] Elliott, A. (1969), Infra-Red Spectra and Structure of Organic Long-Chain Polymers, Arnold, London

[6] Hamermesh, M. (1989), Group theory and its Applications to Physical Problems, Dover Publications Inc., New York

[7] Kirschner, I. and Mészáros, Cs. (2001), Symmetry analysis of static soliton structures and elementary excitations in incommensurately modulated crystals, J. Phys. Condensed Matter, Vol. 13, pp. 5399-5411.

[8] Streitwolf, H.-W. (1967), Gruppentheorie in der Festkörperphysik, Akademische Verlagsgesellschaft, Portig & Geest, Leipzig

[9] Vainshtein, B.K. (1966), Diffraction of X-Rays by Chain Molecules, Elsevier Publ. Co., Amsterdam

[10] Vujičić, M., Božović, I.B. and Herbut, F. (1977), Construction of the symmetry groups of polymer molecules, J. Phys. A: Mathematical and General, Vol. 10, pp. 1271-1279.

Quantification of multiple adulterants in whey protein based sports supplement by nir spectroscopy

Z. KOVACS[1], M. LUKACS[1], Gy. BAZAR[2]

[1]Department of Physics and Control, Faculty of Food Science,
Szent István University, Somlói street 14-16., Budapest, H-1118, Hungary
[2]Department of Nutritional Science and Production Technology,
Faculty of Agricultural and Environmental Sciences,
Kaposvár University, Guba Sándor street 40, Kaposvár,
H-7400, Hungary

Abstract

Protein based sports supplements have a significant growth on the market. Most of the techniques used for protein determination rely on total nitrogen content determination. Sports supplements are exposed to adulteration with cheaper nitrogen sources. Rapid methods for protein content evaluation are required. The objective of our work was to develop near infrared spectroscopy based models for quantification of adulterants in protein powders. Adulterated whey protein concentrates were analyzed with Dumatherm system and FT-NIR spectroscopy. Dumas method gave significantly higher apparent protein content than the expected values. NIR based PLSR models provided average prediction error lower than 0.5% for the adulterants.

Keywords

1. Introduction

Protein is an important component of our meal not only due to its high impact on the sensory and rheological characteristics, moreover, due to its nutritional value (Domingo, Tirelli, Nunes, Guerreiro, & Pinto, 2014). Most of the sports supplements contain protein in very high quantity. These protein based sports supplements are therefore, mainly evaluated by their protein content. The most commonly applied techniques of protein determination rely on the standard Kjeldahl method i.e. on the measurement of total nitrogen content, thus, cannot distinguish if nitrogen derives from different source (Lin, 2009; Moore, DeVries, Lipp, Griffiths, & Abernethy, 2010). Therefore, similarly to other milk or milk powder based products, protein based sports supplements are also often exposed to adulteration when cheaper ingredients with high nitrogen content, for instance melamine or urea, are added to the product to increase its apparent protein content. The available analytical methods most often used to detect or quantify

nitrogen based adulterants apply ELISA, UV-visible spectroscopy, Raman spectroscopy, mass spectrometry, gas chromatography (GC), high-performance liquid chromatography (HPLC) and ion-chromatography (Desmarchelier, Guillamon Cuadra, Delatour, & Mottier, 2009; Koh et al., 2011). However, these techniques are often expensive, time-consuming and require trained manpower above the output of chemical waste (Ezhilan et al., 2016). Therefore, reliable, rapid methods for protein content evaluation are highly required (Mauer, Chernyshova, Hiatt, Deering, & Davis, 2009). Mid- (MIR) and near-infrared (NIR) spectroscopy were successfully applied to detect melamine in dairy products, such as infant formula, milk powder, or liquid milk (Balabin & Smirnov, 2011). Studies show NIR spectroscopy has been successfully applied for the simultaneous detection and quantification of mixed adulterations in case some food products (Qin, Chao, & Kim, 2013). Forchetti & Poppi, (2016) proved that near-infrared spectral imaging combined with multivariate curve resolution can be used for the simultaneous detection and quantification of three different adulterants (starch, urea and whey) in milk powder. Results of an analytical method by means of Dumas and NIR spectroscopy was compered by Ingle et al. (2016) to quantify protein content in whey protein powders. Authors reported 2% standard error of prediction of the PLSR model based on NIR data for protein content determination. However, there are no available studies that introduce comparison of the Dumas method and NIR spectroscopy for quantification of mixed adulterants such as urea and amino-acids in protein based sports supplements.

Thus, the objective of our work reported here was to develop near infrared (NIR) spectroscopy based models for rapid quantification of adulterants in protein powders used to produce sports supplements.

2. Materials and methods

Whey protein samples
A total of 31 samples (20 g each) were prepared, using whey protein concentrate (WPC) as base component mixed with different adulterants such as urea, L-histidine, L-taurine and urea in different ratio. The mixing ratio of the samples was designed in a way that the quantity of the added nitrogen shows a linear increase. The tested samples together with their mixing ratio are summarized in This finding shows that the addition of 3% urea can cause a significant difference between the APC and PPC values. The present results indicate, that there are several ways to adulterate whey protein products, which remain obscure for the Dumas analysis. For instance, it is possible to use a few percentage of urea or histidine to boost nitrogen values in whey protein concentrate to mimic whey protein isolate (~90% < protein content), which is a significantly more expensive substance (e.g. sample number 5, 20). Another way is to mix components with low (e.g. taurine) and high (e.g. urea) nitrogen content to keep the pseudo protein content on the base level, while filling the product up with cheaper components (e.g. sample 23, 30).

Results of near infrared spectroscopy analysis

The second derivatives of the average spectra of the samples containing the highest adulteration levels (sample 5, 10, 15, 20, 25, 30) are shown in Figre 3. The most important absorbance peaks are marked with vertical lines. The second overtone region with C-H stretches is the most distinctive for histidine (black), including the peak at 1108 nm, which is visible in all samples that contain histidine. Samples containing histidine also show peaks at 1626, 1692 and 1728 nm, which is in agreement with the literature (Madhavan, Aruna, Anuradha, Premanand, & Potheher, 2007). Spectra of samples containing taurine (green) present peaks at 1176 and 1592 nm. In the case of urea (blue), the first overtone region with N-H stretches has the most distinctive absorbance peaks which agrees with earlier studies (Forchetti & Poppi, 2016).

Table 1. The table can be separated into blocks (1-5; 6-10; 11-15; 16-20; 21-25 and 26-30) showing the linear increase of the individual or multiple adulteration. The elements of the different blocks of the table can be matched by the added nitrogen value. For instance, samples 1, 6, 11, 16, 21 and 26 have the same amount of added nitrogen. The nitrogen content of the adulterants was considered when the mixing levels were determined (nitrogen content: urea ~ 47%, L-histidine ~ 27%, L-taurine ~ 11%, declared by supplier). Components were blended manually by adding the respective quantity of the given adulterants to WPC and shake it inside plastic containers for two minutes.

Methods

Determination of the apparent protein content using Dumas method

The total nitrogen content of the pure WPC and the samples indicated in Table 1 was measured by the Dumatherm system (C. Gerhardt GmbH & Co. KG, Königswinter, Germany) in triplicates (samples were chosen to provide representative distribution of the tested population). The measured protein content of pure WPC (78.94 ± 1.28%) provided the value for the calculation of the actual protein content (APC) of all the tested samples using the WPC percentage of the samples. For example, sample number 1 has an average APC value of 78.15%, which is the result of multiplying the amount of whey protein the sample contains (99%) by the Dumas results of the WPC material (average 78.94%). Measurements with the Dumas method required additional sample preparation, in the form of packaging 20-25 mg of the samples into tin foil. The device, according to the Dumas method, combusts each sample in oxygen rich environment while detecting and analyzing emerging gases, including nitrogen. The Dumatherm instrument was controlled by Dumatherm Manager software (v. 205, C. Gerhardt GmbH & Co. KG, Königswinter, Germany). The software automatically converted the results to protein percentage, using the general factor value of 6.38. This measured protein content was considered as the actual protein content (APC) of WPC, and the pseudo (apparent) protein content (PPC) of the mixed samples.

Near infrared spectroscopy

NIR spectra of all the 31 samples were acquired using a Fourier transform-near infrared (FT-NIR) spectrometer model MPA (Bruker Optics, Ettlingen, Germany). Reflectance spectra of the samples were measured at room temperature (25 ± 1 °C) using an integration sphere and a sample rotator. Each spectrum was measured in the entire range of the instrument (12500-3600 cm^{-1} or 800-2750 nm, resolution 32 cm^{-1}). Samples were analyzed in three repeats in three different days using randomized order with three consecutives and a background scan prior to each three consecutive measurements. Total number of sample spectra is 279. Control of spectral acquisition was performed with the OPUS Spectroscopy Software (v. 7.2, Bruker Optics, Ettlingen, Germany).

Data evaluation

PPC and APC values of the tested samples were compared using t-test to analyze the statistical significance of the observed differences. Visualization, evaluation and transformation of NIR spectra were performed with chemometric tools. First, raw spectra of the samples were visualized to make observation of typical absorbance peaks and spectral regions. Multivariate data analysis was performed with principle component analysis (PCA)) (Cowe & McNicol, 1985) and partial least squares regression (PLSR) (Naes et al. 2002). The PLSR models based on the NIR spectra and reference values were cross-validated with one-sample-out cross-validation. With future developments in mind, the spectral range most often covered by recent NIR based handheld devices (950-1630 nm) was used for the data evaluation. Raw spectra were smoothed using Saviztky-Golay (SG) filter (Naes et al. 2002), with 2nd order polynomials and varying smoothing points from 11 to 25. Additional pre-treatments (Naes et al. 2002) were used such as standard normal variate (SNV), multiplicative scatter correction (MSC), linear detrend and second derivative. Prediction was performed with the iteration leaving out data of one day of measurements at a time. During this validation process, two third of the data set (training set) was used for calibration and the remaining one third for prediction. The PLSR models were evaluated by comparing the determination coefficients (R^2) and root mean square errors (RMSE). For the analysis of the Dumas results, Microsoft Excel (Microsoft Corporation, USA) was used. The analysis of NIR spectroscopic data was performed with R-project (v. 3.3.2, The R Foundation for Statistical Computing, Vienna, Austria; using R package: aquap2, Pollner and Kovacs 2016).

3. Results and discussion

Results of Dumas analysis

Results of the comparison of PPC i.e. protein content determined with Dumas analysis and APC i.e. actual protein content achieved by calculation using t-test statistics are summarized in This finding shows that the addition of 3% urea can cause a significant difference between the APC and PPC values. The present results indicate, that there are several ways to adulterate whey protein products,

which remain obscure for the Dumas analysis. For instance, it is possible to use a few percentage of urea or histidine to boost nitrogen values in whey protein concentrate to mimic whey protein isolate (~90% < protein content), which is a significantly more expensive substance (e.g. sample number 5, 20). Another way is to mix components with low (e.g. taurine) and high (e.g. urea) nitrogen content to keep the pseudo protein content on the base level, while filling the product up with cheaper components (e.g. sample 23, 30).

Results of near infrared spectroscopy analysis
The second derivatives of the average spectra of the samples containing the highest adulteration levels (sample 5, 10, 15, 20, 25, 30) are shown in Figre 3. The most important absorbance peaks are marked with vertical lines. The second overtone region with C-H stretches is the most distinctive for histidine (black), including the peak at 1108 nm, which is visible in all samples that contain histidine. Samples containing histidine also show peaks at 1626, 1692 and 1728 nm, which is in agreement with the literature (Madhavan, Aruna, Anuradha, Premanand, & Potheher, 2007). Spectra of samples containing taurine (green) present peaks at 1176 and 1592 nm. In the case of urea (blue), the first overtone region with N-H stretches has the most distinctive absorbance peaks which agrees with earlier studies (Forchetti & Poppi, 2016).
Table 1. As the stars indicate in all but two cases (sample number 1, 6) the PPC was found significantly higher than the APC.

This finding shows that the addition of 3% urea can cause a significant difference between the APC and PPC values. The present results indicate, that there are several ways to adulterate whey protein products, which remain obscure for the Dumas analysis. For instance, it is possible to use a few percentage of urea or histidine to boost nitrogen values in whey protein concentrate to mimic whey protein isolate (~90% < protein content), which is a significantly more expensive substance (e.g. sample number 5, 20). Another way is to mix components with low (e.g. taurine) and high (e.g. urea) nitrogen content to keep the pseudo protein content on the base level, while filling the product up with cheaper components (e.g. sample 23, 30).

Results of near infrared spectroscopy analysis
The second derivatives of the average spectra of the samples containing the highest adulteration levels (sample 5, 10, 15, 20, 25, 30) are shown in Figre 3. The most important absorbance peaks are marked with vertical lines. The second overtone region with C-H stretches is the most distinctive for histidine (black), including the peak at 1108 nm, which is visible in all samples that contain histidine. Samples containing histidine also show peaks at 1626, 1692 and 1728 nm, which is in agreement with the literature (Madhavan, Aruna, Anuradha, Premanand, & Potheher, 2007). Spectra of samples containing taurine (green) present peaks at 1176 and 1592 nm. In the case of urea (blue), the first overtone region with N-H stretches has the most distinctive absorbance peaks which agrees with earlier studies (Forchetti & Poppi, 2016).

Table 1. Composition of the tested protein samples showing the applied analytical methods and average pseudo (apparent) protein content (PPC) measured by the Dumas method compared with the calculated average actual protein content (APC) and significance levels (* or ** show that difference was found between PPC and APC values at *=p<0.05 or **=p<0.01 significance level, respectively).

Sample number	WPC (%)	Urea (%)	Histidine (%)	Taurine (%)	APC (%)	NIRS	Dumas	PPC (%)	Difference (%)
1	99.00	1.00	0.00	0.00	78.15	✓	✓	80.14	1.99
2	98.00	2.00	0.00	0.00	77.36	✓			
3	97.00	3.00	0.00	0.00	76.57	✓	✓	81.73	5.16**
4	96.00	4.00	0.00	0.00	75.78	✓			
5	95.00	5.00	0.00	0.00	74.99	✓	✓	87.82	12.83**
6	98.26	0.00	1.74	0.00	77.56	✓	✓	79.36	1.80
7	96.52	0.00	3.48	0.00	76.19	✓			
8	94.78	0.00	5.22	0.00	74.81	✓	✓	83.11	8.30**
9	93.04	0.00	6.96	0.00	73.44	✓			
10	91.30	0.00	8.70	0.00	72.07	✓	✓	85.50	13.43**
11	95.73	0.00	0.00	4.27	75.56	✓	✓	78.44	2.88*
12	91.45	0.00	0.00	8.55	72.19	✓			
13	87.18	0.00	0.00	12.82	68.82	✓	✓	76.39	7.57**
14	82.91	0.00	0.00	17.09	65.45	✓			
15	78.64	0.00	0.00	21.36	62.07	✓	✓	76.23	14.16*
16	98.63	0.50	0.87	0.00	77.85	✓	✓	80.42	2.57*
17	97.26	1.00	1.74	0.00	76.77	✓			
18	95.89	1.50	2.61	0.00	75.69	✓	✓	83.35	7.66**
19	94.52	2.00	3.48	0.00	74.61	✓			
20	93.15	2.50	4.35	0.00	73.53	✓	✓	88.50	14.98*
21	97.36	0.50	0.00	2.14	76.86	✓	✓	80.53	3.67*
22	94.73	1.00	0.00	4.27	74.77	✓			
23	92.09	1.50	0.00	6.41	72.69	✓	✓	79.99	7.30**
24	89.45	2.00	0.00	8.55	70.61	✓			
25	86.82	2.50	0.00	10.68	68.53	✓	✓	82.04	13.51**
26	96.99	0.00	0.87	2.14	76.56	✓	✓	79.66	3.10*
27	93.99	0.00	1.74	4.27	74.19	✓			
28	90.98	0.00	2.61	6.41	71.82	✓	✓	78.47	6.65**
29	87.97	0.00	3.48	8.55	69.44	✓			
30	84.97	0.00	4.35	10.68	67.07	✓	✓	81.90	14.83**
31	100.00	0.00	0.00	0.00	78.94	✓	✓	78.94	0.00

Figure 2. Second derivative (SG, 2nd order polynomial and 21 points) spectra in the 800-2500 nm wavelength interval (average of three consecutive scans and three repeats each) of mixture samples (offsets were applied for visualization). WPC = whey protein concentrate (without adulterants); WPC+histidine (8.70%); WPC+taurine (21.36%); WPC+urea (5.00%); WPC+histidine (4.35%) +taurine (10.68%); WPC+urea (2.50%) +histidine (4.35%); WPC+urea (2.50%) + taurine (10.68%).

The PCA score plot calculated based on the 950-1630 nm spectral interval presents notable separation of the different adulteration levels of urea (Figre 3). The loading vectors show the highest importance around 1460-1530 nm, which region is typical for urea (Forchetti & Poppi, 2016).

Figre 3. The PCA scores and loading vectors of WPC samples using the 950-1630 nm region (using Savitzky-Golay filter, n=21). a, PCA scores colored by urea concentration, b, PCA loading vectors.

The parameters of the best PLSR models built for the quantification of the different adulterants and protein content are summarized in Table 2. SNV was found to be the best pre-treatment combined with Savitzky-Golay smoothing for

the prediction of the quantity of all the three adulterants and protein. Results also show the prediction of the adulterants was possible with lower than 0.5% root mean square error of prediction (RMSEP).

Table 2. Results of PLSR models (average and standard deviation of the three independently predicted datasets) defining the quantity of different adulterants and protein content in the 950-1630 nm spectral range. (R^2=determination coefficient; RMSE=root mean square error (%); C=calibration; CV=one-sample-out cross-validation; P=prediction; SG=Savitzky-Golay filter and number of smoothing points)

	Urea	Taurine	Histidine	Protein
Pre-treatment	SG 25 + SNV	SG 25 + SNV	SG 11 + SNV	SG 11 + SNV
Nr of latent variable	4.000 ± 0.000	7.667 ± 0.577	7.667 ± 1.528	7.333 ± 0.577
R^2c	0.987 ± 0.003	0.998 ± 0.000	0.994 ± 0.002	0.991 ± 0.002
RMSEC	0.152 ± 0.017	0.284 ± 0.010	0.174 ± 0.032	0.374 ± 0.052
R^2cv	0.984 ± 0.003	0.996 ± 0.000	0.988 ± 0.002	0.982 ± 0.005
RMSECV	0.166 ± 0.018	0.366 ± 0.011	0.256 ± 0.015	0.529 ± 0.072
R^2p	0.981 ± 0.006	0.995 ± 0.001	0.988 ± 0.002	0.973 ± 0.023
RMSEP	0.183 ± 0.032	0.411 ± 0.045	0.250 ± 0.019	0.616 ± 0.265

Model built for the prediction of urea concentration presents the lowest RMSEP (Figre 4). The regression vector emphasizes major peaks in the 1300-1600 nm region which covers the peaks found with 2nd derivative (Figre 3).
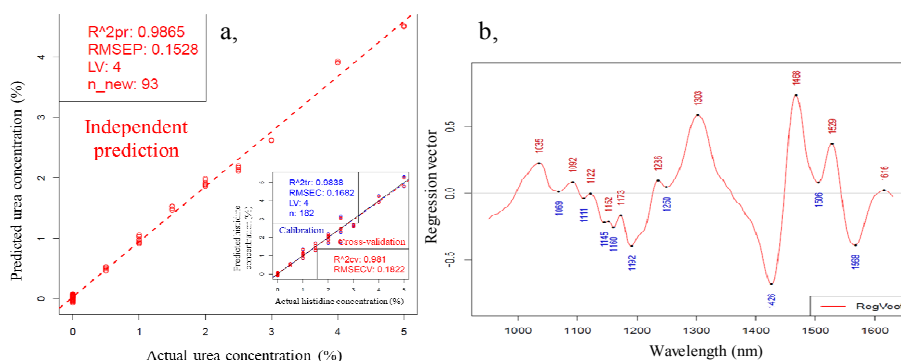
Figre 4. a, Y-fit and b, regression vector of PLSR model built for urea concentration (0-5%) in the 950-1630 nm range. a, Full sized figure shows the results of independent prediction with model parameters. Miniaturized figure shows adherent calibration models. R^2=determination coefficient; RMSE=root mean square error (%); tr and C=training (calibration); CV=cross-validation; pr and P=prediction; LV=number of latent variables.

Conclusion

Results of the Dumas measurements showed significantly higher protein content than the actual protein content of the samples in most cases. Our findings also

prove NIR spectroscopy can be used to quantify multiple adulterants in whey protein powder. Accurate prediction models could be built for the prediction of a more conventional adulterant (urea) and a more product specific one (taurine). NIR spectroscopy can also be a useful tool to detect components that are naturally present in the base component, but are also added as an exterior source (histidine). Most accurate models could be achieved with the combination of SNV and Savitzky-Golay smoothing resulting average RMSEP values 0.183, 0.411, 0.250 and 0.616 % for the prediction of urea, taurine, histidine and protein, respectively. NIR spectroscopy combined with proper chemometric tools can provide a quick, cost-effective and accurate alternative to conventional analytical methods to determine the actual protein content of whey protein that is the major ingredient of sports supplements.

Acknowledgements

References

[1] Balabin, R. M., & Smirnov, S. V. (2011). Melamine detection by mid- and near-infrared (MIR/NIR) spectroscopy: A quick and sensitive method for dairy products analysis including liquid milk, infant formula, and milk powder. *Talanta*, *85*(1), 562–568.
https://doi.org/10.1016/j.talanta.2011.04.026

[2] Cowe, I. A., & McNicol, J. W. (1985). The use of principal components in the analysis of near-infrared spectra. *Applied Spectroscopy*, *39*(2), 257–266.

[3] Desmarchelier, A., Guillamon Cuadra, M., Delatour, T., & Mottier, P. (2009). Simultaneous quantitative determination of melamine and cyanuric acid in cow's milk and milk-based infant formula by liquid chromatography-electrospray ionization tandem mass spectrometry. *Journal of Agricultural and Food Chemistry*, *57*(16), 7186–93. https://doi.org/10.1021/jf901355v

[4] Domingo, E., Tirelli, A. A., Nunes, C. A., Guerreiro, M. C., & Pinto, S. M. (2014). Melamine detection in milk using vibrational spectroscopy and chemometrics analysis: A review. *Food Research International*, *60*, 131–139. https://doi.org/10.1016/j.foodres.2013.11.006

[5] Ezhilan, M., Gumpu, M. B., Ramachandra, B. L., Nesakumar, N., Babu, K. J., Krishnan, U. M., & Rayappan, J. B. B. (2016). Design and development of electrochemical biosensor for the simultaneous detection of melamine and urea in adulterated milk samples. *Sensors and Actuators B: Chemical*, 1–10. https://doi.org/10.1016/j.snb.2016.09.100

[6] Forchetti, D. A. P., & Poppi, R. J. (2016). Use of NIR hyperspectral imaging and multivariate curve resolution (MCR) for detection and quantification of adulterants in milk powder. *LWT - Food Science and Technology*, 1–7. https://doi.org/10.1016/j.lwt.2016.06.046

[7] Ingle, P. D., Christian, R., Purohit, P., Zarraga, V., Handley, E., Freel, K., & Abdo, S. (2016). Determination of Protein Content by NIR Spectroscopy in Protein Powder Mix Products. *Journal of AOAC International*, *99*(2), 360–363. https://doi.org/10.5740/jaoacint.15-0115

[8] Koh, G., Chia, R. S. C., Lin, Q., Cheow, P.-S., Teo, T.-L., & Lee, T.-K. (2011). Determination of melamine in milk powder using gas chromatography-high-resolution isotope dilution mass spectrometry. *Journal of Separation Science*, *34*(21), 3043–52. https://doi.org/10.1002/jssc.201100285

[9] Lin, M. (2009). A review of traditional and novel detection techniques for melamine and its analogues in foods and animal feed. *Frontiers of Chemical Engineering in China*, *3*(4), 427–435. https://doi.org/10.1007/s11705-009-0244-z

[10] Madhavan, J., Aruna, S., Anuradha, A., Premanand, D., & Potheher, I. V. (2007). Growth and characterization of a new nonlinear optical L -histidine acetate single crystals, *29*, 1211–1216. https://doi.org/10.1016/j.optmat.2006.04.013

[11] Mauer, L. J., Chernyshova, A. A., Hiatt, A., Deering, A., & Davis, R. (2009). Melamine Detection in Infant Formula Powder Using Near- and Mid-Infrared Spectroscopy. *Journal of Agricultural and Food Chemistry*, *57*(10), 3974–3980. https://doi.org/10.1021/jf900587m

[12] Moore, J. C., DeVries, J. W., Lipp, M., Griffiths, J. C., & Abernethy, D. R. (2010). Total Protein Methods and Their Potential Utility to Reduce the Risk of Food Protein Adulteration. *Comprehensive Reviews in Food Science and Food Safety*, *9*(4), 330–357. https://doi.org/10.1111/j.1541-4337.2010.00114.x

[13] Phatak, A. (2004). A User-Friendly Guide to Multivariate Calibration and Classificationtion, T. Næs, T. Isaksson, T. Fearn, T. Davies. *Chemometrics and Intelligent Laboratory Systems*, *71*(1), 79–81. https://doi.org/10.1016/j.chemolab.2003.12.010

[14] Qin, J., Chao, K., & Kim, M. S. (2013). Simultaneous detection of multiple adulterants in dry milk using macro-scale Raman chemical imaging. *Food Chemistry*, *138*(2), 998–1007. https://doi.org/10.1016/j.foodchem.2012.10.115

Design and sizing of a plastic recycling station into filaments for 3D printer

A. OUSSAI

Institute Of Mechanics and Machinery

Department Of Agricultural and Food Machinery

Faculty of Mechanical Engineering, Szent Istvan University, Gödöllő, Hungary

Abstract

This project consists in finding a solution to fight against the pollution of the environment, so the idea was to focus on the field of recycling. In the beginning we conducted an analysis of the types of plastic widely used in Tunisia and the filaments for 3D printers and the field of three-dimensional printing in general. In our lab, we aim to analyses the types of the most used plastic in Hungary and go over the recycling steps and study the most environmentally friendly solution. Then we specify the recycling operation, its concept, its process and the possibility of its implementation in reality. Finally, decided to design this station which consists of two sub machine: crusher and extruder. We made a thorough study of the field and what type of machine. Then we set a schedule to follow to reach our goal. We made a complete theoretical study spanning calculations to design and dimensioning of our machine. In the future we plan to study the effects of this machine on the company and the 3D printer production.

Keywords

environment, Grinding, SolidWorks, RDM6 ,3D printer.

1. Introduction

Its objective is to enhance the plastic waste which is one of the main factors of pollution of our environment. This valorization is the transformation of these to filaments used three-dimensional printers. For decades and with the appearance of plastic, people have replaced everyday tools (baskets, glass jars ...) with plastic tools, as well as industries. Plastic is everywhere, in markets, stores, houses ... Thousands of bottles, plastic bags, computers, auto parts ... are sold every day. We see the plastic around us all. Although, plastic has become very useful in our everyday life, it is dangerous for the environment since most plastics are non-degradable in nature. After thinking about recycling, we wanted to orient our recycling towards an area that is a trend these days. Additive manufacturing or 3D printing is considered today as a technological revolution. Most personal 3D printers and some industrial 3D printers use plastic in the form of filaments as raw material. So, all these factors pushed us to realize this

project; manifested in a grinding-extrusion machine. Our work has been divided into two main parts: crusher and extruder. The first sub-machine is used to break and grind plastic waste, and the second is to mix, soften and extrude plastic grains from the mill, into a well-defined diameter filament. This idea allowed us to exploit various knowledge acquired during our training at SZIE and other tools that we learned by making this machine. We used, therefore, SolidWorks, ansys, Abaqus, engineering techniques, the drawing guide, and lots of software and tools. In order to answer our problem; we have structured our work into six part, each of which is devoted to an important part of the project.

2. Materials and methods

After conducting the study of plastic and existing crusher and extruder, we found that most plastics have good thermal properties, chemical and physical. However, consulting a few suppliers of three-dimensional printers we find that most of these revolutionary printers use filaments PLA and ABS as raw material in the first place. Secondly, they also use PE-HD. For this, we decided to work on these 3 types of plastics and set our choice as to the solutions that we adopt in this project and after studying the existing Circular blades mill, is a bit more complicated in its machining (gears and several levels...) but it's possible with our means. In addition, it works with two engines (and in the case of 4 or 6 shaft) and it contains no hopper and for the extruder, usually the extruders are all the same but they defer one compared to the other by a few technical details such as dimensions, mechanical solutions, heating method, type of screw extrusion.
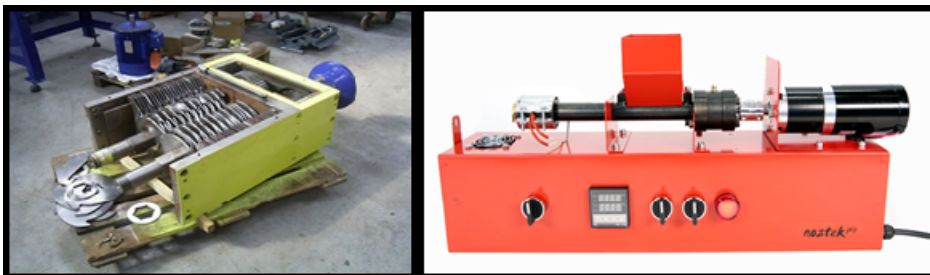
Figure 1. setting the choice for crusher(left side) and extruder (right side)

Functional analysis is to analyze the needs expressed by the company and to characterize, identify and prioritize the features of the product during its lifecycle in order to develop the functional specifications to facilitate and clarify the vision in the choice of the optimal solutions This part enabled us to choose an optimal solution for various components of this project.
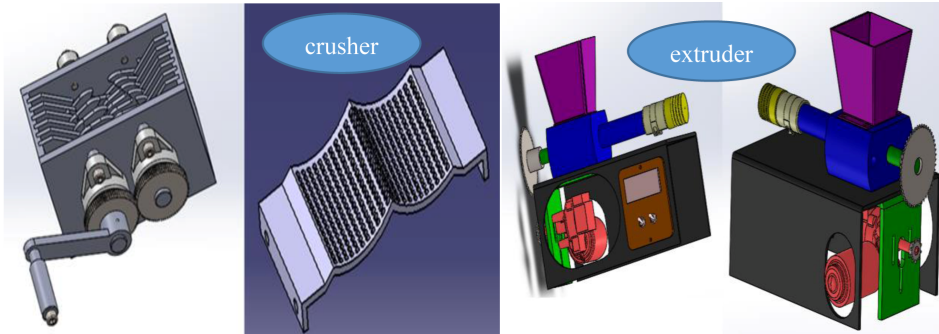
Figure 2. Presentation of solutions for crusher(left side) and extruder (right side)

For the design and sizing the crusher ,the process will begin with description system, as well as the scheme of kinematics. Then we will detail the design of the various blocks of the system and we will assemble; specifying the technical details while using the CAD SOLIDWORKS 2015 software. After this, we will conduct calculations and dimensioning of the Crusher

On the plastic type PE - HD with ultimate tensile strength, σ_{ts} = 31 MPa using the parameter of this plastic, this determine the torque necessary for the breakdown of the plastic

$$\tau = 0, 5\times \sigma_{ts} = 15, 5 \text{ MPa}$$
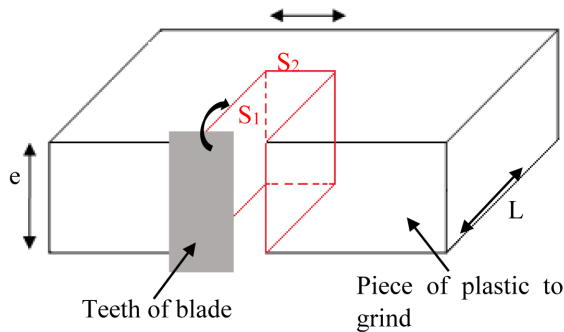
Figure 3. Presentation of the operation of shear

$$F = \sigma_s \times S \quad \rightarrow \quad F = 240{,}25 \text{ N} \tag{1}$$

Then

$$T_{crushing} = F \times d \tag{2}$$

the torque required for the grinding of the plastic. $T_{crushing}$ = 240,25 × 52,5 = 12,6 N.m.

And for sizing of axis and calculations of the thread

$$q = \frac{load}{Length} = \frac{mass \times g}{L} = \frac{3,42 \times 10}{190} = 0,18 \text{ N/mm} \tag{3}$$
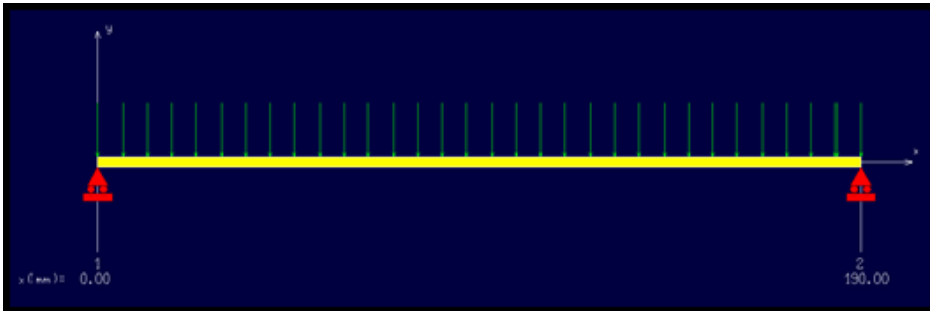
Figure 4. shear force and moments diagram

Applying the two equations of equilibrium yields:

$$\sum \vec{F}_{ext} = \vec{0} \quad \rightarrow R_a + R_b - q \times L = 0 \tag{4}$$
$$\rightarrow R_a = q \times L - R_b$$
$$\sum M_{/A} = 0 \quad \rightarrow - q \times L \times \frac{L}{2} + R_b \times L = 0 \tag{5}$$
$$\rightarrow R_b = q \times \frac{L}{2} = 0,18 \times \frac{150}{2}$$
$$\rightarrow R_b = 17,1 \text{ N}$$
$$\rightarrow R_a = 17,1$$

Now, we will generate the arrow and bending moment by RDM 6 $M_{f,max} = 812$ N.m
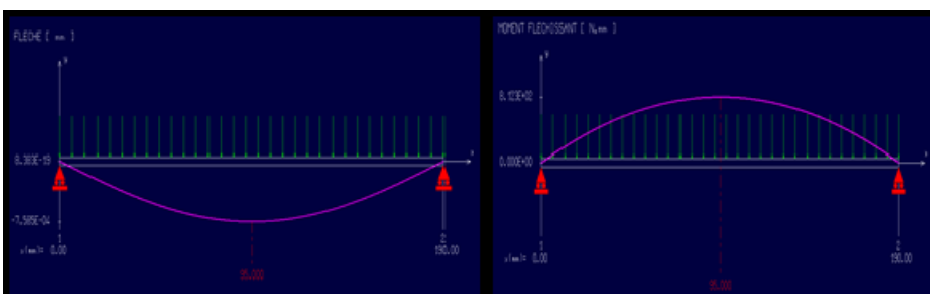
Figure 5. overview of deflection and bending moments

After doing the calculations we did use a calculation of finite elements by SolidWorks Simulation 2015. We have imposed loads on the axis

$$15,6 \text{ MPa} \leq \frac{\sigma_e}{s} = \frac{410}{3} = 136,6 \text{ MPa} \qquad (6)$$

The axes of our grinder can operate safely, validate. And we do the same for the blade and check the validation then design and sizing the extruder
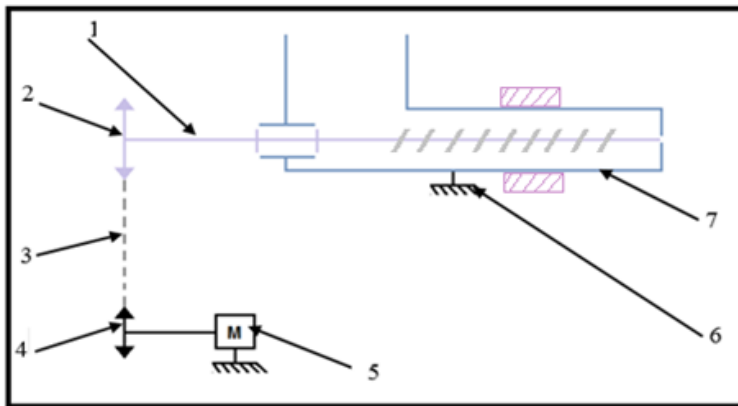

Figure 6. presentation of the solution for the extruder
1: Extrusion screw, 2: Large gear wheel, 3: Transmission Chain, 4: Small gear, 5: Engine, 6: Frame, 7: Extrusion chamber, 8: Heater band

And sizing the most important part in the extruder:
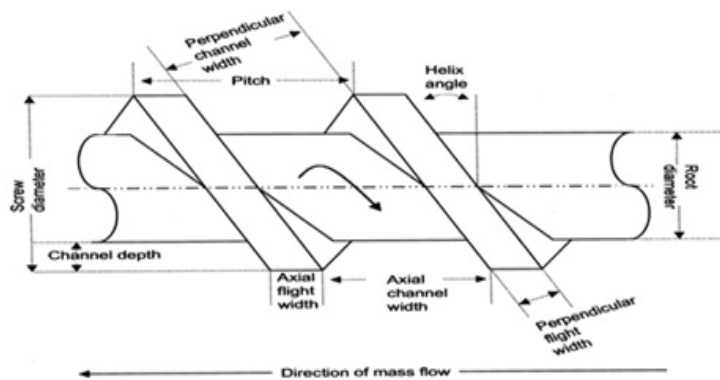
Figure 7. parameter of extrusion screw

$$T_{screw} = K \times D^2 \times L \qquad (7)$$

With: K = 469200 N/m²: Coefficient k of the empirical relationship of plastic. [regular formula for pe-hd extruder coef]

C_{screw} = 469200 × (0,020)² × 0,25 = 46,92 N.m

We want to produce a meter filament per minute:

$$Velocity = 1 meter / minute$$

$$N_{screw} = \frac{Velocity}{\pi \times D} = 15,9 \ \ rev/min \approx 16 \ rpm \tag{8}$$

driving power:

$$P_{driving} = \frac{T_{screw} \times 2 \times \pi \times N_{screw,max}}{60} = 78,61 \ W \tag{9}$$

So the power delivered by the engine is: $P_{en} = P_{driving} = 87,34$ W

Then the best soulition is the D76R(72)-1245-150 dc electric motor 24v 100w 100rpm

When designing of a new construction, the effective and economic operational aspects also have to be considered. Nowodays the machinery management is supported by modern diagnostic control, and remote maintenance systems [1,2]

Conclusion

In this paper we study the types of plastics and diagnose the pollution caused by the latter. This project also allowed us to design and size a recycling station of plastic into filaments for three-dimensional printers. This station which, for us, will contribute to the fight against pollution.The station consists of two machines for grinding of the plastic and the other for the extrusion of the desired filaments. We were able to make a theoretical academic study on both machines and also we designed with SOLIDWORKS 2015. The theoretical study is spread of the mechanical calculations necessary to the design and validation of the structure using the tools. As the prospect of this project, we want to complete the achievement of this station while completing the crusher and extruder mechanically. Then switch to electric and electronic parts (introduction of engines, sensors and wiring...). Next we want to automate this station to make it autonomous.

Nomenclature

SLA- Stereo Lithography **FDM-** Fused Deposition Modelling **ABS-** Acrylonitrile Butadiene Styrene **PE-HD -**Polyethylene high density

References

[1] Z. Bártfai, A. Nagymányai, L. Siklósi, Z. Blahunka: Developing of the lubrication technology service of ENI Hungaria ZRT
Synergy 2013, SZIE GÉK, Gödöllő

[2] Z. Blahunka, Z. Bártfai, R. Lefánti: Wireless Sensor Network Ad Hoc Measurement
Mechanical Engineering Letters, Szent István University, Gödöllő, 2012

[3] Saif al qaisi : American university of Beirut : Effect of Handwheel Height and Angle on Operators' Torque Production Capabilities [April 2015]

[4] Makershop e-shop: 3D printers , scanners , consumables:
http://www.makershop.fr/ [February 2017]

[5] Article by Kate Communs : the rises of additive manufacturing: [25 may 2010]

[6] Ph.D. thesis: The national polytechnic institute of Toulouse France"Physico-chemical properties and use of composite materials with degradable charge produced by co-grinding "Abdula Seyni [11 December 2010]

Effect of ethylene treatment on ripening of pear after cold storage

L.L.P. NGUYEN[1,3], L. Sz. HORVÁTH[1], T. ZSOM[1], M. S. DAM[3], L. BARANYAI[2], G. HITKA[1]

[1]Department of Postharvest Science and Sensory Evaluation, Szent István University
Villányi út 29-43, Budapest, H-1118, Hungary
[2]Department of Physics and Control, Szent István University
Villányi út 29-43, Budapest, H-1118, Hungary
[3]Biotechnology and Food Technology Institute, Industrial University of Ho Chi Minh City, 12 Nguyen Van Bao, Go Vap District, Ho Chi Minh, 700000, Vietnam

Abstract

The efficacy of ethylene treatment and storage temperature on ripening of 1-MCP treated pears after long storage were investigated. Fruits treated with 1-MCP were kept at 0°C for 6 months, then exposed to 150 ppm ethylene at 20°C for 24 hours, split randomly into three groups and stored separately at 0, 10 and 15°C for 2 weeks. Ethylene could trigger the ripening of pear after long storage period. It was observed that samples treated with ethylene ripened evenly compared to non ethylene treated pears The results showed that ethylene treatment had benefit in resuming normal ripening of 1-MCP treated pear.

Keywords

1-MCP, ethylene, ripening, storage, treatment

1. Introduction

The efficacy of 1-methylcyclopropene (1-MCP) in maintaining fruit quality in case of tomato, apple, pear, plum, avocado and melon (BLANKENSHIP & DOLE, 2003, HITKA et al., 2014) have been widely reported. However, in some cases 1-MCP treated pears could not resume the normal ripening after storage (Rizzolo et al., 2015). It was said that ethylene can induce the ripening of pear (Hiwasa et al., 2003). Therefore, the aim of this study was to evaluate the effect of ethylene treatment on 1-MCP treated pear after 6 months of storage at 0°C.

2. Materials and methods

Materials
Fresh samples of 'Kieffer' pears (*Pyrus communis* L.) were harvested while at a green color from an experienced grower in September 2016, Hungary. Fruits

were transported to the Faculty of Food Science of the university in Budapest, Hungary.

1-MCP (SmartFresh®, AgroFresh, Philadelphia, USA) as an application of SmartFresh® system was provided by Rohm and Haas Polska Sp.z.o.o.

1-MCP treatment
Fruits were selected for uniformity of size, shape and freedom from external damage. Samples were treated with 625–650 ppb gaseous 1-MCP (standard commercial application rate) for 24 hours in an air-tight plastic box, and then samples were stored at 0°C for 6 months.

Ethylene treatment
After 6 months of storage at 0°C, samples were randomly divided into 6 groups: 3 ethylene treated groups and 3 non ethylene treated groups. Each group had 20 fruits. Three groups were treated with 150ppm ethylene at 20°C for 24 hours. During 24-hs ethylene treatment, three non ethylene treated groups were kept at 20°C. Then all samples were stored at 3 different temperatures including 0°C, 10°C and 20°C for 2 weeks.

Measurements
Measurements were carried out on day 0 (before ethylene treatment), 7th and 14th day of storage.

Acoustic firmness. Acoustic firmness (S, $10^6 \cdot Hz^2 \cdot g^{2/3}$) of the samples was determined at two opposite sides on the exterior circumference of each fruit, using an AWETA table top acoustic firmness sensor model DTF V0.0.0.105 (AWETA, Nootdorp, The Netherlands).

Ethylene production. Ethylene production was determined by an ICA-56 hand-held ethylene analyzer (International Controlled Atmosphere Ltd., UK) upon the measured ethylene production of the samples being held for a given time (about an hour) in a hermetically closed plastic container. Results were expressed in microliter of ethylene produced per kilogram of fruit in 1 h ($\mu l \cdot kg^{-1} \cdot h^{-1}$).

Respiration rate. Respiratory intensity as carbon dioxide production was measured for an hour in a closed respiratory system containing several hermetically closed plexi glass containers equipped with FY A600-CO2H carbon dioxide sensors connected to an Almemo 3290-8 data logger (Ahlborn Mess-und Regelungstechnik GmbH, Germany). Results were expressed in milliliter of CO_2 produced per kilogram of fruit in 1 h ($ml \cdot kg^{-1} \cdot h^{-1}$).

Chlorophyll fluorescence parameters. Chlorophyll fluorescence parameters were determined at three equidistant points on the external circumference of each fruit by a PAM WinControl-3 controlled MONI-PAM multi-channel chlorophyll fluorometer (Heinz Walz GmbH, Germany). Obtained data were minimal, maximal chlorophyll fluorescence (F_0, F_m) and potential quantum yield of photosystem II (F_v/F_m).

Statistical analysis

All data were processed by SPSS (SPSS Inc, USA) using analysis of variance (ANOVA) followed by Tukey's method with a significance level of P< 0.05. The results were reported as a mean with standard deviations.

3. Results

Ethylene production of all samples increased during the storage period but at different rates (Fig. 1). Samples treated with ethylene showed higher ethylene production than those. When stored in cold temperature, the level of ethylene production was significantly reduced. Pears treated with ethylene and stored at 15 °C resumed the ripening more rapidly than others.
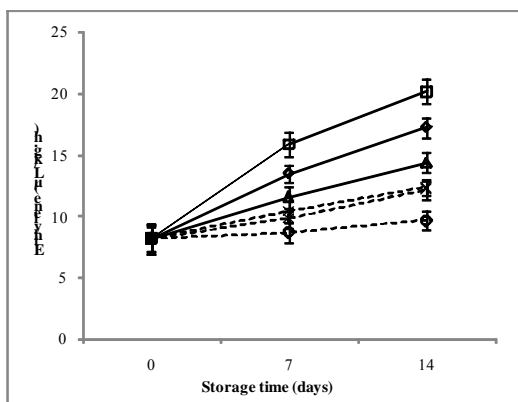
Figure 1. Effect of ethylene treatment on ethylene production of pears during 2 weeks of storage (−□− Ethylene treatment 15°C, −◇− Ethylene treatment 10°C, −Δ− Ethylene treatment 0°C, --×-- Control 15°C, --✳-- Control 10°C, --○-- Control 0°C)
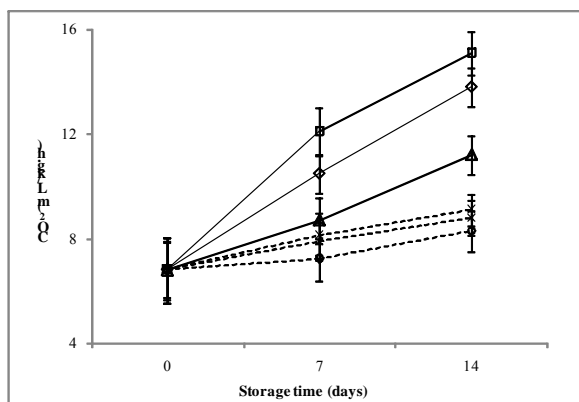

Figure 2. Effect of ethylene treatment on carbon dioxide production of pears during 2 weeks of storage (−□− Ethylene treatment 15°C, −◇− Ethylene treatment 10°C, −Δ− Ethylene treatment 0°C, --×-- Control 15°C, --✳-- Control 10°C, --○-- Control 0°C)

The increase in CO_2 production was probably due to the effect of ethylene treatment and storage temperature on fruits by inducing the ripening (Fig. 2). The results were in agreement with the report of Hiwasa et al. (2003) for 'La France' pears.

Firmness of pears reduced throughout storage period both in ethylene treated and non ethylene treated samples. However, pears kept at 0°C were firmer than those stored at 15 and 10°C (Fig. 3). Softening of fruits is due to biochemical processes such as hydrolysis of pectin by enzyme during ripening (Ali et al., 2010). The ethylene exerted its activity in resuming the normal ripening of ethylene treated fruits (Aharoni et al., 1993), whereas the ripening of non ethylene treated samples was uneven. After 14 days of storage, the ethylene treated pears at 15°C showed the lowest firmness. When stored at high temperature, there were a significantly decline in firmness compared to cold temperature.
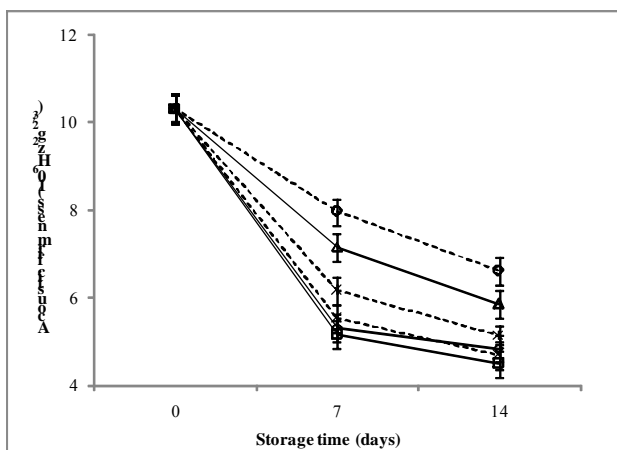

Figure 3. Effect of ethylene treatment on acoustic firmness of pears during 2 weeks of storage (−□− Ethylene treatment 15°C, −◇− Ethylene treatment 10°C, −△− Ethylene treatment 0°C, --×-- Control 15°C, --✳-- Control 10°C, --○-- Control 0°C)

Chlorophyll fluorescence parameter declined during storage (Fig. 4). The decrease of chlorophyll content was due to ripening throughout storage period (Bron et al., 2004; Pongprasert et al., 2014). The color change from green to yellow is often the sign of ripening. There was a color shift from light green to yellow after the first 7 days of storage in case of samples treated with ethylene and stored at 15°C and 10°C. Treating with ethylene and storing at 15 and 10°C increased the color change of pears throughout the storage (data not shown).

Figure 4 reflected a significant loss in chlorophyll content at the end of experiment, because fruits reached the advancing ripeness stage. This could be explained by the effectiveness of ethylene in inducing the ripening.
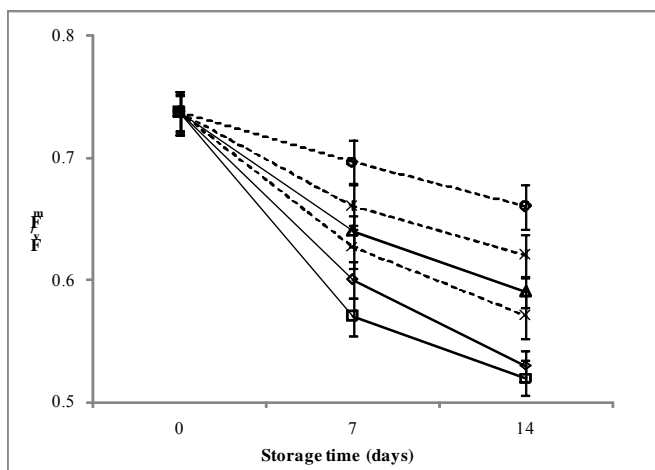
Figure 4. Effect of ethylene treatment on F_v/F_m of pears during 2 weeks of storage
($-\square-$ Ethylene treatment 15°C, $-\diamond-$ Ethylene treatment 10°C, $-\triangle-$ Ethylene treatment 0°C,
$--\times--$ Control 15°C, $--\ast--$ Control 10°C, $--\circ--$ Control 0°C)

Conclusion

The results of this study provided the basic information about the effect of ethylene treatment on ripening of 1-MCP treated pears that could be useful in commercial practice. 1-MCP treated 'Kieffer' pears could resume the normal ripening after 6 month of cold storage when exposed to ethylene. However, further study should be carried out to investigate the effect of concentration, treatment time and treatment temperature on ripening of pear.

References

[1] Aharoni, Y., Copel, A., & Fallik, E. (1993). StoringGalia'melons in a controlled atmosphere with ethylene absorbent. HortScience, 28(7), 725-726.

[2] Ali, A., Maqbool, M., Ramachandran, S., & Alderson, P. G. (2010). Gum arabic as a novel edible coating for enhancing shelf-life and improving postharvest quality of tomato (*Solanum lycopersicum* L.) fruit. Postharvest Biology and Technology, 58(1), 42-47.

[3] Blankenship, S. M., & Dole, J. M. (2003). 1-Methylcyclopropene: a review. Postharvest Biology and Technology, 28(1), 1-25.

[4] Bron, I. U., Ribeiro, R. V., Azzolini, M., Jacomino, A. P., & Machado, E. C. (2004). Chlorophyll fluorescence as a tool to evaluate the ripening of 'Golden' papaya fruit. Postharvest Biology and Technology, 33(2), 163-173.

[5] Hitka, G., Zsom, T., Nguyen, L., & Balla, C. (2014). Effect of 1-methylcyclopropene on 'Bosc Kobak' pears. Acta Alimentaria, 43 (Supplement 1), 73-77.

[6] Hiwasa, K., Kinugasa, Y., Amano, S., Hashimoto, A., Nakano, R., Inaba, A., & Kubo, Y. (2003). Ethylene is required for both the initiation and progression of softening in pear (*Pyrus communis* L.) fruit. Journal of Experimental Botany, 54(383), 771-779.

[7] Pongprasert, N., & Srilaong, V. (2014). A novel technique using 1-MCP microbubbles for delaying postharvest ripening of banana fruit. Postharvest Biology and Technology, 95, 42-45.

[8] Rizzolo, A., Grassi, M., & Vanoli, M. (2015). Influence of storage (time, temperature, atmosphere) on ripening, ethylene production and texture of 1-MCP treated 'Abbé Fétel' pears. Postharvest Biology and Technology, 109, 20-29.

Drive characteristics affecting the speed loss of V-belt drives

P. GÁRDONYI, L. KÁTAI, L. SZÉKELY, I. SZABÓ

Faculty of Mechanical Engineering, Szent István University,
Páter K. u. 1., Gödöllő, H-2100, Hungary

Abstract

The efficiency of V-belt drives is determined by several factors collectively: the slip, the external and inner friction. In this paper the slip of the V-belt was studied as loss intensity as a function of drive parameters. The individual effects of V-belt drive parameters on speed loss are determined using one-factor-at-a-time (OFAT) test method. It was justified in the scope of the major characteristics affecting power loss that by ideally selecting the parameters of the V-belt drive power loss can be measurably reduced. Based on earlier results as well, a regression model was used to examine the slip of the V-belt. On the bases of the test results optimal parameters can be calculated to give references for V-belt drive design.

Keywords

V -belt, Efficiency, Power loss, Slip, ANOVA

1. Introduction

When designing V-belt drives, the power requirements as well as the geometric and kinematic parameters of the driven machine unit are considered as the basis by the engineers, which is adapted to the drive characteristics of the power source by changing the drive. Power transmission can be achieved with several belt drive designs, so it is the designer's task to define the optimal drive design considering different aspects. The study of the drive characteristics affecting the power loss of V-belt drives helps with designing the optimal V-belt drive.

The efficiency (η) of V-belt drive is the ratio of useful and input power. The useful power appears on the driven shaft, which is the product of the peripheral force (F_{t2}) and the peripheral speed (v_2) delivered to the pulley. The input power is fed into the system on the drive side, via the drive pulley (Kátai and Szabó, 2015):

$$\eta = \frac{P_h}{P_b} = \frac{F_{t2} \cdot v_2}{F_{t1} \cdot v_1},\tag{1}$$

belt slip occurring during power transmission:

$$s = \frac{v_1 - v_2}{v_1}.$$
(2)

By further converting the efficiency equation, we get an equation of two members. The part in the bracket means the lost motion, and κ means the losses occurring on the peripheral force.

$$\eta = \frac{F_{t2}}{F_{t1}} \cdot (1 - s) = \kappa \cdot (1 - s)$$
(3)

Typically, the studies published so far have dealt with the power loss of V-belts through the study of motion loss and other torque losses. According to Gervas and Pronin (Gervas and Pronin, 1967, 1969) the torque loss of V-belt drives is partly derived from the inner friction of the tractive element, which in addition to the deformation caused by the belt side forces mainly comes from its bending, and from the radial friction loss, which is generated by the belt element entering and exiting the pulley groove. The loss of motion is made up of the circumferential belt slips. According to Gerbert's tests (Gerbert, 1972, 1974) losses occurring during the power transmission of belt drives are mainly due to the friction of the contacting surfaces and the inner friction occurring due to the repeated use of the belt (hysteresis). The losses of V-belt drives are essentially due to friction losses made up of the molecular inner friction due to the repeated use of the tractive element and the macroscopic friction of the contact areas. The mentioned friction losses are manifested in a complex manner in the form of thermal energy and the movement of the belt relative to the pulley groove. Balta and his co-authors (Balta et al., 2015) studied the speed losses of Poly-V belt drive with the difference in the angular speed of the shafts when the drive parameters are changed. A belt slip model was created:

$$\text{slip}\,(\%) = 0.42 + 0.2 \cdot X_2 - 0.072 \cdot X_3 - 0.17 \cdot X_4 - 0.039 \cdot X_2 \cdot X_3 - 0.65 \cdot X_2 \cdot X_4 +$$
$$0.33 \cdot X_3 \cdot X_4 + 0.059 \cdot X_4^2 + 0.038 \cdot X_5^2.$$
(4)

The variables of the function:

$$X_1 = \frac{\omega - \omega_0}{\frac{\Delta\omega}{2}};\quad X_2 = \frac{M - M_0}{\frac{\Delta M}{2}};\quad X_3 = \frac{T - T_0}{\frac{\Delta T}{2}};\quad X_4 = \frac{D - D_0}{\frac{\Delta D}{2}};\quad X_5 = \frac{E - E_0}{\frac{\Delta E}{2}}.$$
(5)

where the angular speed ω, torque M, pre-tensioning T, pulley diameter D, and the elastic modulus of the V-belt material E are the test factors; ω_0, M_0,

T_0, D_0, and E_0 are the mean values of the factors; $\Delta\omega$, ΔM, ΔT, ΔD, and ΔE are the difference between the largest and the smallest values.

The loss of the belt drive is basically determined by the drive parameters, through the optimum choice of which the efficiency of the drive can be improved. The presented equation provides assistance in designing belt drives of favourable efficiency, but the empirical equations created are difficult to understand and do not provide obvious assistance for practicing engineers. Our goal is to create a mathematical model which clearly defines the effect of drive parameters on belt slip (loss of motion).

2. Material and method

The drive parameter experiments were carried out on a test bench designed for testing drives. The test bench consists of a drive and brake unit mounted on a grooved table (Figure 1). The torque provided by the drive belt is supplied by two force cooled three-phase asynchronous motors (NERIMOTORI IEC 34-1, 1.5 kW). The values of the revolutions and the braking torque can be adjusted using two Fuji Electric 5E1S-7E inverters. The drive parameters were recorded with an 8-channel HBM Spider 8 measurement data collector. The torque values are supplied by the NCTE 2200-17.5 torque measuring cells (measuring range: 0 to 17.5 Nm; accuracy class 1). The revolution and the angular speed were measured using Hengstler 0538633 RI76TD/5000ED incremental revolution encoders with a resolution of 5000 pulses per revolution. The diagram of the electric and metering system of the test bench is shown in Figure 2.
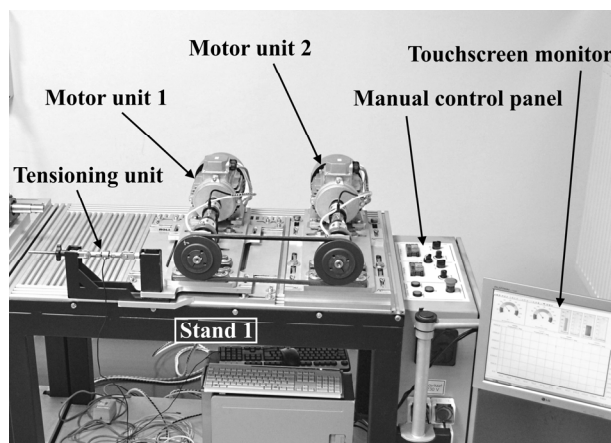

Figure 1. The construction of the test bench

V-belts Profile Z/10 and 5 pulley diameters (d_1= 60; 90; 118; 150; 180 mm) were used for the measurement. The ratio used was 1:1 and with the fixed value

of the free belt section length (345 ± 10 mm) the same flexibility of the different drive settings was ensured. The revolution was determined between the 10 and 20 s^{-1} belt bending frequency values generally occurring in practice. The V-belt drive was loaded with the largest torque calculated on the basis of the given pulley diameter and bending frequency, and it was studied without power transmission. The pre-tensioning of the different experimental settings was determined from the drive sizing, and it was set at 50, 150, and 150 % of that.
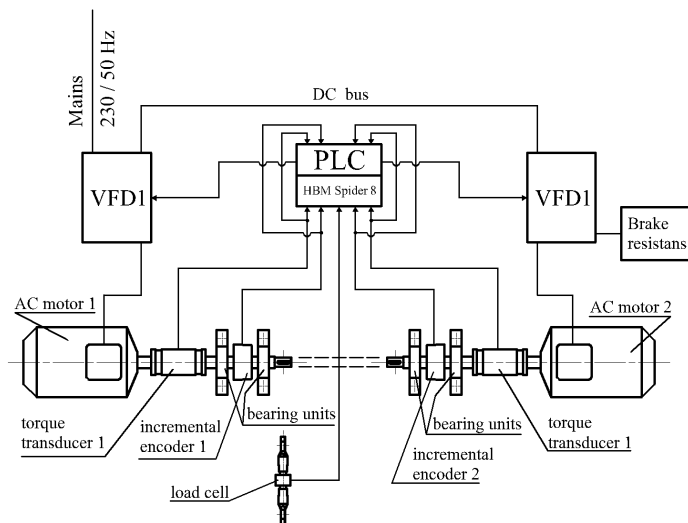
Figure 2. Schematic diagram of the electrical and measuring system

In order to study the drive parameter the measurement program was compiled on the basis of a traditional test method (One-Factor-at-a-Time), where at one time one of the drive parameters was modified with the fixed value of the other drive characteristics. A multiple regression model was used to qualitatively analyze the measured data, which was set up for the torque loss κ examinations. The adequacy of the model was verified by variance analysis (ANOVA), and the value of the coefficients of the variables in the model was calculated. The weight of the individual factors was determined i.e. how each drive characteristic affects the dependent variable compared to the other independent variables. The data were analyzed using the software Statistical Package for Social Science (SPSS).

Based on the regression model used to describe the torque loss κ of the V-belt drive the effect of the drive parameters on motion loss s was examined. The regression model:

$$s = a_0 + \frac{a_1}{d} + a_2 \cdot f + a_3 \cdot M + a_4 \cdot F_H, \tag{6}$$

where the function parameters are:

$$a_0 \ [\%], \qquad a_1 \left[\frac{mm}{\%}\right], \qquad a_2 \left[\frac{\%}{s^{-1}}\right], \qquad a_3 \left[\frac{\%}{Nm}\right], \qquad a_4 \left[\frac{\%}{N}\right].$$

All the independent variables in the model are linear, which contributes to the usability of the model.

3. The results of the tests

The belt slip measured during the tests was studied in the running state of the drive. The regression equation created for the torque loss test carried out by the research group was used to find the factors influencing the motion loss of the V-belt drive among the drive parameters. The result of the analysis of variance is shown in Table 1.

Table 1. The table of variance of slip s

	Sum of squares	Degree of freedom	mean square	F/T value	p
Model	12.84	37	3.76	81.780	<0.001
$1/d$	3.55	4	8.89	5.007	<0.001
f	0.11	1	0.11	-1.554	0.132
M	7.40	2	3.70	12.873	<0.001
F_H	0.71	2	0.36	-3.695	0.001
remainder	1.56	34	0.05		

Table 2. Correlation of parameters in the regression model

Model	coefficient	Standardized regression coefficient Beta	t	p
Constant	-0.081		-0.605	0.549
M	1.147	0.801	12.873	<0.001
$1/d$	49.144	0.314	5.007	<0.001
F_H	-0.379	-0.224	-3.695	0.001

The analysis of variance verified the validity of the model, so it can be used to qualitatively describe the belt slip. The correlation coefficient of the fitting of the model is $R^2 = 0.868$. From the independent variables, the significance level for the bend frequency is high ($p > 0.05$), so it does not affect the tested phenomenon. In

Table 2 the relationship of the individual parameters was examined in the regression model, where the standardized regression coefficient makes the correct comparison of the factors possible. The Beta value shows how much the independent variable influences the dependent variable. The load M has the largest effect on belt slip, the reciprocal of the disc diameter and pre-tensioning have a smaller effect.

According to Table 2, entering the specific values of coefficients, the model is:

$$s = 1.147 \cdot M + \frac{49.144}{d} - 0.379 \cdot F_H. \tag{7}$$

Additional measurements were performed in order to verify the correctness of the model, where optionally selected drive parameters were present in an identical experimental layout. The relative difference between the estimated and measured values of slippage in some cases exceeds 15% (Table 3).

Table 3. Test results of Model Verification

	Pulley diameter d [mm]	Belt bending frequency f [s⁻¹]	Brake torque M [Nm]	Pre-tensioning F_H [N]	Measured value S [%]	Calculated value S [%]	Relative difference [%]
1	180	20	$1/3 \cdot M_N$	$1 \cdot F_H$	0.24	0.28	15.5
2	118	15	$0 \cdot M_N$	$1 \cdot F_H$	0.0	0.04	-
3	150	20	$1/3 \cdot M_N$	$1 \cdot F_H$	0.30	0.33	11.5

Conclusions

The power loss of V-belt drives comes from the loss occurring on the motion and peripheral force. The mathematical model of the motion loss was set up on the basis of the regression model used for the examination of the V-belt drive torque loss. It was justified in the scope of the major characteristics affecting the motion loss that by ideally selecting the parameters of the V-belt drive, loss can be measurably reduced. It was concluded with the help of the analysis of variance that from the drive parameters the load of the drive (M) determines the belt slip. The bending frequency (f) and the revolution of the shafts involved in the drive have no influence on the examined phenomenon. The effect of the pulley diameter and its reciprocal ($1/d$) and pre-tensioning F_H is almost identical, at the same time it has a smaller effect than the load does.

Acknowledgements

References

[1] AL - MALIKI Hayder, ZSIDAI László, KALÁCSKA Gábor, KERESZTES Róbert, SZAKÁL Zoltán, FRICTION TESTS OF DIFFERENT POLYMERS TREATED BY PLASMA TECHNOLOGY. Proceedings of the 4th International Scientific Conference on Advances in Mechanical Engineering (ISCAME 2016). Debrecen. pp. 211-216. (ISBN: 978-963-473-944-9)

[2] B. Balta, F. O. Sonmez, A. Cengiz (2015): Speed losses in V-ribbed belt drives, Mechanism and Machine Theory, 86, pp. 1–14

[3] B. G. Gerbert (1972), Force and slip behaviour in V-belt drives, Acta polytechnica Scandinavica, Mechanical engineering series, Helsinki, 67

[4] B. G. Gerbert (1974), Power loss and optimum tensioning of V-belt drives, Journal of Engineering Industry Trans. ASME, 96, pp.877-885.

[5] G Kalácska, R Keresztes, M Kozma (2009), Friction research of polymer-steel gear pairs. ÖTG Symposium 2009 - Lebensdauer und Energieeffizienz - Product Life and Efficiency: Herausforderung im Maschinenbau und in der Schmierungstechnik - Challenge in Mechanical- and Lubrication Engineering. Wien: Österreichische Tribologische Gesellschaft, pp. 207-211. (ISBN: 978-3-901657-34-4)

[6] K. J. Gervas (1969), Determining the power losses in V-belt drives during flexure, Soviet Rubber Technology, 28 (2) 42.

[7] K. J. Gervas and B. A. Pronin (1967), Calculation of power losses in belt drives, Russian Engineering Journal, 47 (3), pp. 26-29.

[8] Kátai L, Szabó I. (2015), Identification of V-belt power losses with temperature measurement. Journal of Mechanical Science and Technology 29: (8), pp. 3195-3203.

The importance of 3D printing in the development of knee prosthesis geometry

G. P. BALASSA, G. KOPCSÁNYI, I. OLDAL

Department of Mechanics and Technical Drawing,, Szent István University

Páter K. u. 1., Gödöllő, H-2103, Hungary

Abstract

In the human knee joint a degenerative wear of the joints can be formed. The common treatment of that disease is the total knee replacement prosthesis implanting. The aim of our research is to develop a knee prosthesis geometry which can fulfil the mechanical and kinematical requirements. We developed a method within we are creating virtual knee prosthesis geometries with the help of the technology genetical algorithm. The generated geometries are produced by 3D printing technology and are examined on a special knee prosthesis qualification equipment. We would like to demonstrate how this technology suitable for the prosthesis geometry development.

Keywords

Biomechanics, 3D printing, knee, knee prosthesis

1. Introduction

The knee joint is the most complex joint in the human body. The human biomechanics operates with its examination and kinematical function. The biomechanics is an interdisciplinary or multidisciplinary knowledge that was come from the synergy of biology and mechanics. Nowadays one of the major orthopedic problems is the proper treatment of the changes in the human knee joint. In the joint the almost frictionless sliding and rolling between the bones is ensured by the cartilage covering joint surfaces and the joint fluid. During the age progresses joint friction can be formed, it is the so called arthrosis. In case of incurable arthrosis, a total knee replacement (TKR) may be required. The current knee prostheses don't achieve the movement of the healthy knee joint and they change the original kinematics of the joint (Ostermeier et al., 2004). In case of a healthy knee the walking and the movement of the knee joint is coordinated to each other (Fekete et al., 2014) but this will change with the implantation of the knee prosthesis. As the perfect knee prosthesis geometry currently not available we set the goal for us to developing our own geometry. The actual results are reported in our present study.

If the created movement by the knee prosthesis isn't approach enough the movement of the healthy knee during the walking it is also forced to that

movement by the nerve and muscle system. That compulsion causes an overload on the prosthesis - and what the problem causes - on the prosthesis-bone relationship as well. This is occurring at every step a repetitive load which is causing during the time inflammation of the joints and knee prosthesis loosening. With the proper prosthesis geometry this overload can be minimized. As known the human knee joint has six degrees of freedom. The moving possibilities are shown on the Figure 1.
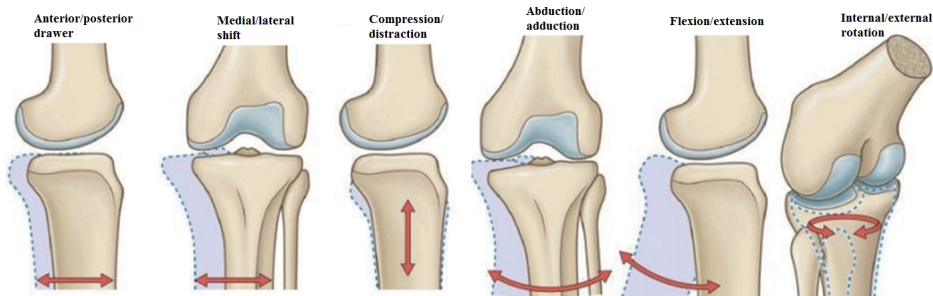

Figure 1. Knee joint motion in three dimensions, which is described using six independent variables (Standring, 2008)

From these movements the most important is the tibia internal/external rotation values under the flexion/extension. That movement has the most significant effect to the prosthesis loosening. Two stages of the rotational movement can be separated. They are the spontaneous and the intentional. The spontaneous rotation (also so called initial rotation) during flexion and the ending rotation during extension aren't muscle tone result (Miltényi, 1980). At the beginning of the bending movements and at the end of the stretching movements approx. 5° rotation is generated. It is created by the geometry of the joint surfaces and the lateral/collateral ligaments. In our research we use this hypothesis that the rotational movement (relevant in relationship with the walking) is created by the geometrical features in the knee joint. That means by the developing of the proper prosthesis geometry the movement of the healthy knee joint can be served. The intentional rotation is the specialty of the human knee joint. In this case the knee joint can ensure 20° internal rotation and 40° external rotation (Donáth, 2005) which is provided by the appropriate loosened ligaments.

If we want to create a good knee prosthesis is seems obvious to copy an image of a healthy human knee joint geometry with a CT or MRI. However this is not the good solution. Instead of the three main components: femur, tibia, meniscus the prosthesis consists of only two components (femur and tibia) which we would like to create the original movement. Furthermore during the knee prosthesis implantation process not only the joint surfaces are replaced but the untouched ligament-system changes as well.

For the development of knee prosthesis geometry it is essential to know the movement of the real human knee joint. The Biomechanical Research Group of the Szent István University determined the specific rotation-flexion function of the human knee joint (Fig. 2.). The movement was with three linear functions approximated as the movement has three main phases. That function is the so called reference function (Katona et al., 2013). For a prosthetic geometry development, this is used such as input parameter to be achieved. The research group has developed for the cadaver machine a knee prosthesis measuring and qualification system (M. Csizmadia B. et al., 2013). In this case the new prosthesis geometry can be adequately tested and compared with the cadaver results.
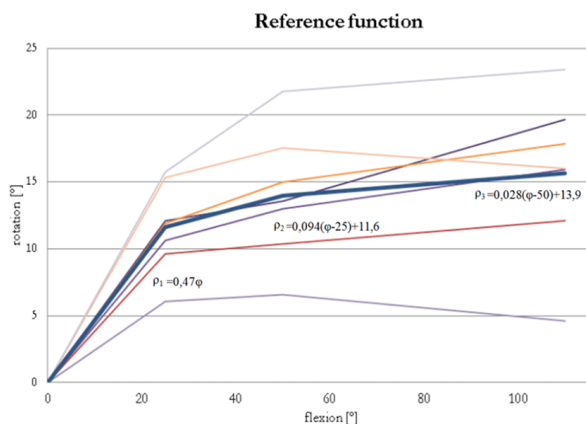
Figure 2. Reference function for the prosthesis development (Katona et al., 2013)

2. Materials and methods

The knee prosthesis is consisting of two components they are the tibia and the femoral component. The so called reference function must be achieved with its adequate geometry. During our research we started our investigations based on commercially available knee prosthesis geometry (Fig. 3.). The femoral component was the commercial and to that component we designed various tibia plateau geometries.

For the development of the geometry we used the genetical algorithm (Sivanandam SN, et. al., 2008) form the evolutionary algorithms. With the use of that algorithm we optimized the tibia joint surfaces. The algorithm generates the starting population on the base of the commercial prosthesis. The prosthesis individuals approach the required function (reference function) in a specific way and then it performs the necessary operations (mutation, crossing etc.) on the individuals. The created individuals are created as parametrical models in Solid Edge ST9 environment. They are manufactured with the technology 3D printing

and examined on the knee prosthesis test rig. The basis of our qualification is the determined difference between the reference function and prosthesis geometry generated function.

During our research we created a genetical algorithm which is suitable for developing knee prosthesis geometry. The result of our work is the generated prosthesis geometries which are decoded as individuals. The algorithm is suitable for the geometry reproduction and to creating new populations whose evolutional results will produce better and better individuals (prosthesis geometries). We tried several methods for the model parametrizing but only one method was appropriate. It is based on the layer by layer 3D printing technology. The virtual prosthesis model (parametrical) was constructed form layers of 0,1mm thickness (Fig. 3.) and the functional surface consist of circles. As a result of the process our prosthesis model is described with 68 layers and 1150 parameters. The value of the 1150 parameter as gene creates the geometry of the individual.
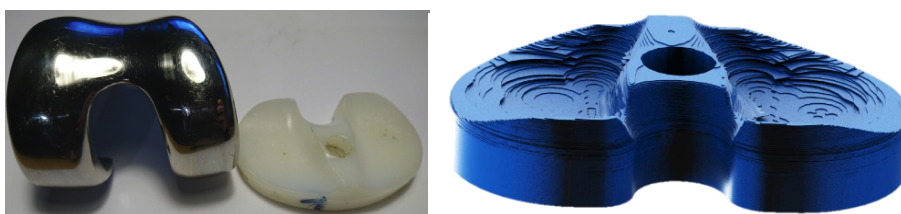

Figure 3. The commercial knee prosthesis and our virtual parameterable model

Making the prosthesis specimens – 3D printing

The 3D printing is one of the newest manufacturing technologies of the XXI. Century. Its use is widespread in prototype models. The technology has been developed by the Massachusetts Institute of Technology (MIT). The first 3D printer was released in 1994. During our work we created the specimens using the FDM (Fused Deposition Modeling) technology. The basic material for the FDM technology is a coiled thin and thermoplastic plastic wire. The most common diameter is the 1,75mm and the materials are ABS (acrylonitrile butadiene styrene) and PLA (polylactic acid). Our printed prosthesis specimens were printed out PLA material with a wire diameter of 1,75mm. During printing a stepper motor shaft drives the polymeric fiber. The polymeric fiber melts on the extruder head and the injector at the end of the extruder forms the printed layer (Kovács, 2004). The full geometry is made up of those layers. The designed specimens were printed using that technology with the help of the Poly-D-Engineering Ltd. The slicing of the STL files was carried out for each individual on the same slicer program with the following settings:
- layer thickness: 0,1mm
- object infill: 30 %
- number of shells: 2

– filament diameter: 1,75mm

For each individual population the print parameters are as follows:

- Print speed: 40mm/s
- Temperature of printer table: 70 °C
- Temperature of printer nozzle: 200 °C
- Travel speed: 70 mm/s
- Diameter of nozzle: 0,4 mm
- The cooling is 70 % after printing the third layer

The boundaries of the printing layers were compensated with grinding paper of 180 particle size, after the printing (Fig. 4.). This was due to the resolution of the models. On the other hand, trimming of roughness peaks due to printing technology was necessary.
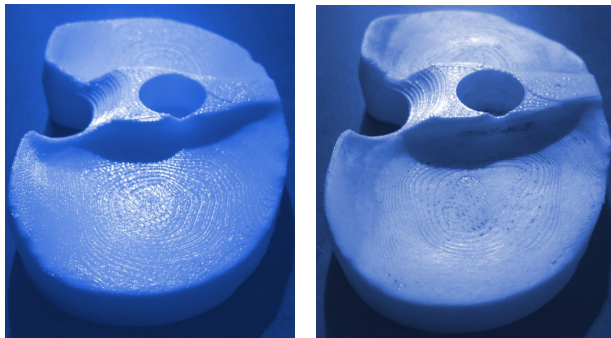
Figure 4. Printed prosthesis before and after surface treatment

Creating of prosthesis models – CNC milling

During the production of 3D print samples, the model validation was required. The tibia component of the real knee prosthesis is made of UHMWPE polymer by CNC milling. If we produce 3D geometry models with 3D printing and CNC milling, then an experimental comparison of the models is possible. That means we can examine the most important issue of our present study that how can be used 3D printing for knee prosthesis geometries development under research conditions.
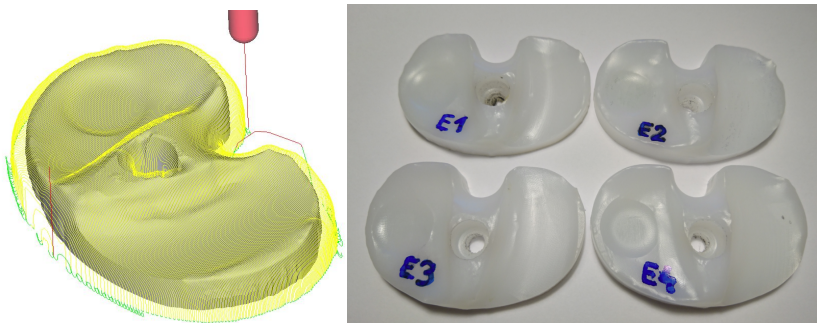

Figure 5. The process of 3D milling in a CAM software and the real milled specimens

To demonstrate this hypothesis, we prepared our prosthesis model with CNC milling as shown in Figure 5. We tested models of one population which consists of 4 elements in each case. Comparison of printed geometries and milled geometries is presented in the next chapter.

3. Results and discussion

Both the 3D prints and the CNC milled designs were tested on the knee prosthesis test apparatus. Our measurements were carried out under the same conditions:

- – 120-300N quadriceps muscle strength range,
- – 0-100° flexion range.

The measurement was performed on the experimental test machine shown in Figure 6. The flexion of the knee prosthesis components is performed by a stepper motor. The rotation-flexion values are recorded by two incremental rotary encoders with a resolution of 0.18°. Due to the high-stepping restore accuracy of the stepper motor all measurements were carried out in the same range of flexion. The quadriceps muscle strength was continuously recorded during the flexion process with a Spider 8 measuring data collector. All measurements were performed with 5 repetitions. The average measurement results of each setting are shown in Figure 7.
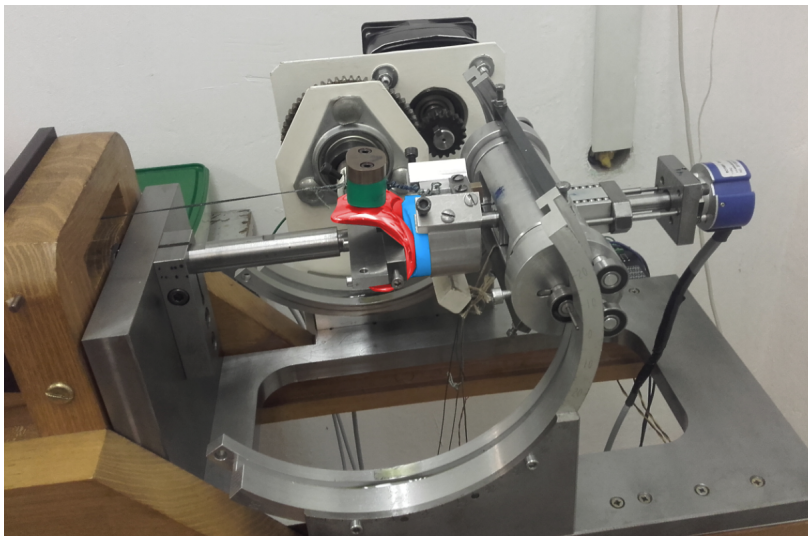

Figure 6. Knee prosthesis under measurement
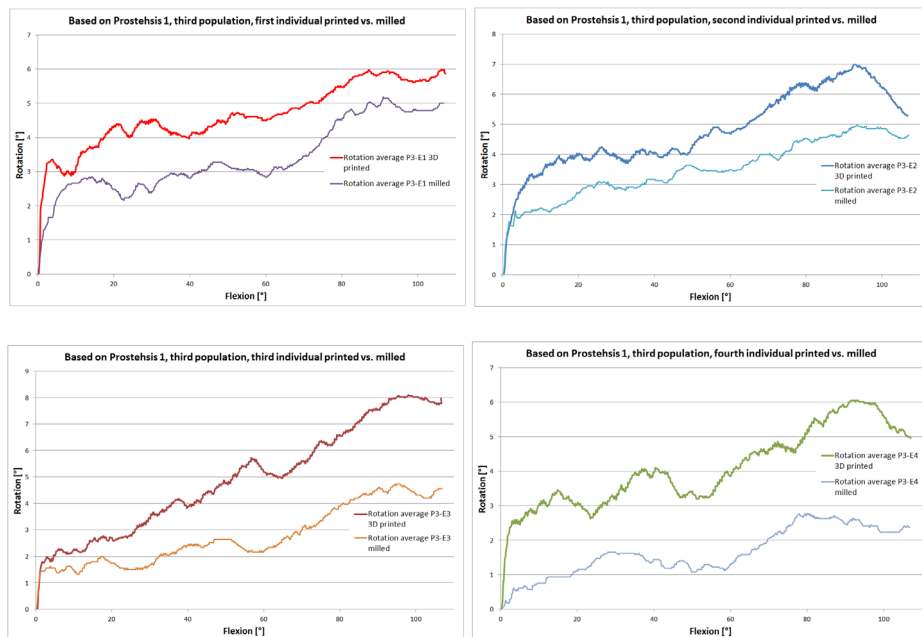
Measurement results (Fig. 7.):

Figure 7. Measurement results

The Figure 7. shows that we didn't get the same results for same geometry models created by 3D printing and CNC milling. For each individual the rotation-flexion functions show a similar pattern, but on average 1-2 degrees, and in extreme cases 3-4 degrees of deviation is possible. As there is no difference in the geometry the quality of the surfaces and the different friction conditions of the individuals give the difference. The main features of the two methods are summarized in Table 1.

Table 1. Technological comparison – advantages and disadvantages

	Advantage	Disadvantage
3D printing	Easy accessible	Slow printing > 2h
	Cheaper than CNC milling	Not the definitive material quality
CNC milling	Definitive material quality	Difficult to access
	Fast processing <0,5h	Expensive technology: tool + machine

It can be stated that 3D printing is suitable for the development of prosthesis geometry, but during the designing of the final geometry, the built-in prosthesis production technology must be used (milled prosthesis). Hereby the surface quality does not cause uncertainty during the prosthesis qualification.

Conclusions

As a result of our research we can conclude that with the use of our algorithm prosthesis geometry can be created and it can also fulfil the prescribed conditions. During the geometry development the 3D printed specimens are suitable for the contact surface qualification. However as a reason of the printed surface we can't achieve better results than a few degrees of the target function. For the final, precise fit a CNC milled model is required. The sensitivity of behavior to surface quality has been demonstrated, but it raises further questions, further research is needed on this subject.

Nomenclature

Greek letters

ρ rotation $°$
φ flexion $°$

Acknowledgements

References

[1] Donáth T. (2005), Anatómia – Élettan. Medicina Könyvkiadó Zrt. pp. 57-71.
[2] Fekete G., M. Csizmadia B, Magd A. Wahab, Patric De Baets, Libardo V. Vanegas-Useche and István Bíró (2014), Patellofemoral model of the knee joint under non-standard squatting. Dyna Colombia; 81 (183), pp. 60-67.
[3] Katona G, M. Csizmadia B and Andrónyi K. (2013) Determination of reference function to knee prosthesis rating. Biomechanica Hungarica, 6 (1), pp. 293- 301.
[4] Kovács NK. (2004), Prototípus fröccsöntő szerszámozás technológiájának fejlesztése – PhD értekezés, pp. 11-40.
[5] M. Csizmadia B, Katona G, Szakál Z and Bíró I. (2005) Kísérleti berendezés cadaver térdízület mozgásanalíziséhez, kísérleti méréssorozat értékelése, Gödöllő.
[6] M. Csizmadia B, Balassa G.P. and Katona G. (2013), The first steps to the development of the knee prothesis rating method. Biomechanica Hungarica; 6 (1), pp. 39-45.

[7] Miltényi M. (1980), A sportmozgások anatómiai alapjai. Budapest: TF, pp. 164-185.

[8] Ostermeier S, Hurschler C and Stukenborg-Colsman C. (2004), Quadriceps function after TKA – an in vitro study in a knee kinematic simulator, Clinical Biomechanics, Vol. 19, pp. 270-276.

[9] Sivanandam S.N. and Deepa S.N. (2008), Introduction to Genetic Algorithms, Springer, pp. 2-36.

[10] Standring S. (2008), Gray's Anatomy. The anatomical basis of clinical practice, New York: Churchill- Livingstone: Elsevier Press, pp. 4300-4354.

Isobus application possibilities in engineering informatics

A. LAGYMANYOSI, N. GÖNCZ, I. SZABÓ, L. BENSE

Faculty of Mechanical Engineering, Szent István University

Páter K. u. 1., Gödöllő, H-2100, Hungary

Abstract

ISOBUS is known as a communication protocol in agricultural and partly in industrial applications, aiming at ensuring standardized data transfer between tractors and implements. This standard enable the centralized data acquisition, and there is no need for a separate system for different implements, one terminal can be used for different procedures. ISOBUS as an information system enables increasing productivity and efficiency. This technology serves as the basic infrastructure for precision agricultural technologies. The large amount of data generated during system operation, can be used for further analyses in developing agricultural technologies. Embedded measuring and data collection systems of the tractor-implement units attached to ISOBUS network can be used for IT developments, as well as processing information in an automatic manner and enabling precise control of the agricultural production and mapping fieldborn data. The paper covers some historical aspects of ISOBUS application technologies and its related concepts, and also the possible use of ISOBUS data exchange in farm machinery development. Application development options based on ISOBUS are presented, such as a remote monitoring system that can be used to provide real-time data acquisition. Presented work describes a designed application example to engine rotation speed monitored based on NI cRIO-9073 FPGA controller and LabView.

Keywords

agricultural informatics, embedded systems, process control

1. Introduction

ISOBUS is a communications protocol created for the agricultural sector designed to provide the standards of communication between tractors and machinery. With the compatibility of tractors and machinery data collection is also centralized, it is not necessary to have a separate terminal for each machine, one terminal can be applied for different machinery.

At the beginning of the 1990s custom solutions were developed by the machinery manufacturers to connect the operation of the tractor and machinery. The manufacturer-specific solutions made it difficult to coordinate the equipment of different manufacturers and the application of the different terminals was also uncomfortable for the drivers.

With advances in technology there was a higher and higher demand to establish a uniform communications system. The negotiations were started between the manufacturers including AGCO, John Deere, New Holland as well as CLAAS, Amazone, Grimme, Kverneland and Pöttinger.

By 2001 they had agreed upon uniform connectors as well as the method of signal and data transfer. As a result, the ISO 11783 standard was created (Tractors and machinery for agriculture and forestry - Serial control and communications data network), also known as the ISOBUS.

The basis for the ISOBUS is given by the CAN protocol developed for the automobile industry and the standard number SAE J1939 describing the internal network of lorries, trucks and buses.

The CAN (Controller Area Network) is the bus system developed in order to simplify the electrical network of vehicles. Its development was started by Bosch and Intel engineers in 1983, and in 1986 it officially appeared in the Society of Automotive Engineers (SAE) conference. In 1987 the first CAN chip appeared from Intel, and in 1990 the CAN specification by Bosch was submitted for international standardization.

The different versions of the CAN system are now found in most passanger cars as well as the more modern agricultural equipment and machinery. In addition CAN has become a widely used communication protocol in many areas of the industry.

The SAE J1939 (Serial Control and Communications Heavy Duty Vehicle Network) is a CAN based communications network used for the communication and diagnostics of commercial vehicles. Since its publication it has become widespread, first in the United States and then in other parts of the world. J1939, ISOBUS and NMEA 2000 use the same high level of protocol.

The embedded measurement and data collection systems used for engineering informatics developments support CAN-based communication therefore can be well adapted to the ISOBUS networks. Based on systems designed for real-time analysis, postprocessing and data logging, on the ISOBUS data flow it is possible to further improve the current technology.

With CAN compatible development tools it cannot be difficult to show the content of the message identifiers and the associated data field, however, on a general CAN network the structure of these is determined by the manufacturers, therefore the data obtained is difficult to interpret.

Since the purpose of the ISOBUS is the standardisation of communication, the identifiers of the messages and the structure of the data field is determined by the high-level protocol mentioned above. For this the 29-bit identifier, extended message format of the CAN protokol is used, data transmission is aligned to the SAE J1939 standard.

2. Applied materials and method

The CAN identifier of message J1939 is structered as follows: the first 3 bits determine the prioroty, the next 18 bits are the number of the parameter group (PGN, Parameter Group Number), the last 8 bits are the source address.

The ISOBUS standard precisely specifies the parameter group numbers and the structure of the associated data field, so they are the same in the case of any manufacturer. This also means that the data obtained from the network can be already interpreted in the possession of the standard.

A suspect parameter number (SPN, Suspect Parameter Number) is assigned to each parameter of a parameter group or component. This is used for diagnostic purposes.

The following example will show how the content of a message can be interpreted. The following data is available about the parameter group "Electronic Engine Controller 1":

Transmission Repetition: engine speed dependent
Data Length: 8
Default Priority: 3
Parameter Group Number: 61444

Start Position	Length	Parameter Name	SPN
1.1	4 bits	Engine Torque Mode	899
2	1 byte	Driver's Demand Engine - Percent Torque	512
3	1 byte	Actual Engine - Percent Torque	513
4-5	2 bytes	Engine Speed	190
6	1 byte	Source Address of Controlling Device of Engine	1483
7.1	4 bits	Engine Starter Mode	1675
8	1 byte	Engine Demand - Percent Torque	2432

Based on the above the structure of data field belonging to the parameter group number 61444 is clear, but for the interpretation of the different parameters further information is necessary. The Engine Speed parameter is defined by the standard in the following way:

Actual engine speed which is calculated over a minimum crankshaft angle of 720 degrees divided by the number of cylinders.

Data Length: 2 bytes
Resolution: 0.125 rpm/bit, 0 offset
Data Range: 0 to 8,031.875 rpm
Type: Measured
Suspect Parameter Number: 190
Parameter Group Number: 61444

With this all the information is available to have the engine speed value measured in revolution/minute shown in the example.

The previous example illustrates clearly that the identifiers of the CAN messages and the associated data field can be converted into information having real physical content in the knowledge of the PGN and SPN numbers.

The above example will be shown in practice bellow through the known embedded measurement and data collection system of National Instruments. For this a NI cRIO-9073 controller and an NI 9853 two-channel, high speed CAN module was used.

First the speed is set to the 250kbit/s value set out in the standard. Out of the formats available for transmitting and receiving data with the NI 9853 CAN modul the CAN cluster is used [1]. The program is prepared for the FPGA target.

The type, identifier and data variables of the CAN cluster are used [2], first the PGN number is created from the identifier. For this the resulting value must be shifted to the right by 8 bits [3], and then through the 18 bit masking of the modified value [4] the PGN number is generated. The data frame type and the 61444 PGN number are set as default, and then within this the program part necessary for creating the SPN of 190 is made.
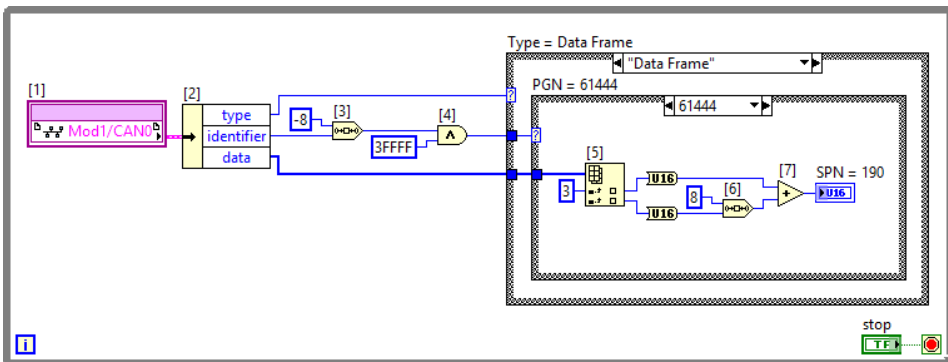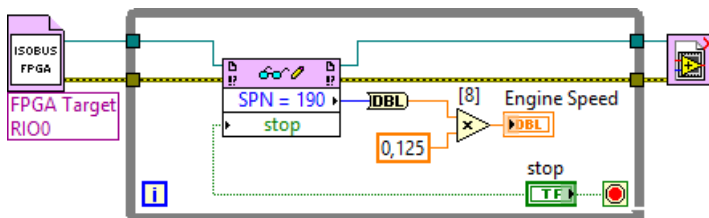

Figure 1. The data frame

Figure 2. The floating point creation

The bytes of the data field are contained in an 8-element array, the engine speed is 2 bytes in length on the fourth and fifth byte. Since the indexing of the array is started from 0, this means the index 3 and 4 element [5]. The index 4

element of the array must be shifted to the left by 8 bits [6], adding the resulting value to the index 4 element of the array [7] a 16-bit positive integer value arises.

The resulting value is taken over to the RT target, and then converted into a floating point number for creating the revolution/minute volume and multiplied by the given 0.125 value [8]. With this the revolution/minute value of the engine speed can be displayed on the Front Panel.
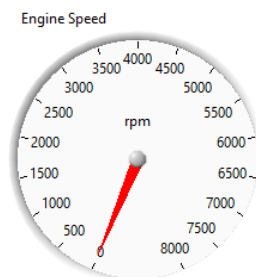

Figure 3. The rotation speed display

As the above example shows the data obtained from the ISOBUS network can be easily processed with the embedded measurement and data collection systems. These systems include a number of built-in options for real-time analysis, postprocessing and data logging so the engineering informatics application of the ISOBUS system provides an opportunity to utilize the amount of data generated during the operation of the system.

The above system can be well used in the early stages of the development, but in order to have the opportunity to test more ISOBUS compatible devices it will be necessery to create a more cost-efficient, task-specific system which is designed according to the extreme operating conditions so it is suitable for the use of the equipment data generated in the agricultural land.

Two systems can be used together too, so in this case the site data logging is combined with postprecessing performed in the laboratory.

Some of the possible solutions for recording and using the data originating from the agricultural land will be discussed below.

The simplest is the data logging through an embedded system with local data storage. The advantage of the solution is its simplicity, it does not require more than installing the system on the vehicle, and the disadvantage is that the logged data should be read out by the user.

If the above system is supplemented with data transmission through a wireless network, a little more complex but user-friendly solution is generated. In this case the data is also recorded into an integrated date storage, but the reading is performed through the wireless network installed in the machine shed. The data can even be sent to a remote server and low transfer speed is sufficient for this with the intermediate data storage.

The most complex system described in the article can be used for real-time analysis and remote diagnostics. This solution differs from the above ones in that the data is transmitted directly to the server through a network suitable for long-range transmission of data. For this a high speed wireless network needs to be established on the agricultural land.

It can be seen from the above that there are numerous options for recording and analyzing the data generated in the ISOBUS system, from which the most suitable one can be selected in the light of the amount of data to be processed.

3. Application examples

So far the possible ways of data processing and recording have been discussed, now the possible application examples will be described. The most obvious application is mapping the conditions of the production area on the basis of available data.

A simple but spectacular example of this may be the preparation of the yield map, which is based on the ISOBUS integration of the yield monitor systems available on the market, on the GPS data coming from the ISOBUS network and on the embedded measurement and data collection system discussed above.

With yield monitor systems the amount of yield and its moisture content can be measured to a high degree of accuracy, however the distribution of these in the field is only available in the case of the most expensive, GPS based systems.

If the data of a simple yield monitor system is added to the ISOBUS network, the yield map of the field can be obtained using the available GPS data. Data can be added to the ISOBUS network in the form of new messages whose structure is set out in the standard. The data can be logged with any of the above described devices.

Not only a cost-effective system can be created with this but the data added to the network can also be used in other areas. By comparing the data generated during tillage and sowing with the data generated during harvesting further conclusions may be made in respect of the production area.

Another ISOBUS-based application development option is the remote surveillance system that can be used to access data in real time from a PC or a smartphone.

Based on real-time data remote diagnostics can be performed, for example, which will shorten the repair time with the early detection of the fault: until the vehicle reaches the machine shed the spare parts and tools can be prepared.

This can be extremely important during periods when the given machine is indispensable in the workflow, in the case of a combine, for example, during harvest.

The real-time data of power machines and machinery can be used when organising the work processes, during harvest, for example, the transportation and storage of crops can be carried out on the basis of the yield data more efficiently.

During the application development for the ISOBUS system it is not always possible to do it in the presence of the given power machine or machinery therefore it may be necessary to simulate the CAN message traffic of the devices.

In certain cases it is sufficient to create the messages on the basis of the logged data, but it may be necessary to customize the value of the parameters, and also a simulation device making it possible to send incorrect data may be needed.

The already mentioned embedded measurement and data collection systems including the above described National Instruments CompactRIO and And LabVIEW platforms used for engineering informatics developments can also offer the solution to the above issues.

Conclusions

It can be seen from the above that the ISOBUS is not a standard with a long history, therefore there are still numerous opportunities in the related application development. By utilizing the data obtained during the operation of the system the current technology can be further developed, the results of the developments can be used in precision agriculture.

The tools of engineering informatics developments create the opportunity to quickly and simply manage application development and data processing.

Acknowledgements

References

[1] https://en.wikipedia.org/wiki/ISO_11783
[2] https://www.can-cia.org/fileadmin/resources/documents/proceedings/
    2003_fellmeth.pdf
[3] https://www.agronaplo.hu/szakfolyoirat/2016/03/gepesites/isobus-kommunikacio-
    traktor-es-munkagep
[4] https://en.wikipedia.org/wiki/CAN_bus
[5] https://www.can-cia.org/can-knowledge/
[6] https://en.wikipedia.org/wiki/SAE_J1939
[7] http://www.simmasoftware.com/j1939-pgn.html
[8] http://www.simmasoftware.com/j1939-spn.html

Modelling of agricultural machine movement

J. RÉDL[1], J. MAGA[2], G. KALÁCSKA[3]

[1]Department of Machine Design, Faculty of Engineering,
Slovak University of Agriculture in Nitra, Slovakia
[2]Department of Machines and Production Biosystems, Faculty of Engineering,
Slovak University of Agriculture in Nitra, Slovakia
[3]Institute for Mechanical Engineering Technology,
Szent István University, Gödöllő, Hungary

Abstract

In this contribution we deal with the modeling of movement of agricultural off-road vehicle operating on sloped ground. The modeled machine was Reform Metrac H6X. We prepared a three dimensional mathematical model with three degrees of freedom. The machine movement was defined with system of non-linear differential equations. Analyzed vehicle had a constant speed of center of gravity. Acting forces between of wheel and ground was modeled with exact method. Nonlinear system of moving equations was solved in PTC Mathcad© Prime 4 environment. The solved kinematical parameters are useful in process of design and testing of prototypes.

Key words

ride stability, vehicle dynamic, tire properties, mathematical modeling

1. Introduction

Ride stability and it control is the very important parameter to prevent the agricultural off road vehicle overturn. Researchers try to predict the situation occurs until machine moving on uneven ground. The best way to have the optimal information is the realization of experimental ride or simulation with mathematical model. Predicting ride stability of vehicle with 2D models was analyzed with many researchers like [8], [5] and [6]. These models withhold the dislocations of real vehicles until the moving. Nowadays the researchers focused on the ride stability and its control. The better knowledges about the acting forces and moments arising between the ground and the tires helps to define these relationships, [9], [4], [1],[2]. The presented methodology is three-dimensional model and allows trace the dislocation and orientation of the lateral forces in the ride and maneuvers. Centripetal component of the lateral force affecting on the wheels and are most relevant. Lateral force was generated by usual way how it described in [1] with respect to the normal reaction of the ground and yaw angle of tire. The model is defined with system of nonlinear moving equation where the

explicit analytical solution is difficult. For this reason the problem was solved numerically. The results of this solution define the lateral dynamics of the vehicle movement more precisely like the linearization or simplification of the corresponding moving equations. Model is usable for most agricultural machines construction configurations as described [7].

2. Material and methods

Mathematical model
For analyses we chose the space model where we considering the tire stiffness and vehicle kinematic maneuvers. The modeled vehicle has a constant velocity of center of gravity. The model is depicted on the figure 1. For this model we consider these assumptions:
1. lateral force depend on the vertical load of the tire,
2. velocity of each wheels are the sum of the velocity of center of gravity and cross product of the angular velocity of the wheel and dislocation vector of center of the wheel.
   The lateral force F_y is defined as follows:

$$F_y = C_\delta \cdot \delta \tag{1}$$

where C_δ is the corner stiffness expressed with the next equation:

$$C_\delta = \lim_{\delta \to 0} \left(\frac{\partial F_y}{\partial \delta} \right)$$
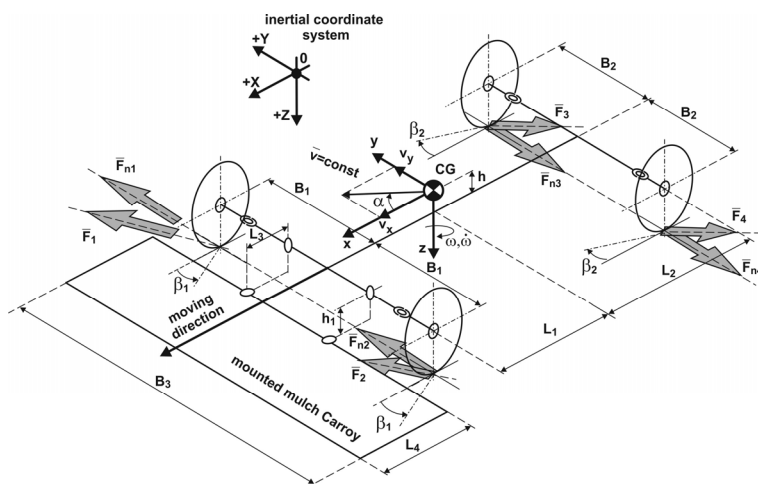
and δ is a slip angle.

Figure1. Vehicle model

The components of the velocity vectors are:

$$\frac{dx_i}{dt} = \frac{dx}{dt} + r_i \cdot \frac{d\varphi}{dt} \cdot \cos\left(\gamma_i + \frac{\pi}{2}\right)$$

(2)

$$\frac{dy_i}{dt} = \frac{dy}{dt} + r_i \cdot \frac{d\varphi}{dt} \cdot \sin\left(\gamma_i + \frac{\pi}{2}\right)$$

(3)

Angle of velocity vector carrier orientation defined in the eq.4 derived from the figure 2.

$$\alpha_i = arctg\left(\frac{\dfrac{dx_i}{dt}}{\dfrac{dy_i}{dt}}\right)$$

(4)

where :

– $\dfrac{dx_i}{dt}$ is the travel speed,
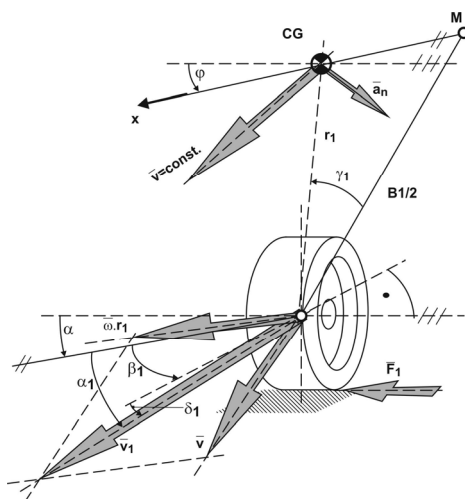
– $\dfrac{dy_i}{dt}$ is the lateral velocity.

Figure 2. Tire model

Tire slip angle will be:

$$\delta_i = \beta_i - \alpha_i \tag{5}$$

Vehicle moving with constant velocity and then the absolute value of velocity vector of center of gravity is constant. With respect this assumption we consider the tangential acceleration is equal to zero like bellow in eq.6.

$$\frac{dy^2}{dt} = 0 \tag{6}$$

In this direction is static equilibrium. We predict the reciprocally compensation of the normal and tangential forces. We neglect the normal components of the driving force. Acting only normal component of the lateral forces defined bellow:

$$F_{ni} = F_i \cdot \cos(\beta_i - \alpha_i) \tag{7}$$

Vehicle is turning when acting these forces pairs. The moving equations satisfactory to these conditions are defined bellow:

$$m \cdot \frac{dx_i^2}{dt} = \sum {}_{i=1}^{i=m} F_{ni} \tag{8}$$

$$I \cdot \frac{d\varphi_i^2}{dt} = \sum {}_{i=1}^{i=m} F_{ni} \cdot r_i \cdot \cos(\gamma_i - \alpha) \tag{9}$$

After managing the equations we got:

$$m \cdot \frac{dx_i^2}{dt} \cdot \left(\frac{d\varphi}{dt} + \frac{d\alpha}{dt} \right) = \sum {}_{i=1}^{i=m} F_{ni} \tag{10}$$

$$I \cdot \frac{d\varphi_i^2}{dt} = \sum {}_{i=1}^{i=m} F_{ni} \cdot r_i \cdot \cos(\gamma_i - \alpha) \tag{11}$$

Rewriting the equations to the solvable form:

$$\frac{d\varphi_i}{dt} = \left[\frac{1}{m \cdot \frac{dx_i}{dt}} \left(\sum {}_{i=1}^{i=m} F_{ni} \right) \right] - \frac{d\alpha}{dt} \tag{12}$$

$$\frac{d\varphi_i^2}{dt} = \frac{1}{I} \left[\sum {}_{i=1}^{i=m} F_{ni} \cdot r_i \cdot \cos(\gamma_i - \alpha) \right] \tag{13}$$

$$\frac{d\varphi}{dt} = \omega \tag{14}$$

$$\frac{dx_i}{dt} = \frac{dx}{dt} \cdot \cos(\alpha + \varphi) \tag{15}$$

$$\frac{dy_i}{dt} = \frac{dy}{dt} \cdot \sin(\alpha + \varphi) \tag{16}$$

Systemic vehicle

The REFORM Metrac is a municipal services tool carrier designed for extreme slopes and difficult terrain. It is distinguished by cutting edge technology and highest efficiency. With its outstanding versatility, the Metrac is ready to roll in all working situations and provides unique working convenience as defined in [3]. The mounted tool is a mulcher Carroy. Technical parameters of vehicle and tool are described in table 1 and table 2.

Table1. Parameters of off-road machine

Parameter	Value	Unit
Manufacturer	Reform-Werke	
Type	Metrac H6 X	
Engine	VM-D 754 SE 3	
Tires	33x15.50-15 BKT	
Weight	2370	kg
Weight with tool	2780	kg
Wheel base	1,995	m
Wheel track	1,630	m
L1	0,815	m
L2	1,180	m
h	0,7	m
B1	0,815	m
I_z moment of inertia	1723,4	kg.m^2

The slope travelling ability was at 55 - 60 % in traverse lines and at 60-65% in fall line at good driving conditions (dry ground with maximum grip). If the electronic weight transfer system is adjusted in an optimal way, working up hill of nearly 70 % can be reached on perfect conditions. This may not be the case everywhere and can only be achieved – as aforementioned – on optimal conditions and with excel lent knowledge of driving and terrain [3].

Table 2. Parameters of tool

Parameter	Value	Unit
Manufacturer	DSP Production Sas	
Mark	Carroy	
Type	GF 2072 RE7F C6 2S	
Description	mulch-laying adapter	
Weight	410	kg
Length	1,0	m
Width	2,270	m
Height	1,10	m

3. Results and discussion

The position of hand steering is determined by the deviance between the longitudinal axis of vehicle and required direction of movement. For the better riding the difference between the moving direction of vehicle and immediate moving direction of center of gravity will be minimal. This vehicle is controlled by operator very easy. To testing of ride variants we used the simulations with constant velocity and the same valued steering angle of all wheels. The ride maneuver has a circular form. The second variant was an obstacle avoidance maneuver.
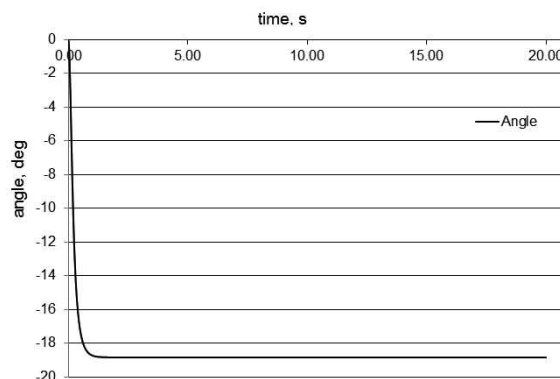

Figure 3. Direction angle change of velocity vector

Algorithm contains the function of continual changing of wheels steering angle. In the simulation we used the steering angle $\beta=8deg$ and the center of gravity velocity $v=2m.s^{-1}$. Change of the angular velocity is depending on the time. This relationship is described in the figure 4.
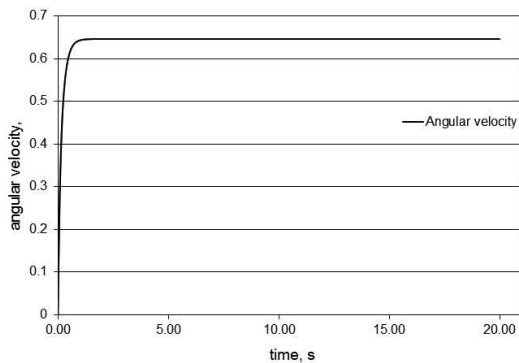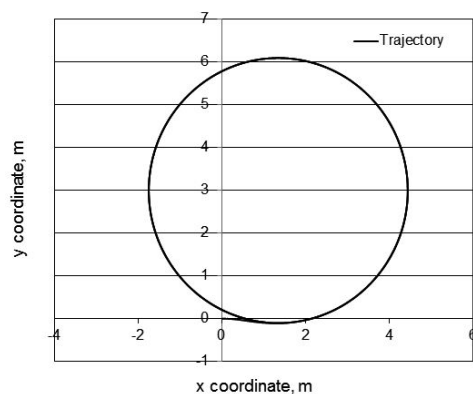
Figure 4. Angular velocity

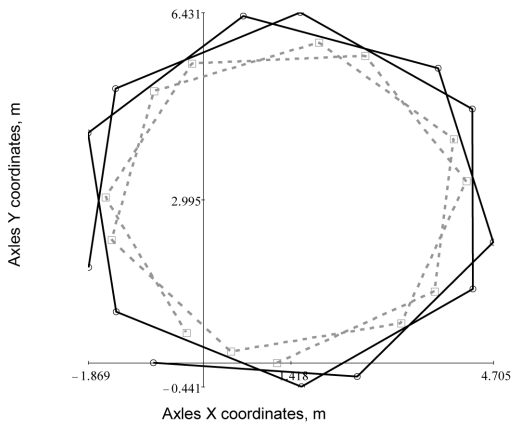*Figure 5.* Trajectory of center of gravity of vehicle

Figure 6. Vehicle axles trajectory

Modification of the tractor is relevant at the 2 second and characterized the rolling of the vehicle. The rolling is influenced with used periodical function.

The influence of adhesion changing is not significant. The second important solved parameters were the dislocations of center of gravity in the inertial coordinate system. Trajectory is depicted in the figure 5. The form of trajectory is typical for turning ride maneuver. The trajectory of front end and the rear axle is depicted in the figure 6. For the illustrative purpose we chose only 155 positions. When the very fast turning occurs at the beginning of the maneuver the longitudinal axis of vehicle is not changing significantly with respect to the axis X in the inertial coordinate system. This is described in the figure 3, when the angle change has a linear character.
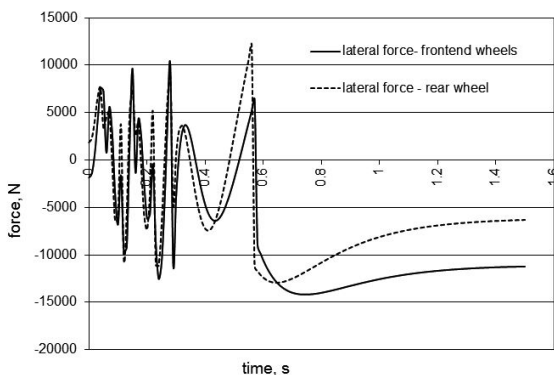

Figure 7. Lateral forces

To modelling the lateral force with eq.(1) according to the [1] we use these parameters :
- vertical force range (vertical load on one wheel) Fz=5000-7000 N,
- corner stiffness $C\alpha$=1680 N.deg^{-1},
- slip angle δ=8deg.

The modelled lateral force for the frontend and rear wheels are in the figure 7. The major changes of later forces are described only for 1,6s time interval. To the end of the simulation the forces has the consolidate course.

Conclusion

We defined the practical maneuvers of agricultural off road vehicle with the mathematical model with three degree of freedom and described with system nonlinear differential equations. The kinematic problem was solved numerically with Mathcad Prime 4: environment. We solved these parameters:
- dependence of the angular velocity from the time in the turning ride in the chosen maneuver,
- trajectory of center of gravity in the inertial plane,
- dislocation of the vehicle, defined with the dislocations of the vehicle axis (front end and rear).

Designed mathematical model is utilizable in the process of design and testing of prototypes and in the optimization process of vehicle construction. The model is adapted for modeling of the AWS systems and various theories of generating the lateral forces acting in the wheel-ground relationship and predicts the steering angle of wheel with tire.

References

[1] Guiggiani, M. 2014. The Science of Vehicle Dynamics, Springer Science+Business Media Dordrecht 2014. p.364. ISBN 978-94-017-8532-7.

[2] Chen,W. -Xiao,H. - Wang,Q.- Zhao,L.- Zhu,M. 2016. Integrated Vehicle Dynamics and Control, 2016 John Wiley & Sons Singapore Pte. Ltd. p.373. ISBN: 9781118379998

[3] Metrac Pruefberichte, Available at:
http://www.josephinum.at/fileadmin/content/BLT/Pruefberichte/g2008253.pdf

[4] Pacejka, H. 2005. Tire and Vehicle Dynamics. Butterworth-Heinemann 2005. p.672, ISBN-13: 978-0-7506-6918-4.

[5] Rajamani, R. - Zhu, C. – Alexander, L. 2003. Lateral control of a backward driven front-steering vehicle. In: Control Engineering Practice 11 (2003) 531–540. ISSN 0967-0661

[6] Renfroe, D. – Roberts, A. – Gilbert, M. 2006. Vehicle rollover maximum limits, In: Int. J. Vehicle Design, Vol. 40, Nos. 144 1/2/3, 2006. ISSN 0143-3369.

[7] Simoník, J. - Jobbágy, J. 2010. Earth-moving machinery (Stavebné stroje), 1.st.edition. Nitra: Slovenská poľnohospodárska univerzita, 2010. 187 s. ISBN 978-80-552-0514-4.

[8] Šesták, J. – Rédl, J. – Pršan, J. Pohyb terénneho vozidla po nerovnej podložke. In Nové trendy v konštruovaní a v tvorbe technickej dokumentácie 2002. Nitra: Slovenská poľnohospodárska univerzita, 2002, s. 87--93. ISBN 80-8069-025-1.

[9] Wong, J,Y. 1989. Terramechanics and Off-Road Vehicles. Elsevier Science Publisher, 1989. s.251. ISBN 0-444-88301-0.